Synthesis and Electrochemistry of Novel Conducting Dendrimeric Star Copolymers on Poly(Propylene imine) Dendrimer

Abd Almonam Abd Alsalam Baleg

A thesis submitted in fulfilment of the requirements for the degree

Doctor of Philosophy

in the

Department of Chemistry, University of the Western Cape

Supervisors:

Professor Emmanuel I. Iwuoha

Dr. Nazeem Jahed

October 2011

Synthesis and Electrochemistry of Novel Conducting Dendrimeric Star Copolymers on Poly(Propylene imine) Dendrimer

Abd Almonam Abd Alsalam Baleg

Keywords

Conducting dendrimeric star copolymer

Polypyrrole

Poly(propylene imine)

Dendrimer

Poly(propylene imine)-co-polypyrrole

Hall effect measurements

Conductivity

Electrical conductivity

Electrochemical impedance spectroscopy

Cyclic voltammetry

Platinum electrode

ABSTRACT

One of the most powerful aspects of conducting polymers is their ability to be nanostructured through innovative, synthetically manipulated, transformations, such as to tailor-make the polymers for specialized applications. In the exponentially increasing wide field of nanotechnology, some special attention is being paid to innovative hybrid dendrimer-core based polymeric smart materials. Star copolymers are a class of branched macromolecules having a central core with multiple linear polymer chains extending from the core. This intrinsic structural feature yields a unique 3D structure with extended conjugated linear polymer chains, resulting in star copolymers, which have higher ionic conductivities than their corresponding non-star conducting polymer counterparts. In this study an in-depth investigation was carried out into the preparation and characterization of specialized electronic 'smart materials'. In particular, the preparation and characterization of novel conducting dendrimeric star copolymers which have a central poly(propylene imine) (PPI) dendrimer core with conducting polypyrrole (PPy) chains extending from the core was carried out. This involved, first, the preparation of a series of dendrimeric polypyrrole poly(propylene imine) star copolymers (PPI-co-PPy), using generations 1 to 4 (G1 to G4) PPI dendrimer precursors. The experimental approach involved the use of both chemical and electrochemical synthesis methods. The basic procedure involved a condensation reaction between the primary amine of a diamino functional PPI dendrimer surface and 2-pyrrole aldehyde, to afford the pyrrole functionalized PPI dendrimer (PPI-2Py). Polymerization of the intrinsically contained monomeric Py units situated within the dendrimer backbone was achieved via two distinctly different routes: the first involved

iii

chemical polymerization and the second was based on potentiodynamic oxidative electrochemical polymerization.

The star copolymers were then characterized using various sophisticated analytical techniques, in-situ and ex-situ. Proton nuclear magnetic resonance spectroscopy (^{1}H NMR) and Fourier transform infrared spectroscopy (FTIR) were used to determine the structures. Scanning electron microscopy (SEM) was used to determine the morphology. Themogravimetric analysis (TGA) was used to study the thermal stability of the prepared materials. X-ray diffraction analysis (XRD) was used to study the structural make-up of phases, crystallinity and amorphous content. Hall effect measurements were carried out to determine the electrical conductivity of the chemically prepared star copolymers.

The PPI-co-PPy exhibited improved thermal stability compared to PPI-2Py, as confirmed by TGA. SEM results showed that the surface morphology of the functionalized dendrimer and star copolymer differed. The surface morphology of the chemically prepared star copolymers resembled that of a flaky, waxy material, compared to the ordered morphology of the electrochemically grown star copolymers, which resembled that of whelk-like helixes. In the case the electrochemically grown star copolymers, SEM images recorded at higher magnifications showed that the whelk-like helixes of the star copolymers were hollow tubes with openings at their tapered ends, and had an average base diameter of 2.0 μm. X-ray diffraction analysis of the first generation star copolymer G1PPI-co-PPy revealed a broadly amorphous structure associated with PPy, and crystalline peaks for PPI.

Cyclic voltammetry (CV), square wave voltammetry (SWV) and electrochemical

impedance spectroscopy (EIS) techniques were used to study and model the electrochemical reactivity of the star copolymer materials. Electrochemical impedance spectroscopy data showed that the G1PPI-co-PPy exhibited slightly higher ionic conductivity than pristine PPy in lithium perchlorate. The second generation star copolymer G2PPI-co-PPy electrochemically deposited on a platinum (Pt) electrode had a lower electrochemical charge transfer resistance compared to electrodeposited polypyrrole (PPy) on a Pt electrode, and bare Pt. The decrease in charge transfer resistance was attributed to an increase in the conjugation length of the polymer as a result of the linking of the highly conjugated PPy to the PPI dendrimer.

Bode impedimetric analysis indicated that G2PPI-co-PPI was a semiconductor, with a maximum phase angle shift of 45.3° at 100 MHz. The star copolymer exhibited a 2-electron electrochemistry and a surface coverage of 99%. Results of Hall effect measurements showed that the star copolymer is a semiconducting material, having a conductivity of 0.7 S cm^{-1}, in comparison to the 1.5 S cm^{-1} of PPy.

To the best of my knowledge, these new star copolymers have not been reported in the open literature. Their properties make them potentially applicable for use in biosensors.

DECLARATION

I declare that *"Synthesis and Electrochemistry of Novel Conducting Dendrimeric Star Copolymers on Poly(Propylene imine) Dendrimer''* is my own work, that it has not been submitted before for any degree or assessment at any other university, and that all the sources I have used or quoted have been indicated and acknowledged by means of complete references.

Abd Almonam Abd Alsalam Baleg   October 2011

Signature _____

Supervisors: Prof. Emmanuel I. Iwuoha

Dr. Nazeem Jahed

DEDICATION

I dedicate this thesis to

my dearest wife

Amani Majed Emhameed

and

to my lovely children

Mohamed Abd Almonam Baleg

Moied Abd Almonam Baleg

Malak Abd Almonam Baleg

ACKNOWLEDGEMENTS

In the name of Allah, the most Gracious and the most Merciful

Praise be to Allah the Almighty, for thee (alone) we worship and thee (alone) we ask for help. Praise also is upon Muhammad S.A.W. who guided and led us to the right path.

First of all, I would like to express my gratitude to my family - I thank my wife (Amani) who stood with me throughout the journey of writing this thesis, and my children (Mohamed, Moied and Malak) whose presence gladdened my life. I am also indebted to my family in Libya for giving me the strength and support throughout my studies and especially during those hard and discouraging moments in the history of our nation.

Thanks are also dedicated to the University of the Western Cape, South Africa, for giving me the opportunity to pursue my Doctoral degree. Special thanks go to the Department of Chemistry and SensorLab, University of the Western Cape, for providing all the apparatus and instrumentation required for my research.

I acknowledge my supervisors Professor Emmanuel I. Iwuoha and Dr Nazeem Jahed for keeping their confidence in me and assisting me to complete my work successfully. Their patience, advice, constructive comments and encouragement have greatly helped me complete my research.

I should not forget to thank my colleagues in the SensorLab and all other colleagues for their support and motivation.

I would also like to thank the staff of the Chemistry Department, especially Prof. Priscilla Baker, Prof. Farouk Ameer and Dr. Fanelwa, for their help and support. I highly appreciate the support I got from post-doctoral fellows Drs. Amir Al-Ahmed, Faiza, Nikkie, Jasmina and Tesfaye.

LIST OF PUBLICATIONS

1)   Synthesis and characterization of poly(propylene imine) dendrimer – Polypyrrole conducting star copolymer. **Abd Almonam A. Baleg**, Nazeem M. Jahed, Omotayo A. Arotiba, Stephen N. Mailu, Nicolette R. Hendricks, Priscilla G. Baker, Emmanuel I. Iwuoha. Journal of Electroanalytical Chemistry, 2011, volume 652, pages 18–25.

2)   Spectroelectrochemical dynamics of dendritic poly (propylene imine)-polythiophene star copolymer aptameric 17B-stradiol biosensor. Rasaq A. Olowu, **Abd Almonam Baleg**, Peter M. Ndangili, Chinwe O. Ikpo, Njagi Njomo, Priscilla Baker, Emmanuel Iwuoha. International Journal of Electrochemical Science, 2011, volume 6, pages 1686–1708.

3)   Modulation of the interfacial electrochemistry of surfactant-functionalised polypyrrole chemical sensor systems. Faiza J. Iftikhar, **Abdul M. Baleg**, Priscilla G.L. Baker, Peter M. Ndangili, Stephen N. Mailu, Emmanuel I. Iwuoha. Electrochimica Acta, 2011 (30 May), volume 56(14), pages 5214–5221.

4)   Determination of anthracene on Ag-Au alloy nanoparticles/overoxidized-polypyrrole composite modified glassy carbon electrodes. Stephen N. Mailu, **Abd A. Baleg,** Tesfaye T. Waryo, Peter M. Ndangili, Fanelwa R. Ngece, Priscilla G. Baker, Emmanuel I. Iwuoha. Sensors, 2010, volume 10(10), pages 9449–9465.

5)   Natasha West, Priscilla Baker; Omotayo Arotiba, Nicolette Hendricks, **Abd Almonam Baleg,** Tesfaye Waryo, Fanelwa R. Ngece, Emmanuel I. Iwuoha Overoxidized polypyrrole incorporated with gold nanoparticles as platform for impedaimetric anti-tranglutaminase immunosensor. Analytical Letters, 2011, volume 44(11), pages 1956–1966.

6)   Impedimetry and microscopy of electrosynthetic poly(propylene imine)-co-polypyrrole dendritic star copolymer. Abd Almonam A Baleg, Rasaq A Olowu, Peter M. Ndangili, Chinwe O Ikpo, Faiza J Iftikhar, Nazeem Jahed, Priscilla Baker, Emmanuel Iwuoha. Submitted.

TABLE OF CONTENTS

LIST OF ABBREVIATIONS

ATRP	Atom transfer radical polymerization
HOMOs	Highest of the low-energy orbitals
Pt|bare	Bare platinum electrode
Eg	Band gap
CP	Conducting polymer
CPs	Conducting polymers
R_{ct}	Charge transfer resistance
CV	Cyclic voltammetry
C_{dl}	Double layer capacitance
ΔE_p	Difference in potential peak potentials
DCM	Dichloromethane
$CDCl_3$	Deuterated chloroform
DAB	Diaminobutane
PAMAM	Polyamidoamine Dendrimers
EIS	Electrochemical impedance spectroscopy
FTIR	Fourier transform infrared
PPI-2Py	Functionalized dendrimer
G4PPI	Forth generation poly(propylene imine)
G1PPI-co-PPy	First generation poly(propylene imine)-co-polypyrrole
G1PPI	First generation poly(propylene imine)
Tg	Glass transition temperature
K_{et}	Heterogeneous rate constant
$LiClO_4$	Lithium perchlorate solution
Pt|G2PPI-co-PPy	Modified platinum electrode with second generation poly(propylene imine)-co-polypyrrole

Pt|PPy	Modified platinum electrod with polypyrrole
Pt|G1PPI-co-PPy	Modified platinum electrod with first generation poly(propylene imine)-co-polypyrrole
PPI	Poly(propylene imine) dendrimer
PPI-co-PPy	Poly(propylene imine)-co-polypyrrole
^{1}H NMR	Proton nuclear magnetic resonance spectroscopy
I_{pa}	Peak anodic current
I_{pc}	Peak cathodic current
PPy	Polypyrrole
E_{pa}	Peak anodic potential
E_{pc}	Peak cathodic potential
PBS	Phosphate buffer saline
ROP	Ring-opening polymerization
PANI	Polyaniline
PEDOT	Poly(3,4-ethylene-dioxythiophene)
GPC	Gel permeation chromatography
Pt	Platinum
2-Py	2-Pyrrole aldehyde
PANI	Polyaniline
SEM	Scanning electron microscopy
SWV	Square wave voltammetry
G2PPI-co-PPy	Second generation poly(propylene imine)-co-polypyrrole
G2PPI	Second generation poly(propylene imine)
TGA	Themogravimetric analysis
G3PPI	Third generation poly(propylene imine)
TEM	Transmission electron microscopy
XRD	X-ray diffraction

τ	Time constant (cycle life)
ω_{max}	Frequency at maximum imaginary impedance
LUMOs	Lowest of the high-energy orbitals

UNIVERSITY *of the*
WESTERN CAPE

LIST OF FIGURES

LIST OF TABLES

CHAPTER 1

Introduction

This chapter provides a brief background on the topic of conducting polymers and specifically conducting star copolymers, describes the problem statement and research motivation, and presents the aims and objectives of the study that was carried out.

1.1   Background

An organic polymer that exhibits highly reversible redox behaviour and a combination of properties of metals and plastics is termed as conducting polymer (CP) more commonly, a "synthetic metal". Conducting polymers (CPs) typically contain, as the fundamental structural unit, a linear backbone of repeating conjugated monomers [1]; examples include polyacetylene (PA), polypyrrole (PPy), polyaniline (PANI), and polythiophene (PT) [1]. Electron delocalization is a consequence of the presence of conjugated double bonds in the polymer backbone of CPs. Conductivity values for such polymers varies from 10^{-10} to 10^6 S cm^{-1}, covering the range associated with semiconductors and conducting filled composites at the lower end, to metals at the higher end. Polymers with electrical conductivity or semiconductivity are of interest as lightweight replacements for inorganic metals and semiconductors. Conducting polymers have the potential to replace metal coatings [2]. Organic conducting and semiconducting polymers may be synthetically tailored to optimize desirable material properties, such as the melting point, melt viscosity, solubility, electrical and thermal conductivity.

Conducting polymer composites, resulting from the blending of an insulating polymer matrix with electrical conducting fillers (e.g., carbon black, carbon fibres, metal particles), show many interesting features due to their electrical resistivity variation with thermal solicitations [3-6]. Recent studies have shown that several conducting polymers, e.g., PPy, PANI and poly(3,4-ethylene-dioxythiophene) (PEDOT), all have good biocompatibility [7-8], and have been proven to be useful alternatives for the development of new biodegradable conduits employed for restoring the function of injured peripheral nerves or the regeneration of a nerve gap by using electrical stimulation in situ [9]. Conducting polymers have electrical and optical properties similar to those of metals and inorganic semiconductors, and also exhibit attractive properties associated with conventional polymers, such as (generally) ease of synthesis and processing [10]. Polypyrrole exhibits good electrical conductivity and high air stability and is a useful conducting polymer. Polypyrrole has emerged as an important material because of its wide range of technological applications, in various areas, such as secondary batteries [11], electrochromic display devices [12], light-emitting diodes [13], capacitors [14], sensors [15], membranes [16], and enzyme electrodes [17]. Electrical transport in polymeric materials [18] has become an area of increasing research interest because these materials have potential use in solid-state devices.

However, PPy and other conducting electroactive polymers are limited in their practical use due to their very brittle structure, insolubility, and poor mechanical and physical properties, which restrict their processability [19]. Synthesis of conducting star, graft or block copolymers are some of the effective ways to improve the processability of conducting polymers [20-21]. Preparation of graft, block and star copolymers permit

chemical linkage between the insulating matrix (end groups) and the conjugated polymer, thus enhancing the chemical stability of the material [22].

Star copolymers are a class of branched macromolecules that have a central core to which multiple linear polymer chains are attached. The three-dimensional (3D) structure with extended conjugated linear polymer chains gives star copolymers properties that are different from the typical two-dimensional (2D), linear polymers. Conducting star copolymer materials are particularly useful as coatings because of their spheroidal structure and their ability to pack in three dimensions [23]. These materials are used in their undoped state for applications in which the conductivity requirements are not too high, for example static dissipation, or where the optical property of the polymer coating is of chief importance, e.g., as a pigment or reflective layer. Materials with conductivities in the range 10^{-6} to 1 S cm^{-1} may be suitable for these purposes. Furthermore, the conducting chains can, surprisingly, provide sufficient intermolecular overlap to give solid materials with electrical conductivities higher than the corresponding linear, non-star conducting polymers [23-26]. For example, nylon-6 with a star structure has a melt viscosity and crystallization half-time that are substantially reduced by the branching [27]. The regular 3D structure of star copolymer gels combines the properties of hardness and flexibility, and is being investigated for the making of materials that are hard, without being brittle [23].

The combination of star copolymer and conducting polymer structures offers an approach to making materials that have the favourable properties of both, i.e., improved processability and electrical conductivity. Improved processability results from the

spheroidal structure of hyperbranched, dendrimeric, and starburst polymers. A conducting star copolymer may be constructed in which two or more different conjugated arms radiate from the central core [28]. Doping of conducting star copolymers to increase the electrical conductivity may be achieved using existing methods applicable to the conjugated radiating chain moieties. For conjugated chains based on Py or thiophene units, or derivatives thereof, doping may be achieved by treatment with oxidizing agents such as iodine, ferric chloride, ferric tosylate, gold trichloride, and antimony chloride. If the polymer side chains are composed of PANI, doping can be achieved by treatment with acid [29]. Doping can also be achieved electrochemically by confining the polymer to an electrode surface and subjecting it to an oxidizing or reducing potential in an electrochemical cell. In this way, doped thin films on conducting substrates are obtained. Applications of conducting polymers in batteries, supercapacitors and electrochromic displays frequently entails doping of the polymer by such an electrochemical process [23]. The synthesis of conducting star, graft and block copolymers leading to a new material with modulated properties can be employed [20-21]. Graft and block copolymerization permit the creation of chemical linkage between the insulating matrix (end groups) and the conjugated polymer, thus enhancing the processability and chemical stability of conducting polymers [22]. Electrochemical copolymerization can afford a variety of conducting materials with different optical, electrical and morphological properties, as well as controlled electrochromic properties [30-32].

Poly(propylene imine) (PPI) dendrimers are highly branched macromolecules terminating with amino groups. They have several interesting characteristics, and can be used as hydrogen donors because of their high density of amino groups. Many of the properties of

4

dendrimers are strongly influenced by the terminal groups [33-35]. Dendrimer-like star branched polymers have recently appeared as a new class of hyperbranched polymers. They are recognized as nano-ordered globular macromolecules from their architectures and have many characteristic structural features, such as hierarchic hyperbranched structures, generation-based radial architectures, different branch densities between core (inside) and shell (outside), and many junction points and end-groups [36-37]. Dendrimer-star copolymers [38], with a new type of molecular architecture, in which many linear homo or block copolymer chains are attached to the dendrimers, have been developed because they combine the properties of star copolymers with those of dendrimers [39-44]. Two general methods have been used to prepare the dendrimer-star copolymers. One involves linking monofunctional linear polymers onto the dendrimer surface [39, 43-45]. The other involves growth of armed polymer chains from the surface of the dendrimer by "controlled/living" polymerization reactions, such as anionic polymerization [46], ring-opening polymerization [47], and atom transfer radical polymerization (ATRP) [48].

A series of star-shaped copolymers, using the generation 1 to generation 5 (G1-G5) PPI as the core, have been prepared to investigate their miscibility properties with linear polystyrene [49-50]. The unsaturated end groups of polyisobutylene were converted into anhydride termini by an ene reaction with maleic anhydride, and the product was reacted with the PPI dendrimers to afford PPI-polyisobutylene star copolymers [51]. It is also possible to synthesize a variety of block copolymers with the same branched architectures by introducing different polymer segments at different generation. Such block copolymers generate unique and characteristic nanostructures ordered superstructures and supramolecular assemblies because of their hierarchic hyperbranched architectures.

5

Interesting morphologies and nanostructured materials have been reported by several research groups [52-58]. Hee-Soo Yoo *et al.* [59] synthesized a series of dendrimer-like star-branched polystyrenes by developing an iterative methodology based on the "arm-first" divergent approach, and obtained products with controlled molecular weights and compositions, and narrow molecular weight distributions [59]. Dendritic copolymers are a specific group of dendrimers. There are two different types of copolymers. Segment-block dendrimers are built with dendritic segments of different constitution. They are obtained by attaching different wedges to one polyfunctional core molecule. Layer-block dendrimers consist of concentric spheres of differing chemistry. They are the result of placing concentric layers around the central core. Hawker and Fréchet [60] synthesised a segment-block dendrimer which had one ether-linked segment and two ester-linked segments. They also synthesised a layer-block dendrimer. The inner two generations were ester-linked and the outer three ether-linked.
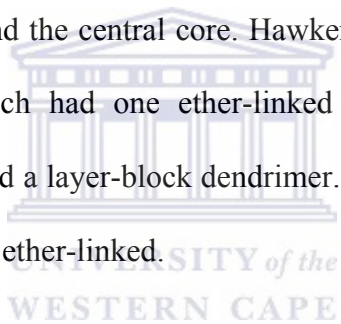
Thus, dendrimer-like star-branched polymers and block copolymers are promising specialty functional materials, with many possible applications to drug, vaccine, and gene encapsulated delivery devices, surface modifiers, functional nanosize spheres and micelles, surfactant, molecular recognition systems, microelectronic materials, etc.

1.2   Problem Statement and Research Motivation

Conducting polymers have become important materials because of their wide range of electronic applications, such as in secondary batteries and sensors; they provide conductive/electroactive carrier matrix platforms to effectively wire enzymes to underlying electrodes. Polypyrrole is a popular conducting polymer because it exhibits

6

good electrical conductivity and high air stability, and is potentially useful in diverse applications. However, the practical uses of PPy and other CPs are limited, due to their very fragile structural stability and insolubility, which give rise to processing difficulties. The synthesis of micronized conducting star copolymers, rather than linear macromolecular polymers, is one of the more effective ways of improving the properties of conducting polymers. In terms of preparative protocols, graft and block copolymerization could be useful, because the chemical linkage between the conjugated polymers can improve the chemical stability of these polymers.

1.3   Aim and Objectives

1.3.1   Aim

There is a rapidly growing need for organic materials with tailored properties. In the past decade, various hyperbranched polymers have been commercialized and are now being used in a number of high performance applications such as sensors, membranes and photo related applications. Dendrimers and dendronized conducting copolymers present polymeric materials with complex macromolecular architectures where the material properties can be tailored for specific advanced applications. However, conducting star copolymers have been synthesized for the first time. In order to tailor these materials for future applications such as super capacitance material, rechargeable batteries, sensor and biosensor applications, as well as optical power limiting materials, new and versatile synthetic tools must be developed. Moreover, the structure property relationship of these materials must be further understood. However, the challenge in the development of electronic smart materials (conducting star copolymers) for the availability of suitable

7

support material by attaching or incorporating the core and shall polymer chains to make copolymers. In electrochemistry this will allow the flow of electrons from the solution to the transducer. This support material is often a conducting polymer, copolymer, or a conducting composite.

In this study, dendrimers were used as platforms to prepare novel conducting star copolymers materials. In particular, the aim of this study was to develop electronic smart materials having a PPI dendrimer core with conducting PPy chains extending from the core. To achieve this, a set of key research questions categorized as a series of objectives is outlined.

1.3.2   Objectives

The following were the specific research objectives:

(i)   Prepare functionalized dendrimers (G1-G4) with Py, to afford PPI-2Py.

(ii)   Chemically and electrochemically copolymerize PPI-2Py with PPy monomer to prepare PPI-co-PPy star copolymers.

(iii)   Characterize the above star copolymers using analytical techniques such as Fourier transform infrared spectroscopy (FTIR), thermogravimetric analysis (TGA), X-ray diffraction spectrometry (XRD), and scanning electron microscopy (SEM).

(iv)   Carry out electrochemical characterization and impedance modelling of the star copolymers in solution, and as electrode modifiers.

(v)   Determine the conductivity of the star copolymers by means of Hall effect measurements.

1.4   Layout of the Document

This document is divided into the following six chapters:

•Chapter 1 presents a general introduction, motivation for the study, the aims and objectives.

•Chapter 2 presents a literature review of the field of study, with focus on conducting polymers and dendrimers.

•Chapter 3 describes the materials and methods used, for synthesis and characterization. Experimental procedures for the chemical and electrochemical syntheses of conducting star copolymer are described. The theory related to selected analytical techniques that were used is included

•Chapter 4 presents the results of the characterization of the products obtained after the chemical and electrochemical syntheses of the conducting star copolymer.

•Chapter 5 presents the results of the electrochemical characterization and impedance modelling of the second generation poly(propylene imine)-co-polypyrrole (G2PPI-co-PPy) star copolymer in solution, and as electrode modifiers.

•Chapter 6 presents conclusions and recommendations for future work.
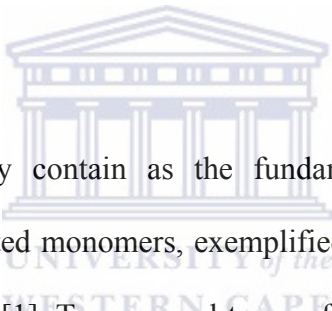
CHAPTER 2

Literature Review

2.1   Introduction

This chapter is an elaborated follow up of Chapter 1. The main focus of this review is to explore the themes of the research: conducting polymers and dendrimers. The scope of this review can be summarized as follows: conducting star copolymers, synthesis and applications of PPI dendrimer copolymers.

2.2   Conducting Polymers

Conducting polymers typically contain as the fundamental structural unit a linear backbone of repeating conjugated monomers, exemplified by polyacetylene, polypyrrole, polyaniline, and polythiophene [1]. Two general types of conducting polymers exist. One group is a composite material that uses a polymer to hold together conducting filler such as metal flakes or carbon black. The second group consists of a set of polymers whose backbone intrinsically propagates charge, making the polymer itself conducting [61]. Conductivity values for such polymers can vary from 10^{-10} to 10^6 S cm^{-1}, covering the range associated with semiconductors and conducting filled composites, at the lower end, to metals at the higher end. Polymers with essential electrical conductivity or semiconductivity are of interest as lightweight replacements for inorganic metals and semiconductors. In addition, conducting polymers have the prospect to replace metal coatings and may be applied by more economical non-vacuum processes, such as from

solution or from the melt [62]. Conducting polymers such as PPy, PT, PA and PANI have experienced much development over the past 25 years. These and other conducting polymers such as polythiophene have been used in a variety of applications ranging from sensors to capacitors to light-emitting diodes and batteries [63-65]. Organic conducting and semiconducting polymers may be synthetically tailored to optimize desirable properties such as melting point, melt viscosity, solubility, electrical and thermal conductivity. In general, conductive/semiconducting polymers consist of a backbone of repeating monomer units with extended pi-electron delocalization. Figure 2.1 shows examples of polymer backbones that are popular for forming conducting or semiconducting polymers.
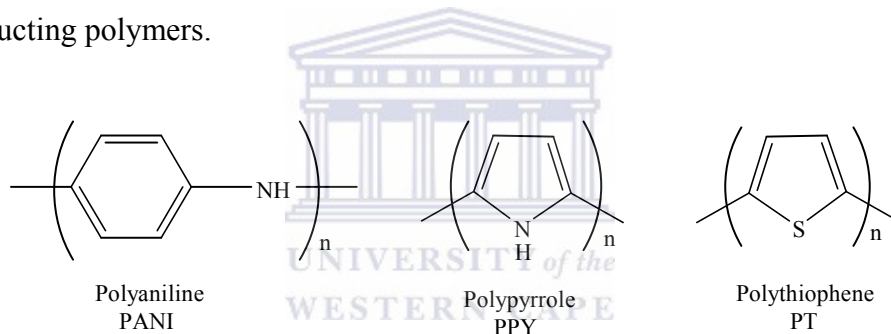
Figure 2.1: Standard conducting polymers.

Electrically conducting properties are frequently observed not only in polymers with hundreds or thousands of repeating units, but also in oligomers with 4 to 10 repeating units. Therefore, the conducting or semiconducting properties of a conducting polymer are enhanced by long-range ordering of the polymer in the solid state reference. Conducting polymer composites, resulting from the blending of an insulating polymer matrix with electrical conducting fillers (carbon black, carbon fibres, metal particles), show many interesting features due to their electrical resistivity variation with thermal solicitations [3-

11

6]. Recent studies have showed that conducting polymers namely, PPy, PANI and PEDOT, all have good biocompatibility [7-8, 66], and have been proven to be promising alternatives for developing new biodegradable conduits used for restoring the function of injured peripheral nerves or the regeneration of a nerve gap by using electrical stimulation in situ [9].

2.2.1 Synthesis of Conducting Polymers

Conducting polymers are either synthesized chemically or electrochemically. Both methods have advantages and disadvantages, as summarized in Table 2.1 [1].

Table 2.1: Comparison of chemical and electrochemical polymerization of CPs

Polymerization approach	Advantages	Disadvantages
Chemical polymerization	-Large-scale production possible -Post-covalent modification of bulk CP possible -More options to modify CP backbone covalently	-Cannot make thin films -Synthesis more complicated
Electrochemical polymerization	-Thin film synthesis possible -Ease of synthesis -Entrapment of molecules in CPs -Doping is simultaneous	-Difficult to remove film from electrode surface -Post-covalent modification of bulk CP is difficult

Chemical synthesis includes unusual methods of either condensation polymerization (i.e.,

step growth polymerization) or addition polymerization (i.e., chain growth polymerization). Condensation polymerization proceeds via the loss of small molecules, such as hydrochloric acid or water. With chemical synthesis of polymers, it is possible to synthesize CPs that is currently not possible with electrochemical synthesis. Electrochemical synthesis is a common alternative for making CPs, particularly because this synthetic procedure is relatively straightforward [1, 67]. This method consists of dissolving monomer into a solvent/electrolyte medium followed by the electrodeposition of a polymer film onto an electrode surface by using pulse, galvanostatic, potentiostatic or sweeping techniques [68]. All CPs can be synthesized chemically, but electrochemical synthesis is limited. The standard CPs (e.g., PPy, PT, PANI and PEDOT) can be polymerized both chemically and electrochemically.

2.2.2 Different Conducting Polymers

For conducting polymers to be used in applications, it needs to have excellent electronic and mechanical properties, solution or melt processability as well as high environmental stability. A list of conducting polymers widely used today is shown in Figure 2.2 and includes polyacetylene, polythiophene, poly(3-alkyl-thiophene), polypyrrole, polyisothiophene, polyethylene dioxythiophene, polyparaphenylene vinylene and polyaniline [69].
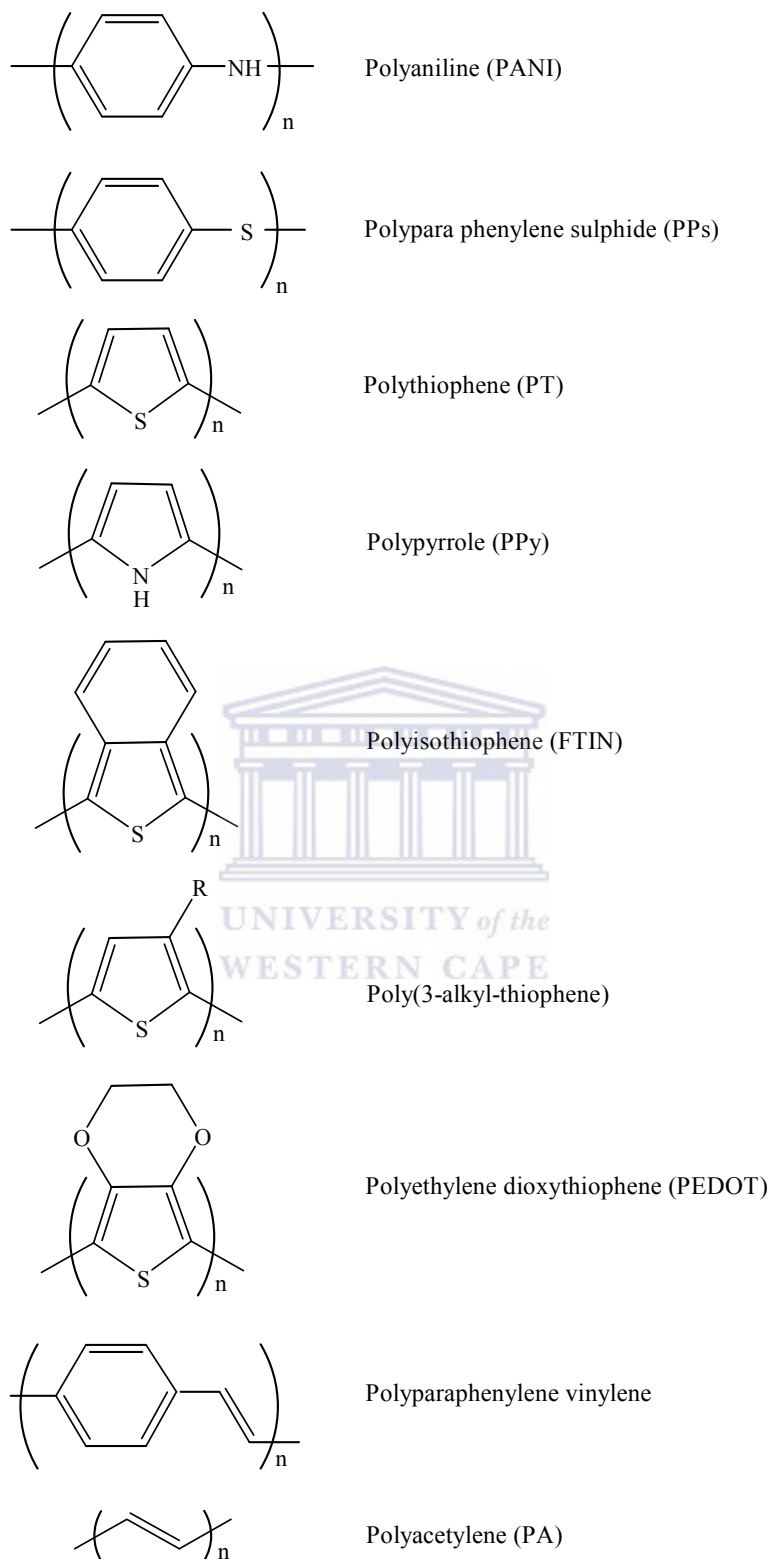
Figure 2.2: Structures of a few conducting polymers [70].

Polyaniline (PANI)

Polypara phenylene sulphide (PPs)

Polythiophene (PT)

Polypyrrole (PPy)

Polyisothiophene (FTIN)

Poly(3-alkyl-thiophene)

Polyethylene dioxythiophene (PEDOT)

Polyparaphenylene vinylene

Polyacetylene (PA)

A change in emphasis in the area of materials science and chemistry has opened new approaches to the areas of analytical sensing, which influences the design of sensors, particularly those that use electrochemical or spectroscopic transduction methods. The application of CPs has been widespread, to include the areas of sensors, actuator components in microsurgical tools, controlled drug delivery systems, corrective implantable aids, life-like prosthetic limbs, actuators and artificial muscles. Since the early 1990s, CPs have been extensively reported to function as thin films for batteries, sensors, ion-selective electrodes and solid-state devices [70-71]. One conducting polymer that has received great attention is PPy, due to its wide range of technological applications in several areas. It has been widely studied, and characterized by thermal analysis and electrochemical techniques, including CV and EIS.

2.2.3   Applications of Conducting Polymers

Conducting polymers have electrical and optical properties similar to those of metals and inorganic semiconductors, but also exhibit the attractive properties associated with conventional polymers, such as ease of synthesis and processing [10]. This unique combination of properties has given these polymers a wide range of applications in the microelectronics industry. Specific industrial application of conducting polymers are charted in Figure 2.3

Led Photocopiers

Transducers

Optical Storage

Photoconducting

Plastic Batteries

Piezoelectric

Super Capacitor
Connectors

Metal

Solid State
Photochemical
Reactions

Sensor

Conducting Composites

Solid
State

Super Conductors

Conducting Polymers

Josephson Juction
Computer Logic
High Field Magnet
Generators

Non-Linear
Optical
Phenomena

Electrochromic

Ferromagnetism

Conductive
Surface
EMI/ESD

Frequency Doubler

Display Devices

Magnetic
Recording

Figure 2.3: Applications of conducting polymers [10].

2.3 Conjugated Polymers

Conjugated polymers are organic macromolecules which consist at least of one backbone chain of alternating double- and single-bonds; they combine the electrical properties of semiconductors with the mechanical properties of plastics. Applications of conjugated polymers in organic electronic devices such as light-emitting diodes and solar cells depend critically on the nature of electronic energy transport in these materials

2.3.1 Electrochemistry

When an electroactive polymer film is adsorbed onto a working electrode and immersed

16

into an electrolyte solution it can be either oxidized, reduced, or both. Cyclic voltammetry provides a convenient method for the analysis of an electroactive polymer because the observed redox processes can vary as a function of the polymer's fundamental electronic structure, morphology, solvent interactions, and electrolyte interactions [72].

2.3.2 Electron Classification

Electrons are essential for conductivity. Electrons are classified into one of four categories in materials. Core electrons are tightly bound to the nucleus and remain on the element's nucleus, with few exceptions. The electrons are found between two bonded nuclei and are responsible for keeping the structure together. The n electrons are thought of with heteroatoms (i.e., O, N, S, P, etc) and have an effect on the reactivity of a bond. The π electrons are involved in binding but form weaker and less localized bonds than the internuclear bonds of an electron. The π electrons are thought to be moving in the field created by the nuclei and the other electrons, and they require the least amount of energy to jump to the next energy state (see Figure 2.4).
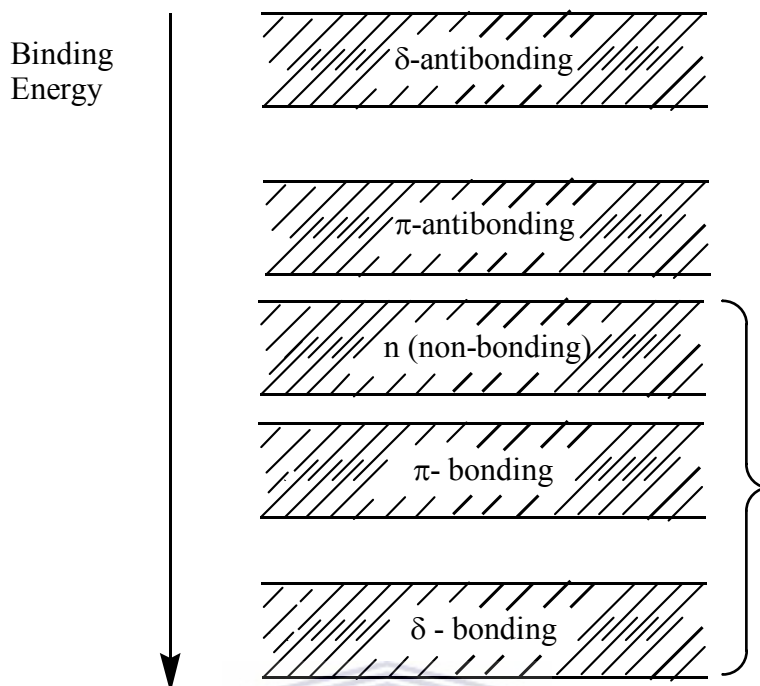
Binding
Energy

Figure 2.4: Binding energy levels of σ, π, and n electron states for organic molecules

[73].
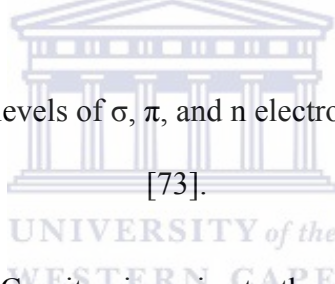
The double bond between the C units gives rise to the conjugated bond. The π electron serves as the one electron per atom that makes conduction possible. Polymers which contain π electrons are known as conjugated polymers.

2.4 Band Theory

Band theory is widely used to understand the electrical conduction. When two identical atoms each having a half-filled orbital are brought together the two orbitals interact to produce two new orbitals, one of lower energy and one of higher energy. The magnitude of this energy difference is determined by the extent of orbital overlap. The two electrons go into the lower-energy orbital. The (now-filled) lower energy orbital is a bonding orbital

and the higher-energy (empty) orbital is an antibonding orbital. There is energy spacing between the highest of the low-energy orbitals (HOMOs) and the lowest of the high-energy orbitals (LUMOs) and this is called the band gap (Eg). In other words, Eg is the energy difference between the valence and conduction bands. In band theory, an insulator has completely filled and completely empty energy bands with a large gap between its energy bands. A conducting material has a number of free electrons in an incomplete energy band (see Figure 2.5). At temperatures higher than 0 K, electrons can jump into the higher energy bands, creating the possibility of conduction. Depending on the size of the electron gap, the material can be an insulator or a semiconductor. In materials with electron gaps of approximately 1 eV or below, the number of electrons that are excited at room temperature becomes more significant, and they are thought of as semiconductors. In general the conductivities of semiconductors can range from 10^3 to 10^{-9} S cm^{-1}.
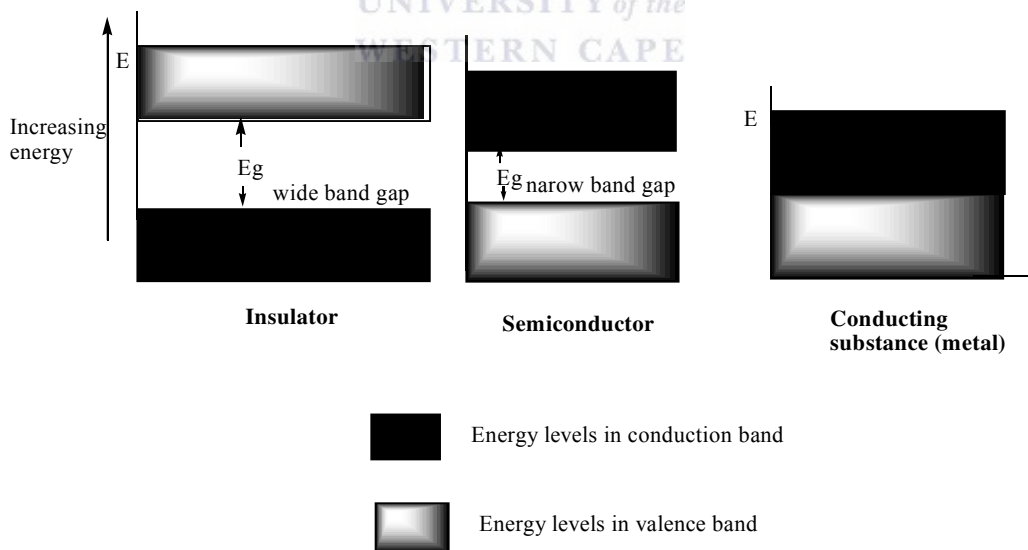
Figure 2.5: Energy gap representation of an insulator, semiconductor and metal [74].

In a metal there is no gap. This means that orbitals are freely available for conduction,

metals generally have conductivities along the lines of 10^6 S cm^{-1}, and insulators are at the other end of the spectrum with magnitudes around 10^{-22} S cm^{-1}. On the other hand, insulators have a very large Eg, and hence thermal excitation of carriers is not possible. Most semiconductors are inorganic, crystalline solids, the magnitude of the gap is such that electrons may be thermally excited across it, putting the electrons into the empty upper band, where they can conduct, and leaving holes in the lower band, which can also conduct [75]. In the case of highly conjugated conducting polymers it can display semiconductor properties without the inorganic, crystalline structure. The difference between energy levels within these two sets of orbitals is so small that the bands may be regarded as continuous and the electron can take any energy within. Doping with an anion or cation can be used to increase the conductivity of these polymers (see Figure 2.6) [74].
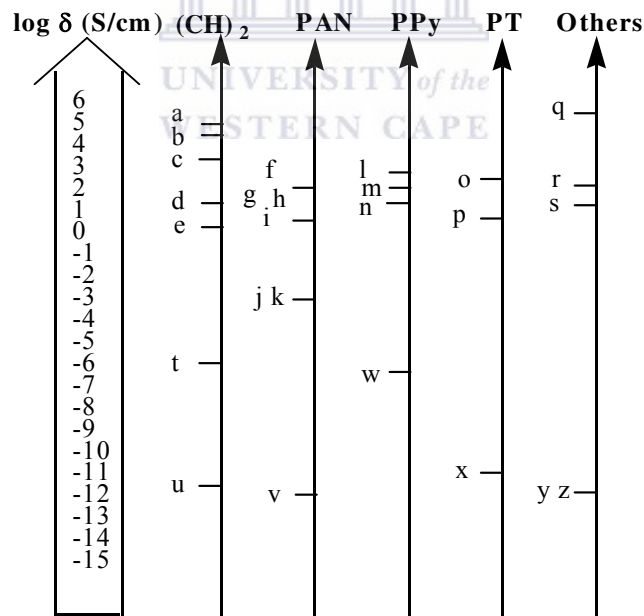
Figure 2.6: The conductivity of various conducting polymers at 24 °C. (a-e) forms of [CH(I$_3$)]x, (f-k) forms of PAN, (l, m) PPy doped with PF$_6$, (n) PPy (TSO), (o, p) forms of PT, (q) PPV (H$_2$SO$_4$), (r) PPP (AsF$_5$), (s) Kr-implanted poly(phenylenebenzobisoazole),

(t-z) undoped versions of the respective polymers [74].

Doping for inorganic and crystalline solids is slightly different to doping in conducting polymers. For inorganic semiconductors, the dopant is at the level of parts per million whereas for conducting polymers, the dopant can form up to 50% of the polymer weight.

2.4.1 Band Theory for Conducting Polymers

Rigid band models like those used in semiconductor physics are not completely accurate for conducting polymer. At first it appears that conducting polymers have similar properties to inorganic crystalline semiconductors, but the movement of electrons varies between these two types of materials. In conducting polymers, oxidizing or reducing the material does not create free electrons or holes at the conduction bands.

This is because structural deformation occurs along the polymer backbone, where the transfer of charge occurs, and creating areas more likely to transmit charge. Conducting polymers all have it-conjugated systems, with alternating single and double bonds along the polymer backbone. They are unusual because they can conduct without having partially empty or filled bands. For conducting polymers, when an electron is excited from the valence band, a polaron is created. Unlike traditional band theory, the hole that the electron leaves is not completely empty. Instead, partial delocalization takes place and results in a structural deformity from several of the surrounding monomer units to balance the energy level created by the electron, thus polarizing the nearby material, which transforms into a new equilibrium condition hence the term polaron. In PPy, bipolarons form and the change affects approximately four monomer units [76].

In the doping process, defects are generated that form radical cations or anions, which are also polarons. A polaron consists of two defects: a charged defect accompanied by a neutral defect, also known as an ion and a radical. Within this framework, two types of conducting polymers exist: those with a degenerate ground state (trans-polyacetylene) and those with a non-degenerate ground state (PPy). For the polymers with degenerate ground states, the initial charge forms a polaron, and a subsequent charge will create another polaron. The two polarons, however, degenerate to form two charge solitons. For non-degenerate polymers, however, solitons are not formed with two charges, but pairs of defects are created called bipolarons. With the degenerate polymers the energy level for the distorted state is equivalent to that of the original structure. For the non-degenerate materials the energy level of the distorted state is not equivalent which causes the bipolaron to form with two charges to maintain balance [77]. For non-degenerate systems (PPy, polythiophene, etc.) at low doping levels, charges are stored as polarons and bipolarons. The polaron is the radical cation or anion accompanied by the lattice distortion resulting from the charge (Figure 2.7).
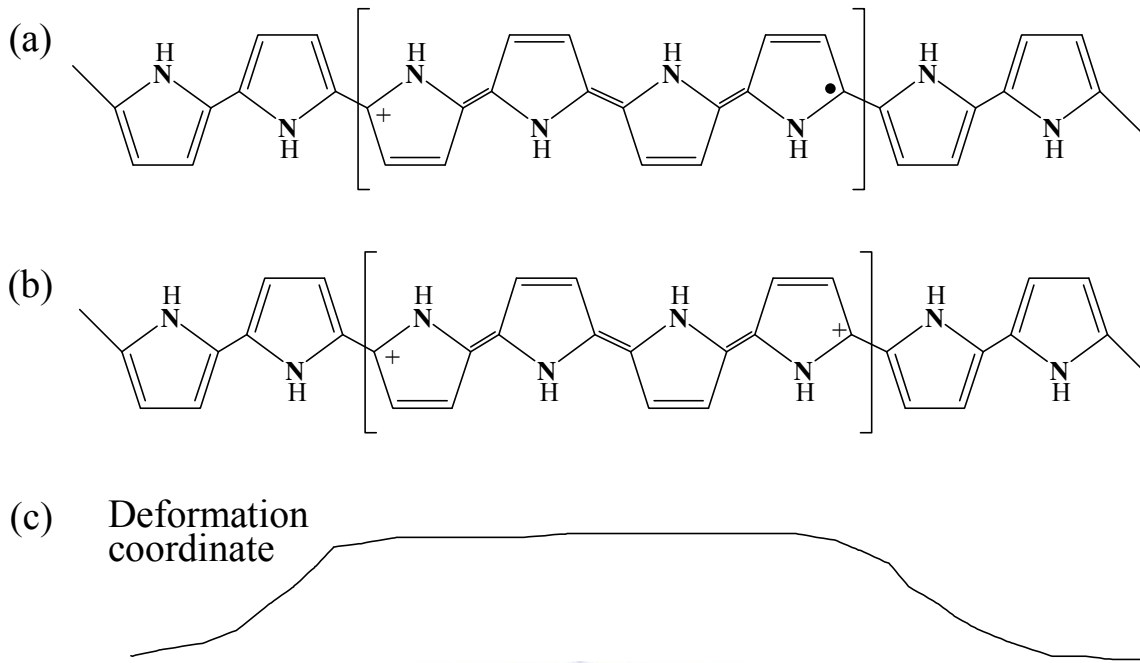
Figure 2.7: Schematic representations: (a) a polaron, and (b) a bipolaron on a PPy chain. The lower schematic (c) represents the deformation of the polymer lattice created from the charge defects [78-79].

Polypyrrole is a highly disordered polymer with as many as one defect for every three rings [79]. These charges defects create an electrically conductive partially filled band. Bipolarons are formed when two polarons form on the same polymer chain. Another method of transport occurs when the polarons and bipolarons hop to nearby chains to carry the electric current. When PPy is oxidized and becomes more conducting, it is a polycation with many of these delocalized positive charges on its backbone which are countered by dopant anions.

The function of polarons and bipolarons can also be considered with Eg analysis (Figure 2.8). When a polaron is formed it forms two energy states equidistant from the centre of the gap. An electron or hole polaron can be formed with the electron polaron having the

lower energy state occupied by two electrons with opposite spins.
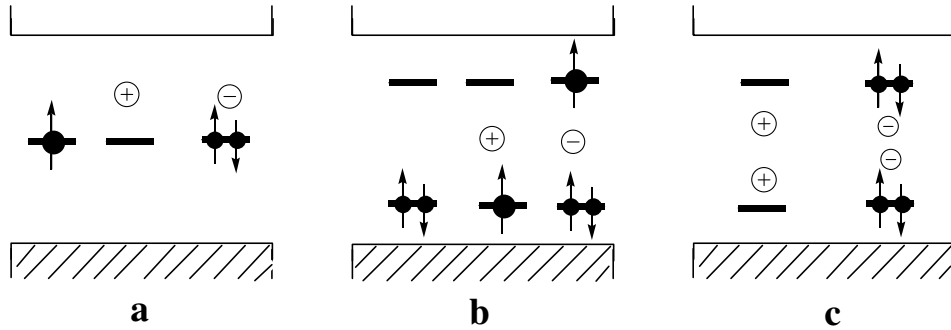
Figure 2.8: Energy levels: (a) soliton (neutral, positively, negatively charged states), (b) polaron (neutral, positively, negatively charged states), and (c) bipolaron (positively and negatively charged states) [77].

In bipolaron formation, both energy states are occupied by two electrons with opposite spin; or, if it is a hole formation, both energy states are empty. In the case of a soliton, only one energy state is formed in the centre of the gap [77]. To maintain conductivity, valence electrons must move into conduction band through the gain of energy. The product of the carrier mobility (μ), the charge (q), and the concentration of carrier (n) is the electrical conductivity (σ).

$$\sigma = \mu * q * n \tag{2.1}$$

For conducting transport, the polarons and bipolarons must be able to overcome the energy barrier and hop from chain to chain. This interchain hopping is the second component of charge transport in conducting polymers.

2.4.2   The Origin of Band Structure

One of the most important concepts in understanding the properties of conducting

polymers is the origin of band structure. As shown in Figure 2.9 for the PPy system [80], molecular orbital perturbation effects lead to energy states that are very close in energy, to the point such that excitations can occur through thermal population.
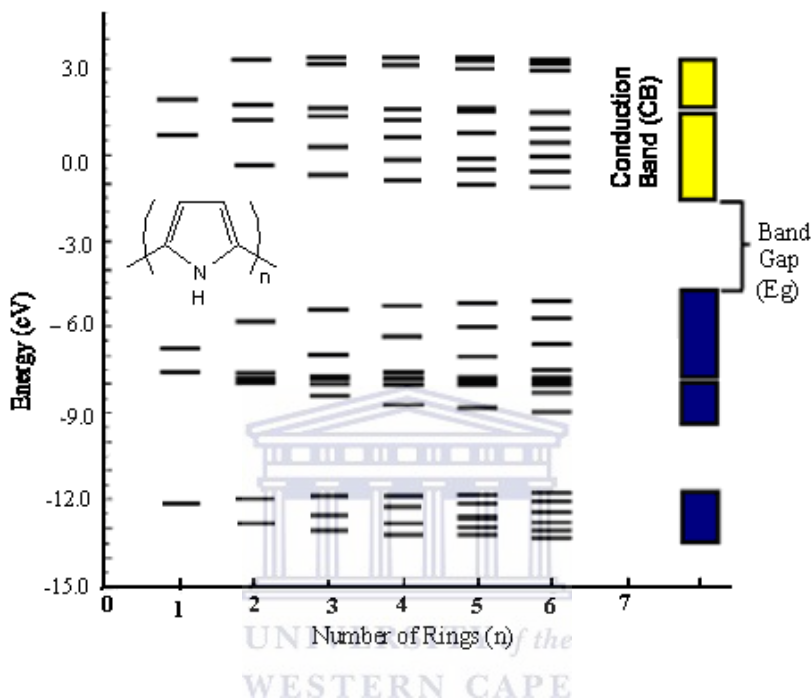
Figure 2.9: The origin of band structure in PPy. Figure adapted with permission from Salzner *et al.* [80].

As the length of the polymer chain increases progressively from 1 to infinity, the occupied valence orbitals form continuous bands called the valence bands, VB, and the empty orbitals coalesce into continuous bands called the conduction bands, CB. The polymer HOMO is thus defined as the highest occupied state in the valence band, and the LUMO is defined as the lowest unoccupied state in the conduction band. The difference in energy between the HOMO and the LUMO is defined as the band gap. The band gap has an enormous effect on the properties of the conducting polymer, with the greatest effect on

the optical absorption spectrum. The band gap represents the lowest energy transition for a photoexcitation, and thus the onset of the polymer absorbance spectrum will be equal to or greater than the band gap [81].

2.5   Conductivity

Electrical conductivity in PPy involves movement of positively charged carriers or electrons along polymer chains and hopping of these carriers between chains. It is generally believed that the intra-chain hopping resistance is much greater than the interchain transport resistance. Conductivity of PPy can range from those of insulators with almost no conductivity ($10^{-5}\Omega^{-1}cm^{-1}$) to 100 $\Omega^{-1}cm^{-1}$ [79]. Doping ions help to decrease the band gap between the energy levels (Figure 2.10). Polypyrrole is conducting because of the ability for electrons to hop along the polymer chains and across interchains due to the x-conjugating bonds. By using smaller counter anions with coplanarity with the polymer chains, the conductivity can be increased [82]. Conductivity within conducting electroactive polymers (CEPs) is a complex issue. A polymer that can exhibit conductivity across a range of some 15 orders of magnitude most likely utilizes different mechanisms under different conditions. In addition to the electronic conductivity exhibited by CEPs, they possess ionic conductivity due to the solvent/electrolyte incorporated during synthesis [83].

Dopants such as hydrogen peroxide, polyethylene oxide, dodecylbenzenesulfonate, and salts containing transition metal ions have all been used [84-86]. Studies have found that longer deposition times, lower plating potentials and temperatures, and higher concentrations of monomer and electrolyte are favourable for conductivity and stability

[87]. Other modifications such as increasing the roughness of the plating surface has also been shown to increase conductivity [82]. The addition of water into the electrodeposition solution also produces a more conducting polymer, possibly because water serves as a better proton scavenger than PPy in the solution [88].
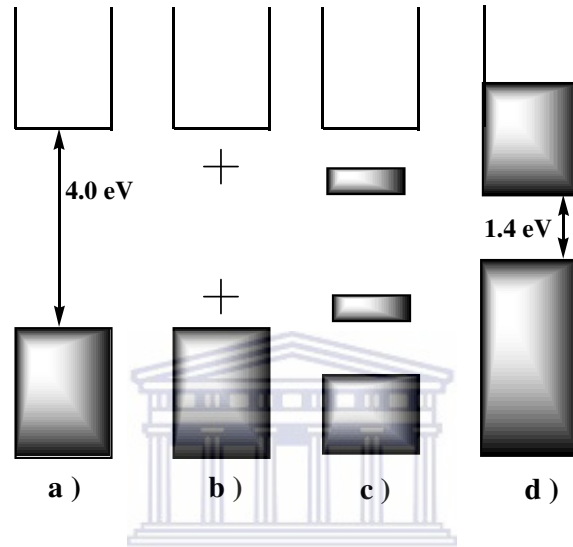
Figure 2.10: Band structure representation of PPy and how it is modified with doping: (a) no dopant, (b) intermediate doping level (bipolarons are non-interacting at this point), (c) 33% dopant per monomer, (d) 100% dopant per monomer. The material changes from an insulator with a band gap of 4.0 eV to a semiconductor with full doping at l.4 eV [89].

2.5.1 Thermal Conductivity

Thermal conductivity is the ability of the material to conduct heat. It depends on the mobility and vibration of the molecules, and also the specific heat of the substance. Lunn *et al.* studied the thermal conductivity of polypyrrole in the temperature range 280-335K [90]. They showed that the relationship between thermal and electrical conductivity for polypyrrole was more complicated than a simple Wiedemann–Franz proportionality.

2.5.2   The Hopping Process

Conduction via localized electrons implies discrete jumps across an energy barrier from one site to the next. In other words, if two molecules are separated by a potential barrier, a carrier on one side can move to the other side either by tunneling through the barrier or by moving over the barrier via an activated state. The latter process is called hopping. Carrier mobility is the main reason of electrical transport in conducting polymers. Mobility of the charge carriers can be restricted as the degree of overlapping decreases in molecular or atomic levels. As the electronic states become increasingly localized, transport of the particle occurs through hopping process. The relative importance of these two mechanisms depends on the shape of the barrier and on the availability of thermal energy. This thermally activated type of mobility will increase with temperature, of course, in contrast to that in band conduction. It is apparent that we can learn much about the conduction process by determination of carrier mobility, e.g., its temperature dependence provides a good criterion by which we can distinguish band and hopping types of mechanisms. Although polymers are amorphous materials, a short-range order prevails in most of these materials. Hence the theory that is used to explain the electronic band structure in crystalline phase can also be applied in amorphous polymers. If the spatial fluctuations in the interatomic distances are large, the correspondingly large and random fluctuations in the height or depth of the potential wells may lead to the localization of states below a certain critical and well-defined energy. When the carrier mobility is low and the mean free path is comparable with interatomic distance, the conduction can be expected to take place by a hopping process in the localized states.

In order to obtain hopping conduction, it is necessary to have an insulating or semiconducting material exhibiting a few intrinsic thermal free carriers at least over a limited energy region, a large density of sites through which charge transfer can take place. There are mainly three types of transport for the carrier mobility: single chain or intermolecular transport, interchain transport and interparticle contact [91]. The intra-chain movement depends on the effective conjugation of the polymer, while the interchain jumping is determined by the stacking of the polymer molecules. In a hopping mechanism, only those carriers with an energy kT, where k is the Boltzman constant and T is the temperature, below the Fermi level have a significant probability of hopping. Mott [92] showed that for strongly localized states, the conductivity at low temperatures must follow a relationship of the ega. 2.2

$$\sigma \approx \exp\left(\frac{-B}{T^{1/4}}\right) \tag{2.2}$$

where: σ is the conductivity and B is a constant related to the hopping mechanism. At high temperatures, deviations from $T^{1/4}$ occur, which can be understood in terms of interchain hopping [92]. A carrier trapped in a chain, after detrapping, may drift along the same chain or may hop into an adjacent chain. In amorphous polymers, the conduction occurs due to two distinct processes: a temperature-dependent trap hopping and a comparatively less dependent interchain hopping.

2.5.2   Solitons, Polarons and Bipolarons

Polymer doping leads to the formation of conjugational defects, solitons, polarons and

bipolarons in the polymer chain. The presence of localized electronic states of energies less than the band-gap arising from changes in local bond order, including the formation of solitons, polarons and bipolarons, has led to the possibility of new types of charge conduction [93]. The ground state structures of such polymers are two-fold degenerate; the charged cations are not bound to each other by a higher energy bonding configuration and can freely separate along the chain. The effect of this is that the charged defects are independent of one another and can form domain walls that separate two phases of opposite orientation and identical energy. These are called solitons; solitons are subdivided into three categories: neutral soliton, positive soliton and negative soliton. An interesting observation at this point is that charged solitons have no spin; however, neutral solitons have spin but no charge. A positively charged soliton occurs when an electron is removed from the localised state of a neutral soliton by oxidation. A negatively charged soliton is produced when an electron is inserted by reduction (Figure 2.11). Solitons produced in polyacetylene are believed to be delocalized over about 12 CH units, with the maximum charge density next to the dopant counterion. The bonds closer to the defect show less bond alternation than the bonds away from the centre. Soliton formation results in the creation of new localized electronic states that appear in the middle of the energy gap. At high doping levels, the charged solitons interact with each other to form a soliton band, which can eventually merge with the band edges to create true metallic conductivity [94-95]. This is illustrated in Figure 2.11.
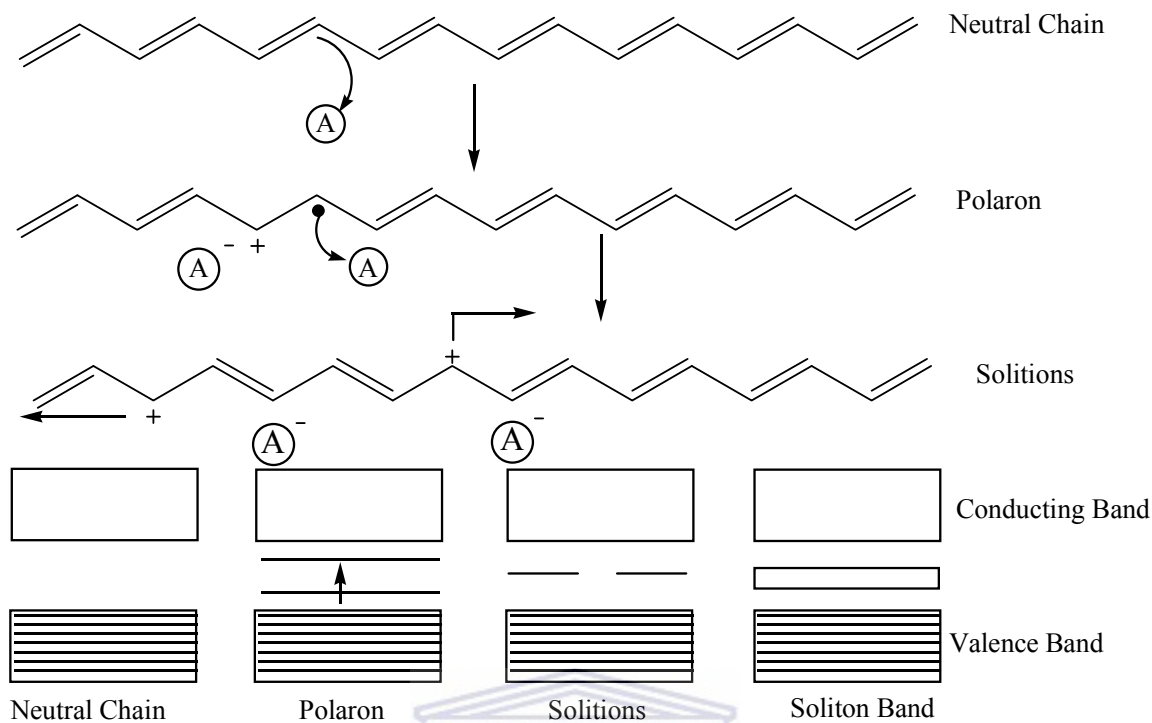
Figure 2.11: Soliton structures of polyacetylene [95].

Polarons are obtained as a combination of a neutral and a charged soliton on the same polymer chain. Further oxidation causes more and more polarons to form and eventually the unpaired electron of the polaron is removed, or two lose polarons can combine to form dications or bipolarons (Figure 2.12) [96-97]. The oxidative doping of PPy proceeds in the following way. An electron is removed from the p-system of the backbone producing free radical and a spinless positive charge. The radical and cation are coupled to each other via local resonance of the charge and the radical. In this case, a sequence of quinoid-like rings is used. The distortion produced by this is of higher energy than the remaining portion of the chain. The creation and separation of these defects costs a considerable amount of energy. This limits the number of quinoid-like rings that can link these two bound species together. The polaron state of the PPy it is believed that the lattice distortion extends over

four Py rings. This could be either a radical cation or radical anion. This creates a new localized electronic state in the gap, with the lower energy states being occupied by a single unpaired electron. The polaron state of polypyrrole is symmetrically located about 0.5 eV from the band edges [98-99]. Bipolarons and polarons are self-localized particle-like defects associated with characteristic distortions of the polymer backbone and with quantum states deep in the energy gap due to strong electron–lattice coupling. A polaron has a spin ±1/2 and an electric charge ±e, whereas a bipolaron is spin less with a charge ±2e. A consistent description of the dynamics of the mechanism of creation, stability and transition of polarons and bipolarons constitutes a critical problem in the understanding of these materials. The polaron-bipolaron transition problem was explicitly addressed by Cik *et al*. in poly(3-dodecyl thiophene) in connection with temperature changes [100]. They found that when the sample was heated and subsequently cooled there was an amplification of the diamagnetic inter- and intra-chain bipolarons. Kaufman *et al*. studied PPy [101] by optical-absorption spectroscopy and ESR and reported that the metastable states possess spin, while the stable states do not. Their data revealed a slow transition, consistent with the diffusion rate limited by the mobility of the dopant. Two mechanisms have been put forward to explain the transition from polaron to bipolaron states: Polarons recombination into bipolaron [100-102], where the bipolaron is generated when polarons with the same electric charge meet each other; and single-polaron to bipolaron transition [103-105], where the polaron structure is transformed by the addition of one extra charge.

The neutral polymer has full valance and empty conduction bands with a separated band gap. Formation of polaron and bipolaron generates new energy levels located at midgap. Upon further oxidation the free radical of the polaron is removed, creating a new spinless

32

defect called a bipolaron. This is of lower energy than the creation of two distinct polarons. At higher doping levels it becomes possible that two polarons combine to form a bipolaron. Thus at higher doping levels the polarons are replaced with bipolarons. The bipolarons are located symmetrically with a band gap of 0.75 eV for PPy. This eventually, with continued doping, forms into a continuous bipolaron bands [98]. Their band gap also increases as newly formed bipolarons are made at the expense of the band edges. For a very heavily dope polymer it is conceivable that the upper and the lower bipolaron bands will merge with the conduction and the valence bands respectively to produce partially filled bands and metallic like conductivity. This is shown in Figure 2.12. Conjugated polymers with a degenerate ground state have a slightly different mechanism. As with PPy, polarons and bipolarons are produced upon oxidation.
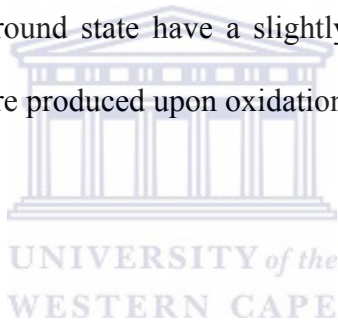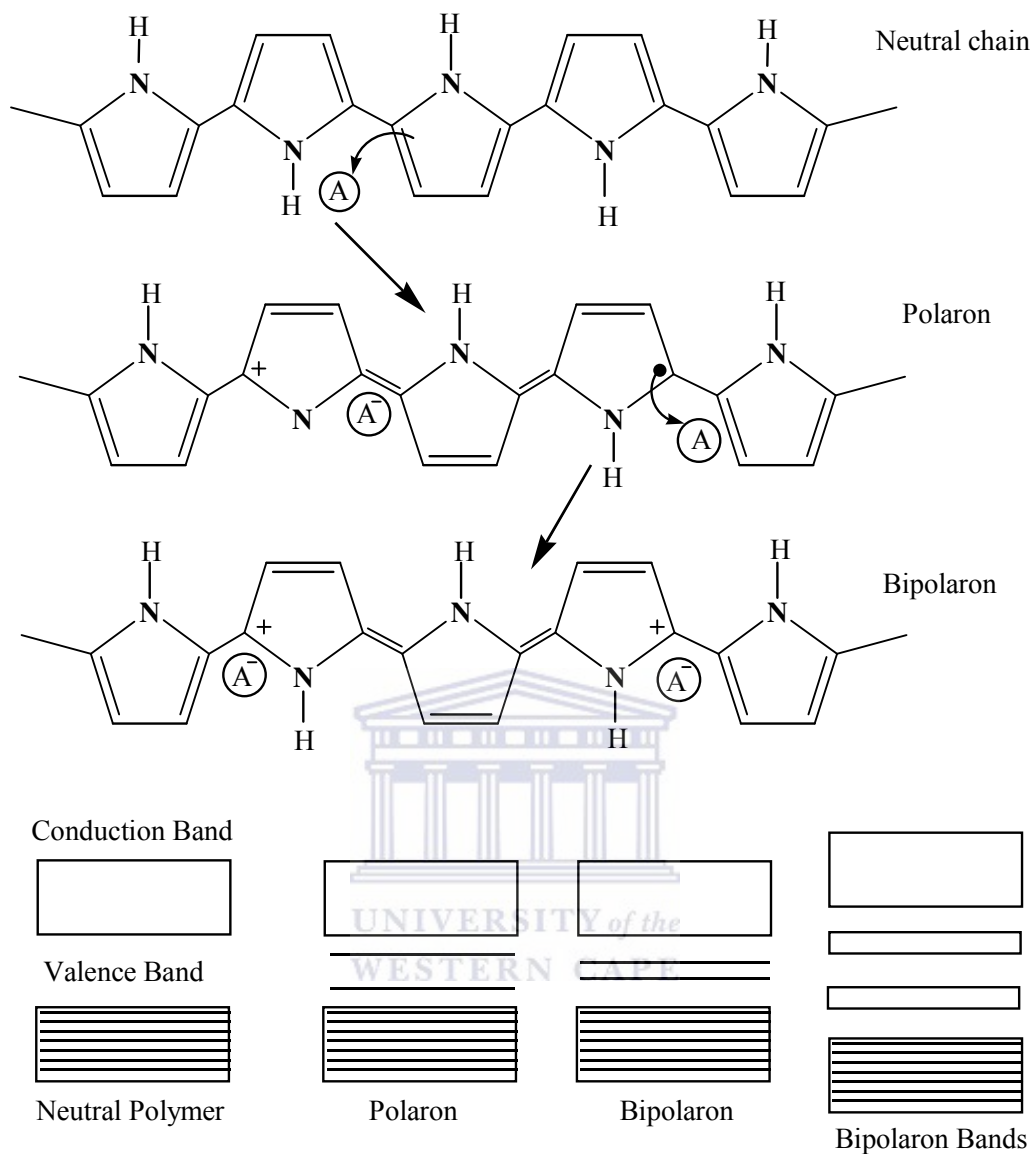
Figure 2.12: Formation of polaron and bipolaron in polypyrrole.

2.6 Polypyrrole

Polypyrrole exhibits good electrical conductivity and high air stability and is a potentially useful conducting polymer. PPy, one of the most studied conducting polymers and has been in wide range of technological applications in several areas such as secondary batteries [11, 106-109], electrochromic display devices [12, 110], light-emitting diodes

[13, 111], capacitors [112-113], sensors [114-117], membranes [118], and enzyme electrodes [119-121]. Electrical transport in polymeric materials [18, 122] has become an area of increasing research interest because these materials have great potential for solid-state devices. PPy was first synthesized in 1916 where it prepared by the oxidation of pyrrole to a powder known as "pyrrole black". In 1968 it was first electrochemically deposited [123]. In addition, PPy has been prepared by electropolymerization of Py onto a variety of substrates with promising results [124-128]. PPy (structure seen in Figure 2.13) is an electrodeposited polymer that can be doped with various agents to alter its physical, chemical and electrical properties [84, 129-130]. Additionally, the properties of PPy can be controlled by plating under various conditions [85, 131].
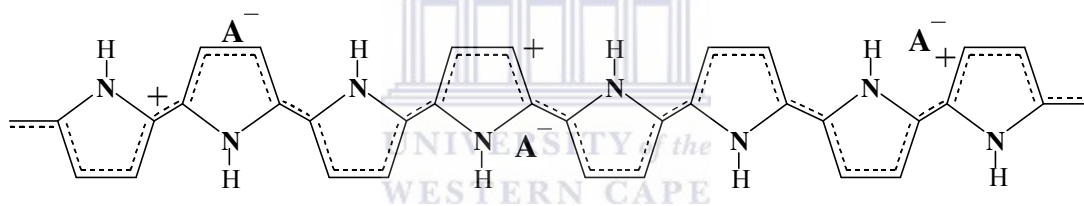
Figure 2.13: PPy with counter ions (A⁻) to balance charge [132].

As a result of its electroactivity, high electrical conductivity and stability it is frequently used in commercial applications such as sensors, batteries, molecular devices and membranes. One of the main advantages of PPy is its stability. Its conductivity decreases only 20% a year in an unprotected environment. It can also withstand temperatures of 100-200 °C, depending on dopant, and is stable in acids [78]. The ability to control the surface properties of PPy, such as wettability and charge density, creates the potential for modifying tissue interactions with the polymer [133]. The power to alter the properties of

PPy through its dopants also adds versatility not seen in other conducting polymers and makes it appealing for biosensor applications. However, PPy itself has rather poor properties in terms of electrochromic behaviour [134]. It is common that further enhancement by doping and sensitizing with various dyes is required for good optical properties [135-136]. Syntheses of conducting star, graft and block copolymers are one of the effective ways to improve the properties of conducting polymers. In order to make them as processable as conventional polymers, several approaches have been developed, one of which is to prepare graft and block copolymers with desired end groups like pyrrole or thiophene [137-140].

2.6.1 Chemical and Electrochemical Polymerization of Pyrrole

Polypyrrole can be obtained chemically or electrochemically. The electrochemical polymerization of Py has been extensively studied because it is easily obtained in the form of freestanding films and has good environmental stability and conductivity. Electrochemical polymerization is performed using a three-electrode configuration (working, counter, and reference electrodes) in a solution of the monomer (Py), appropriate solvent, and electrolyte (dopant) (Figure 2.14). Current is passed through the solution and electrodeposition occurs at the positively charged working electrode or anode. Monomers (Py) at the working electrode surface undergoes oxidation to form radical cations that react with other Py monomers or radical cations, forming insoluble polymer chains on the electrode surface (Figure 2.13). A number of important variables must be considered, including deposition time and temperature, solvent system (water content), electrolyte, electrode system, and deposition charge. Each of these has an effect

on film morphology (thickness and topography), mechanics, and conductivity, which are properties that have a direct impact on the utility of the material for any applications.
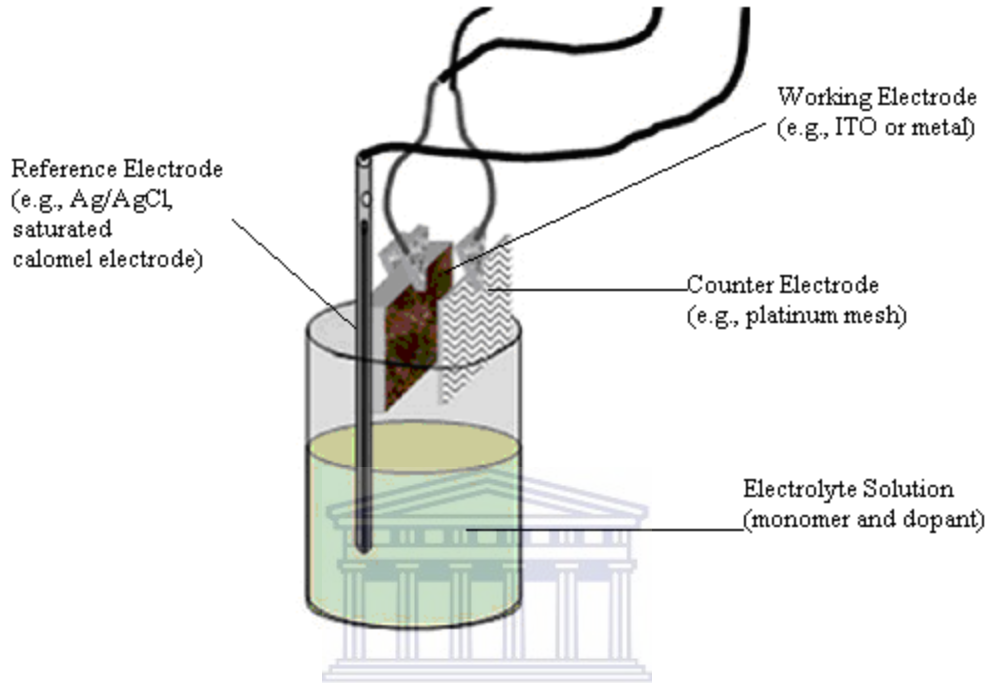
Figure 2.14: Three-electrode setup for electrochemical synthesis: reference electrode, working electrode, and counter electrode [141]**.**
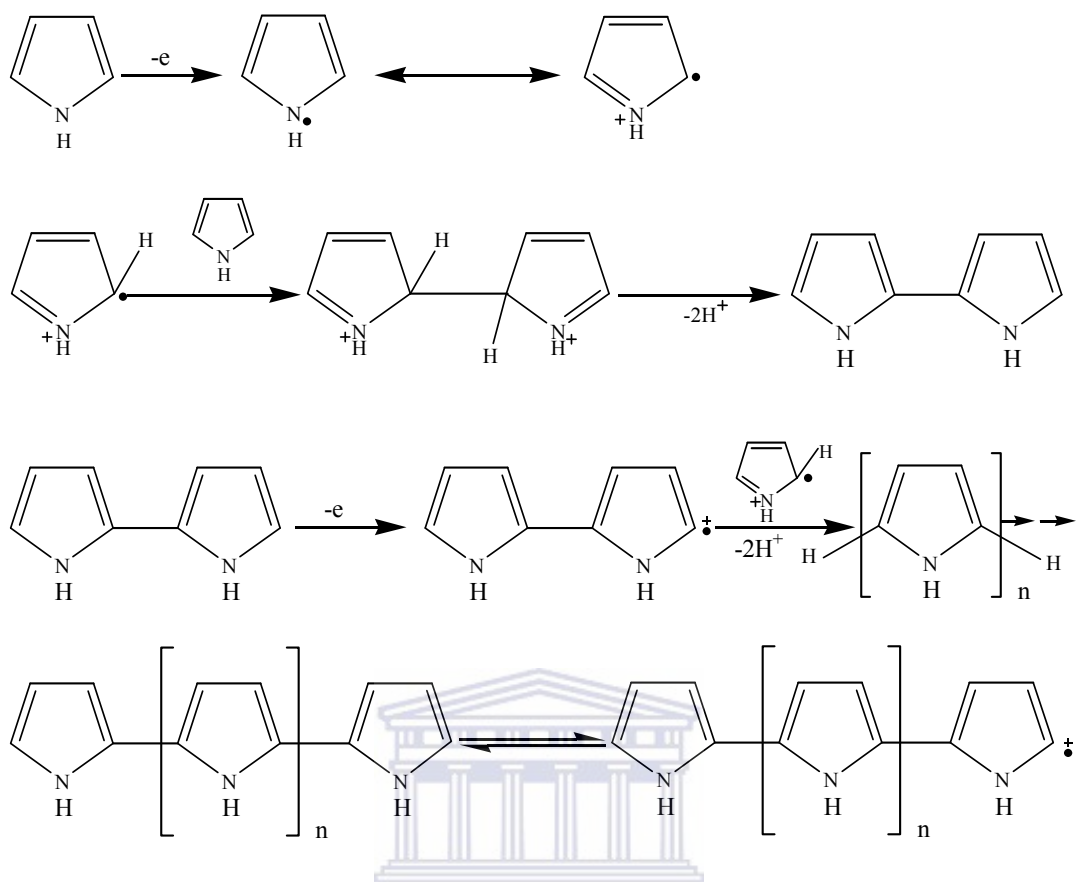
Scheme 2.1: Mechanism for polymerization heterocycles via electrochemical synthesis. This pathway is initiated by the oxidation of a monomer at the working electrode to give a cation species, which can react with a neutral monomer species or radical cation oligomeric species to generate the polymer. Adapted from [141]**.**

2.6.2 Polypyrrole Modification

Ease of modification through dopants has made PPy a popular material to fabricate. Apart from the dopants used, electrodeposition conditions and alteration of the chemical structure have resulted in various forms of PPy. The wide ranges of properties that can be controlled by altering aspects of PPy formation make the polymer an ideal material for many applications. Below are several fabrication factors that can affect the characteristics of PPy. The solvent in which the PPy is electrodeposited is important for chemical

properties. Conductivity and mechanical properties can be altered by using various solvents and altering the amount of water in the plating solution. Conductivity can also be changed just by modifying the percentage of water. Although the mechanism is not understood, since the chemical compositions are identical, it is believed to correspond with changes in the polymer unit chain length [142]. The presence of water vapour during electrodeposition decreases the conductivity of PPy by decreasing the hopping of electrons across the polymer [143]. Film formation is also proportional to the activity of hydrogen ions, anions and the monomer concentration. It has been found that agitation of the solution can decreases the plating rate because hydrogen ions on the surface might have a catalytic effect. One group suggests that the anion forms an intermediate species with the Py [144]. Another method for PPy modification is to functionalize the Py monomer by substituting a desired group in place of the hydrogen molecule. The addition of the new group can have a great influence on the properties of the polymer. For example, if the PPy is formed with N substitutions, the conductivity normally drops by 5 to 6 orders of magnitude. This is believed to be due to the fact that the substitution blocks PPy rings from residing within the same plane [145].

2.6.3   Electrical Conductivity of Polypyrrole

The electrical conductivity of PPy conducting polymers is one of the most important properties for analytical applications. PPy is a conducting polymer which has a nondegenerate conduction band in the ground and start the polaron and bipolarons are the dominant charge carriers in these polymeric conductors, the mechanism of conduction in PPy has not been yet conclusively established because of the persistent structural disorder

of the polymer [146]. The most widely accepted view of conductivity in these systems involves charge transport along the polymer chains, as well as hopping of carriers [147] (holes, bipolarons, etc.). Electrically conducting polymers are semiconductors with a filled valence band and an empty conduction band. These bands are separated by an energy gap. Doping of these polymers creates new bands in the energy gap, making it possible for the electrons to move to these new bands and increasing the conductivity of the materials [147]. The electrical conductivity of conducting polymers is achieved in the film of the conducting polymers by oxidation (p-doping) or reduction (n-doping), followed by the insertion of anionic or cationic species, respectively (see Scheme 2.1) [148].
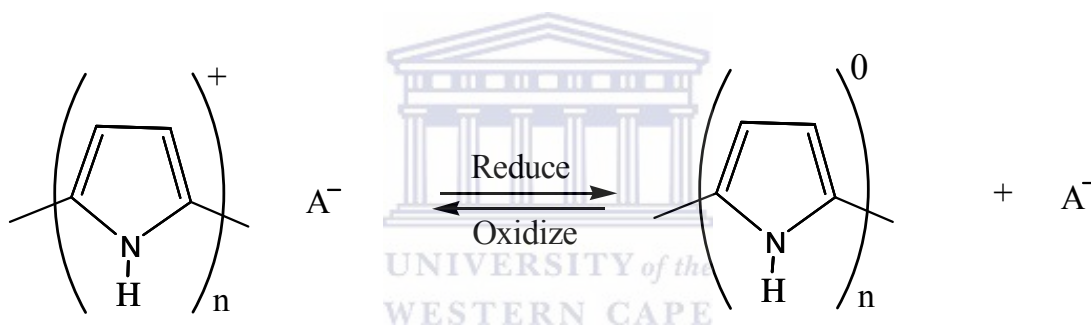
Scheme 2.2: Procedure of ion-exchange behaviour of a conducting polymer.

Due to the double bond alternation in the conjugated polymer backbone, the charged species formed upon doping are able to move along the carbon chain (delocalization), allowing electron transport and thus giving an electronically conducting material [149]. Thus, the hoping of electrons along and across the polymer chains with conjugating bonds gives PPy its electrical conductivity [150]. As a result, more positive PPy, more electron holes available, longer polymer chains and more coplanarity between interchains, are favoured for a higher conductivity performance [151]. The electrical conductivity of PPy

is the product of two important factors: the number of carriers (e$^-$ or holes) and charge carrier mobility. Higher mobilities will occur with more crystalline, better oriented, defect-free materials. Increasing the doping level will increase the density of charge carriers. The conductivity decreases with falling temperature just like that of semiconductors. In contrast, the conductivities of typical metals, like silver, increase with falling temperature. The electrical conductivity of the PPy films are strongly influenced by the preparation conditions, such as the nature/concentration of electrolyte or counterion [152], doping level [153], current density [147], synthesis temperature [154], and solvent [155].

The number of electrons involved in the PPypolymerization process for each monomer is approximately 2.25, one for each of the two α positions to form the polymer and another one for every four monomer units to form the doped polymer. Similarly; one anion per four monomer units is incorporated during doping to maintain charge neutrality [156]. In the undoped state (pristine), neutral PPy is generally non-conducting, having the aromatic and quinoid structures of which the latter posses a higher energy configuration. Generally, the redox mechanism of PPy is described by a one-electron transfer step: [157].

$$PPy \rightleftharpoons PPy^+ + e^-$$

where PPy is the neutral species and PPy$^+$ is the radical cationic species or polaron (one positive charge localized over three to four monomer units). The polaron can further be oxidized:

$$PPy^+ \rightleftharpoons PPy^{++} + e^-$$

PPy^{++} is the dicationic species or bipolaron (two positive charges localized over three to four monomer units). In the presence of dopant, where the dopant maintains electrical neutrality of the polymer during polymerization, the doped form (oxidized) is formed, which manifests as either a polaron and/or bipolaron depending on the doping level, as follows:

PPy + X$^-$ (s) $\rightarrow$ PPy$^+$X$^-$ + e$^-$ polaron

PPy $^+$+ 2X$^-$(s) $\rightarrow$ PPy^{2+}(X$^-$)2 + e$^-$ bipolaron
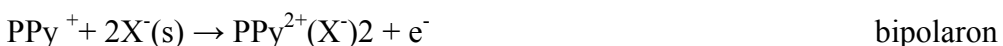
where X$^-$ are anions, (the subscript (s) indicates that they are in solution phase) and PPy represents a segment of the polypyrrole chain.

2.7   Conducting Star Copolymers

Star copolymers are a class of branched macromolecules that have a central core to which multiple linear polymer chains are attached. The 3D structure with extended conjugated linear polymer chains give star copolymers properties that are different from the typical 2D, linear polymers. Conducting star copolymer materials are particularly useful as coatings because of their spheroidal structure and their ability to pack in three dimensions [23]. The conducting star copolymers are used in their undoped state for applications in which the conductivity requirements are not too high, for example static dissipation, or where the optical property of the polymer coating is of chief importance, for example as a pigment or reflective layer. Materials with conductivities in the range 10^{-6} to 1 S cm^{-1} may be suitable for these purposes. Furthermore, the conducting chains, surprisingly, can provide sufficient intermolecular overlap to give solid materials with electrical

conductivities higher than the corresponding linear, non-star conducting polymers [23-26]. For example, nylon-6 with a star structure has a melt viscosity and crystallization half-times that are substantially reduced by the branching [27]. The regular 3D structure of star copolymer gels combines the properties of hardness and flexibility and is being investigated to make materials that are hard without being brittle [23]. The combination of star copolymer and conducting polymer structures open up an approach to making materials that have the favourable properties of both, i.e., improved processability and electrical conductivity. Improved processability results from the spheroidal structure of hyperbranched, dendrimeric and starburst polymers. A conducting star copolymer may be constructed in which two or more different conjugated arms radiate from the central core [28].

Doping of the conducting star copolymers to increase the electrical conductivity may be achieved using methods of prior art applicable to the conjugated radiating chain moieties. For conjugated chains based on Py or thiophene units or derivatives there of doping may be achieved by treatment with oxidizing agents such as iodine, ferric chloride, ferric tosylate, gold trichloride, antimony chloride reference. If the polymer side chains are composed of PANI, doping can be achieved by treatment with acid [29]. Doping can also be achieved electrochemically by confining the polymer to an electrode surface and subjecting it to an oxidizing or reducing potential in an electrochemical cell. In this way, doped thin films on conducting substrates are obtained. The electrolyte provides a source of charge compensating ions flowing in and out of the film accompanying the oxidation or reduction reaction. Applications of conducting polymers in batteries, supercapacitors and electrochromic displays frequently entail doping of the polymer by such an

electrochemical process [23].

2.8   Importance of Conducting Polymers to Biosensors

Polypyrrole has been used for sensor and biosensor applications; several types of biosensors have been developed over the past decades since conducting polymers act as a 3D matrix for the immobilization of enzymes, where reactants can be converted to products. When conducting polymers are immobilized on metal substrates they have an organised molecular structure that permits the 3D structure for the immobilisation of the active catalysts and preserve their activity for long duration. This property of conducting polymers together with its functionality as a membrane has provided several opportunities for the development of sensors [158-160].

The electronic conducting properties and unique chemical and biochemical properties of conducting polymers have ensured that they have numerous (bio) analytical and technological applications. This further allows ease of synthesis and deposition onto a conducting surface of a given substrate from monomer solutions by electrochemical polymerization, with precise electrochemical control of their formation rate and thickness. Once electrodes are coated with conducting polymers under mild conditions, it opens up enormous possibilities for the immobilization of biomolecules and bi-affinity or biorecognizing reagents. The co-immobilization of other molecules such as enzymatic cofactors or charge-transfer mediators through entrapment within the electropolymerized films or by covalent binding on these films permits the fabrication of reagentless biosensors [161-163].

The mode of operation of a chemically modified sensor under amperometric conditions is simple in concept. The redox-active substrate of interest reacts with the catalytically active sites immobilized in the polymer matrix rather than at the underlying support electrode. The electrocatalysis follows a 3D process that is fairly effective. This enables electron transfer between the substrate and the catalytic site, and the kinetics of the substrate/product transformation is normally governed by the properties of the mediating electroactive polymer film. Important factors that may influence reactivity include the degree of conductivity of the polymer film, the catalytic properties of the mediating sites, the nature of the interaction between the active site and substrate, and the morphology of the polymer film [164].

2.8.1 Immobilization of Enzymes on Conducting Polymers

The most commonly reported enzyme immobilization techniques used for designing and development of specific sensors and biosensor include physical adsorption, entrapment, intermolecular cross-linking and covalent binding of the biomaterial.The simplest methods of immobilizing biomolecules on polymer surfaces is adsorption [165]. This includes both physical adsorption and electrochemical adsorption techniques. The latter is achieved by applying a potential to the polymer electrode surface, which enhances electrostatic interactions and hence immobilization [166].

Covalent attachment of biomolecules to the surface of polymers ensures immobilization without leaching of the biomolecules from the substrate surface [167]. Covalent attachment of biomolecules to the monomer prior to polymerization has also been reported [168-169]. This strategy, however, requires lengthy syntheses to produce the

monomer or to modify a preformed surface. Because covalent attachment is usually achieved using a linker, the separation of the biomolecule from the polymer backbone can also have disadvantages in terms of signal transduction and reduced activity of the biomaterial [170]. Self-assembly techniques have been investigated for biomolecule immobilization onto various support materials. Layers formed by self-assembly require a poly-ion to effect biomolecule attachment through strong electrostatic interaction [171-173] and can result in tightly packed structures that limit diffusion [174]. Furthermore, careful control of pH is required to achieve these assemblies and for them to retain stability. Another technique that has been used for the immobilization of biomolecules is the entrapment of the enzyme in the backbone of the conducting polymer in order to have the transfer of electrons between the redox centre and the polymer chain [175-176].

A range of conducting polymers has been employed in the construction of enzyme sensors. These include PPy, PANI, poly(indole) and polyphenol [177-180]. However, of these materials, the most widely used have been films of PPy and its derivatives [181-183]. This may be attributed to the ease with which these films can be grown from aqueous solutions and the high degree of selectivity due to the inherent size exclusion property of PPy films [184-185].

2.9   Dendrimers

Dendrimers are a unique class of macromolecules having highly branched, three-dimensional architectures [186]. The term dendrimer refers to its characteristic appearance. It is derived from two Greek words: 'dendron', which means a tree, and 'meros', which means a part [187-188]. The synthesis of the branched molecular structure

of dendrimers, that resemble ice crystals, Christmas stars or treetops, is reported by Newkome's group [189]. They called them arborols, from the Latin word 'arbor', also meaning a tree. The term cascade molecule is also used, but dendrimer is the best established one, due to their multivalent and monodisperse character [189], the 3D architectures with low polydispersity and high functionality (Figure 2.15) [190-191].
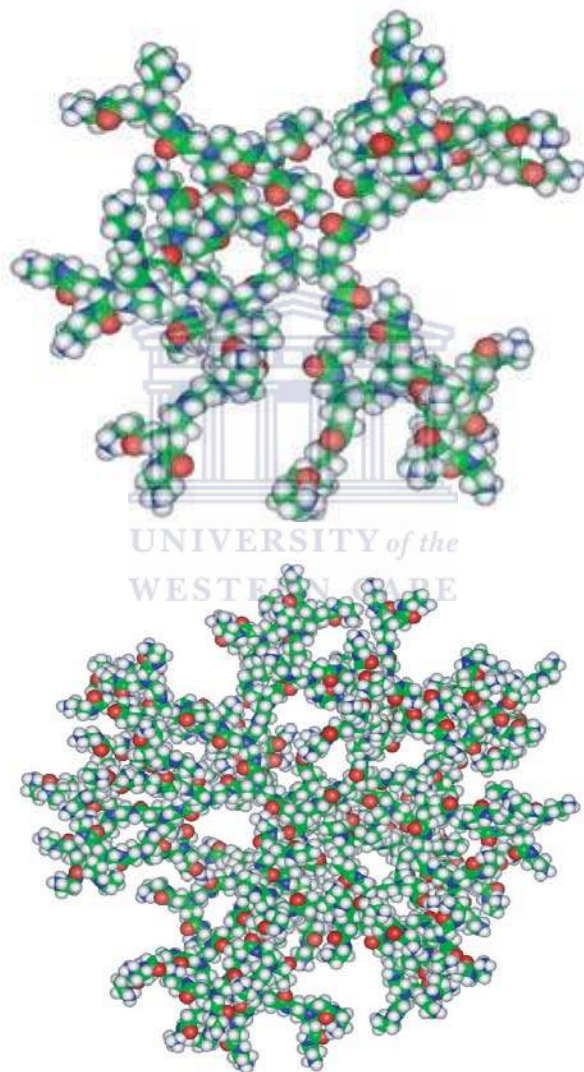
Figure 2.15: Three-dimensional architectures of dendrimers [190-191].

The extremely regular structure of a dendrimer contributes to its nearly perfect spherical

shape; nanostructure ranging from 10 to 200 Angstroms in diameter. A typical dendrimer is built upon an initiator core, with several branching interior layers composed of repeating units and multiple active primary amine groups at its surface (Figure 2.16). The surface of a dendrimer is characterized by the presence of functional groups that together can be utilized as a backbone for the attachment of several types of biological materials [192]. Dendrimers are produced in an iterative sequence of reaction steps, in which additional iteration leads to a higher generation material. The principal difference between a dendrimer and other hyperbranched polymers is that each of the monomer units in the dendrimer has at least one functional unit that allows further branching [193].
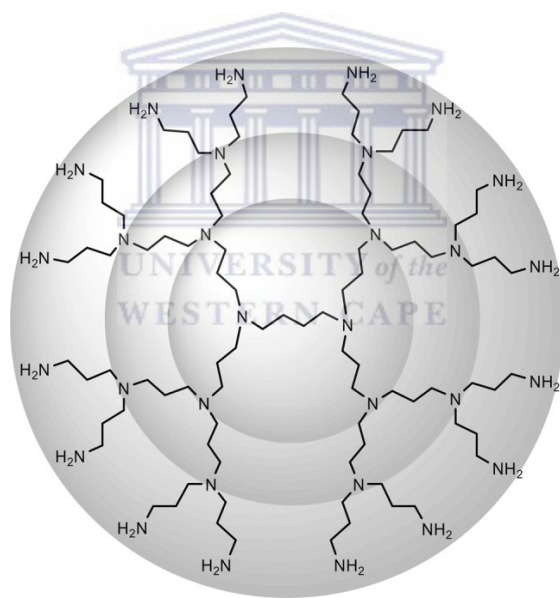
Figure 2.16: Third-generation (G3) PPI dendrimer.

Dendrimers have often been referred to as the "polymers of the 21st century". They were first introduced in 1978 by Vögtle [194] and are globular macromolecules composed of branches emanating from a central core. In 1982, theoretical studies on dendrimer interactions with guest molecules were reported by Maciejewski [195]. He envisioned the

core of the dendrimer as a potential host for guest molecules. But it was not until a few years later, in 1985, that dendrimers were at the forefront of chemistry and were showcased as possible incarceration devices for molecules. Most notably, during this time period, simultaneous work by Newkome [189] and Tomalia [196] demonstrating the synthesis of dendrimer molecules was reported. Since that time, a variety of dendrimers have been developed, different molecules have been attached to the periphery of the dendrimer. The unique architecture and the functionality of dendrimers makes them excellent carrier molecules for use in nanoscale medical applications [197]. They have been explored as light-harvesting agents [198], chemical sensors [199], catalysts [200] and cross-linking agents [201]. They also have been investigated in the biomedical field for drug delivery [202-204], gene therapy [205-206] and as imaging contrast agents [207]. Several dendrimer-based products are under development for the treatment and diagnosis of a variety of diseases. Many of the intriguing properties of dendrimers as well as their syntheses and possible applications are discussed [208-212]. There are many types of dendrimers; the first dendritic structures that were thoroughly investigated and have received widespread attention are Tomalia's PAMAM dendrimers [213].

In this study, PPI dendrimers having a diaminobutane (DAB) core, also denoted as DAB-Amx or PPIx, where x refers to the number of terminal (peripheral) amine groups (see Figure 2.16), were used. The PPIx dendrimers were chosen for many reasons, including their commercial availability, their defined internal hosting locations (cavities), and their very reactive (functionalizable) amine end-groups. There are more than 10,000 published patents relating to dendrimers since the first dendrimer patent was issued to Tomalia [214].

2.9.1 Dendrimers as Unique Macromolecules

Dendrimers have attracted much attention recently owing to their unique molecular architectures. In the last 30 years, dendrimers have exploded onto the scientific scene. The increase in the knowledge about and understanding of dendrimers is evidenced in the dramatic increase in patent literature regarding dendrimers since 1981. From 1981 to 1985, two patents were granted, 51 were granted from 1991 to 1995, and over 1000 were granted from 2001 to 2005 [215]. With increasing publicity about them, dendrimers are now also becoming more widely known outside the scientific community. The synthesis of a dendritic polymer is growing interests for this new family of polymers due to their unique and specific properties. In contrast to linear organic polymers, dendrimers are a novel class of macromolecules possessing a highly branched 3D architecture, and well-controlled size and shape. The large number of end groups of a dendrimer can be chemically modified to associate different functionalities with them. In addition, dendrimers generally have a size in the order of a few nanometres, allowing some critical applications that require a compact multifunctional device on the nanometre scale [216-217]. One remarkable advantage is that the chemical structure of dendrimers is almost limitless. Also, dendrimers have been synthesized with incredible uniformity, which is quite unique in the production of nanoparticles. The true nano-scale size of these molecules lends itself to great precision among their many uses; they have unique linear and nonlinear optical properties depending on their molecular architectures. Applications based on dendrimer's linear optical response have been reported for light-emitting diodes, light harvesters, and fluorescent biomarkers, etc. Nonlinear optical properties of dendrimers have also been investigated recently by several research groups. It was found

that dendrimers containing multi-chromophores can be used to enhance nonlinear optical effects. Nonlinear optical chromophores having large quadratic hyperpolarizability and are commonly incorporated into optically transparent polymers in order to develop organic electro-optical (E-O) devices with large high order E-O response. In contrast to linear-chain polymers, dendrimers having 3D architecture can effectively reduce the intermolecular interactions and prevent the aggregation formation, thus enhancing the nonlinear E-O response [218].

Another use can be found in the therapeutic application of dendrimers [219], such as the anionic poly(amidoamine) conjugates of d(+)-glucosamine and (d)(+)-glucosamine-6-sulfate with immunomodulatory and antiangiogenic properties [220]. Part of the bright future foreseen for dendrimers rises from the incredible systematic control of many of their properties. The control over certain dendrimer characteristics such as size, shape, branch length/density, and surface functionality allows for their customization for use in many fields [221]. Some basic knowledge concerning these topics may be ascertained from other areas. Dendrimers, of course, may be studied using molecular chemistry analytical techniques. However, because of their intrinsic polymeric nature, analytical techniques already in use in the field of polymers may give further insight into the biological activity and toxicity of dendrimers [222].

2.9.2   Synthesis of Dendrimers

Dendrimers are generally prepared using either a divergent method or a convergent one [223]. The poly(propylene imine) PPIx dendrimers are synthesized by the divergent method, which was the first method to be utilized in the formation of dendrimer

macromolecules. In the divergent approach, individual branches are attached to a core or initiator until the number of branches desired is obtained. Each time branches are added, the number of end groups doubles, leading to the use of the term dendrimer generation [224]. The sensitivity of this technique gives a more realistic picture of the purity of a given dendrimer than possible with any other technique. In case of the poly(propylene imine) dendrimers, all generations with amineor nitrile end groups have been fully analyzed with electrospray ionisation-mass spectrometric (ESI-MS) to determine the amount of various side reactions [225].

The PPI*x* dendrimers are commercially available in five generations. These generations are 1, 2, 3, 4, and 5, corresponding to PPI*x*, where *x* = 4, 8, 16, 32, and 64 terminal groups, respectively. In addition to the divergent approach, dendrimers may be synthesized by addition of functionalized branches to a focal point; Frechét [226]. Introduced this convergent approach to dendrimer synthesis. The convergent synthesis route formed more monodispersed dendrimers than the divergent approach due to fewer side reactions and more control over their end-reactive groups [226]. Each of the two methods for synthesizing dendrimers has its own disadvantage: the divergent approach leads to dendrimers with more defects and the convergent approach can only be used to make dendrimers of a limited generation size [224].

Dendrimers made using the divergent approach have more defects in their structure than those made by the convergent method. Those made divergently with defects have similar structures to those containing no defects making separation of these by-products difficult, but a method has been developed for PPI dendrimers [227-228]. The dendrimers made

convergently with defects can be separated from the defect-free dendrimer without difficulty by using gel permeation chromatography (GPC) because the defects are merely small branch molecules. The only drawback of using the convergent method is the limitation of forming higher generation dendrimers. When trying to attach the functionalized branches to the core, steric crowding becomes a problem, which limits the number of end groups [224].
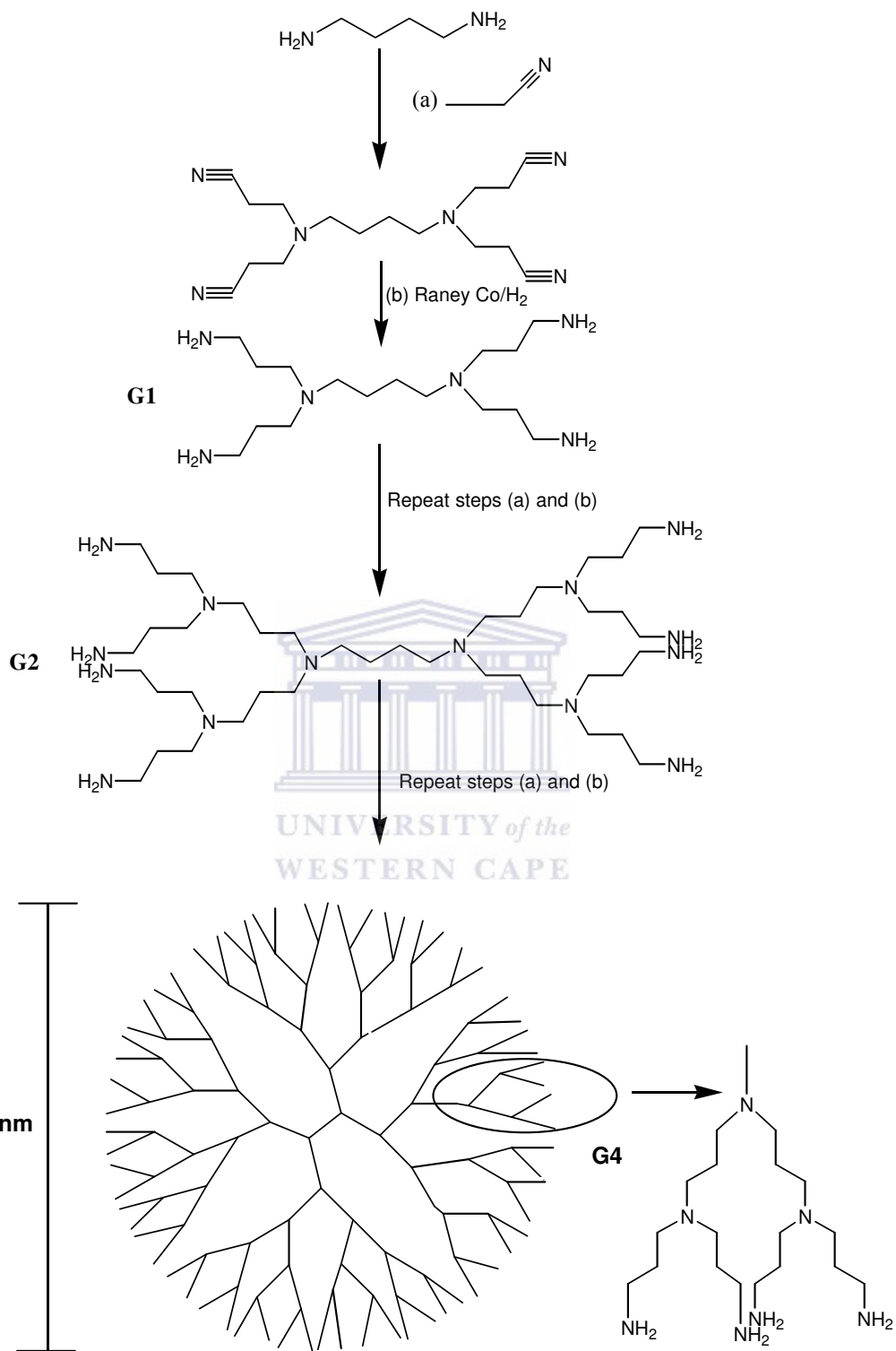
Scheme 2.3: Synthesis and structure of PPI.

The core of dendrimers prepared by either route can host guests by two trapping mechanisms, namely, static and dynamic trapping. Dynamic trapping is the ability of the guest to partition into or out of the dendrimer relatively unhindered [229-230].This trapping technique relies on an equilibrium mechanism, so it is required that an outside source of guests be available to aid in the retention of guest molecules inside the dendrimer core (Scheme 2.3).

2.9.3 Poly(propylene imine) Dendrimers

Poly(propylene imine) dendrimers stand for "poly(propylene imine)" describing the propylamine spacer moieties which is the oldest known dendrimer type developed initially by Vögtle [231]. These dendrimers are generally poly-alkyl amines having primary amines as end groups, the dendrimer interior consists of numerous tertiary tris-propylene amines. PPI dendrimers are commercially available up to G5. In addition, these dendrimers are also sometimes denoted "DAB-dendrimers" where DAB refers to the core structure, which is usually based on Diamino butane [232]. As an alternative name to PPI, POPAM is sometimes used to describe this class of dendrimers. POPAM stands for poly(propylene amine), which closely resembles the PPI abbreviation. The combination of hydrophilicity, highly branched structure and chemical functionality makes poly(propylene imine) dendrimers very interesting building blocks to obtain well-defined amphiphilic superstructures. Dendrimers have gained a growing scientific interest as building blocks in new molecular architectures [233-234].

The physical and chemical properties of dendrimers are determined by the shape and multiplicity of the core and building blocks and by the size and shape of the end groups, in

addition to their chemical [235], it offer us not only the possibility to change the size and molecular weight of the molecule by choosing different generations, but they also allow us to access new molecular structures and self-assembling systems that can be designed to perform one specific function, however the organized structure of dendrimer, ease of modification, and strong adsorption behaviour to a variety of substrates, PPI dendrimers can be used to produce monolayers or stacked film layers, which can be used as sensors to detect hazardous chemical materials [236-237].

Dendrimers are of interest for their unusual physical properties. An important feature of dendrimers is that their viscosity in solution and in melt is lower than that of the linear polymers. Surprisingly, the viscosity decreases with increase in molecular weight, i.e. higher dendrimers are less viscous [195, 238-239]. The glass transition temperature (Tg) depends on the number of end groups and number of branch points [240]. An increase in the number of end groups lowers the Tg, while Tg is increased with an increasing number of branch points and the polarity of the end groups [241], rheological properties [208, 242], an electrically conducting dendrimer has been reported by Duan *et al.* [243]. The solubility of dendrimers in common solvents, compared to their analogous linear polymers, depends predominantly on the properties of their surface groups [244]. Theoretical studies [245] of the PPI dendrimers have led to predictions of interesting characteristics for the molecule depending on the pH and salt concentrations of the aqueous environment. At low pH and low salt concentration, the interior tertiary amine groups are protonated leading to a repulsion of charges. This charge repulsion results in what is considered an "extended conformation" of the PPI dendrimer. At high pH and high salt concentration, the tertiary amines are no longer protonated, causing a collapse of

the dendrimer onto itself (see Figure 2.17) [245]. An important property of dendrimers is their tendency to form cationic structures under physiological conditions (pH 7.4). Under these conditions, the primary amines on the surface of the dendrimer readily protonate. This creates a polycationic dendrimer with ammonium terminal groups, which leads to a more basic solution [246]. The work described in this dissertation will show, for the first time, that conducting star copolymer can be observed with a modified PPI dendrimer. Table 2.2 shows Increase in PPI parameters with the number of generations and the calculated properties of amine surface functional PPI dendrimers by generation.

Table 2.2: Increase in PPI parameters with the number of generations [247]

Generation	End groups [number]	Diameter [Å]	Molar mass [g]
1	4	4.4	317
2	8	6.9	773
3	16	9.3	1687
4	32	11.6	3514
5	64	13.9	7168

Figure 2.18 shows a G3 (PPI dendrimer. T there are three generations of branches, and the outermost shell is composed of 16 -NH$_2$ groups.
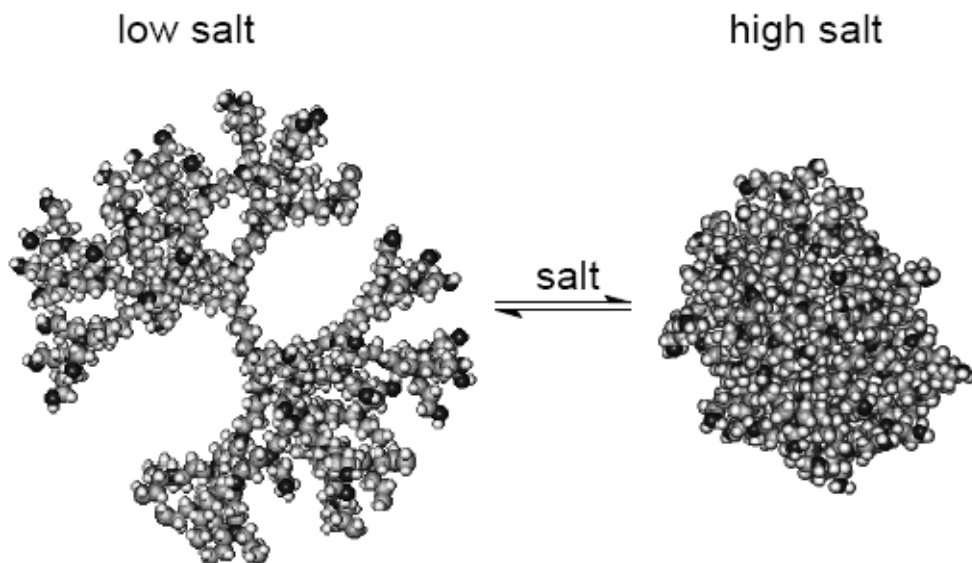
Figure 2.17: The occurrence of a dense shell (left) or a dense core conformation (right) of poly(propylene imine) dendrimers is dependent on ionic strength of the solution [245].
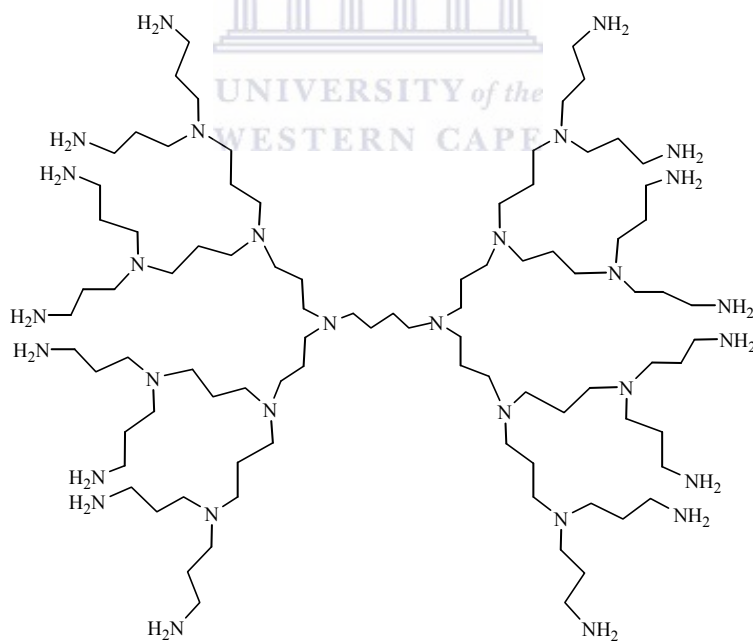
Figure 2.18: Generation 3 poly(propylene imine) dendrimer.

2.9.4 Applications of Poly(propylene imine) Dendrimers

The surface functionalities, interior and core of the dendrimers can be tailored for a variety of applications, including molecular electronics, molecular recognition, catalysis, sensors and electroluminescent devices [70-74, 248]. Dendrimers containing photoactive or redox active components can serve as molecular antennae for light harvesting and can be exploited in electrochemical sensors. Research is also active in applications as diverse as polymer additives [248]. The behaviour of dendrimers as hosts is essential if they are to find success as solubilising agents [249-250]. Dendrimer catalysts are already commercially utilized in the production of pesticides [251]. The dendritic boxes with encapsulated guest molecules can be opened and closed reversibly by means of an external stimulus and can be useful in controlled drug-delivery applications [252]. The structural precision with high specificity along with the nanodimensions of the dendrimers has led to a variety of biomedical applications. Extensive interest in their use as protein mimics, genetic material transfer agents, targeted drug-delivery agents, magnetic resonance imaging contrast agents, antiviral and antitoxin agents, angiogenesis inhibitors and artificial enzymes can be found in literature [253-255]. Novel applications of terminated PPI dendrimers in the nanotechnological by generating the molecular print boards for structured surfaces [256-257]. Hybrid polymers were prepared by grafting living cationic poly(THF) onto the surface of the PPI dendrimers [258].

2.9.5 Poly(propylene imine) Dendrimers Star Copolymers

Poly(propylene imine) dendrimers are highly branched macromolecules terminating with amino groups. They have a number of interesting characteristics. They can be used as

hydrogen donors because of their high density of amino groups. Many of the properties of dendrimers are strongly influenced by these terminal groups [33-35]. Dendrimer-star copolymers [38], a novel type of molecular architecture, in which many linear homo- or block copolymer chains are attached to the dendrimers, have been developed because they combine the properties of star copolymers with those of dendrimers [39-44]. Two general methods have been used to prepare the dendrimer-star copolymers. One is to link monofunctional linear polymers onto the dendrimer surface [39, 43-45]. The other is to grow armed polymer chains from the surface of the dendrimer by "contolled/living" polymerizations, such as anionic polymerization [46], ring-opening polymerization (ROP) [47], and atom transfer radical polymerization (ATRP) [48]. A series of star-shaped copolymers, using the G1 to G5 PPIs as the core, were prepared [49-50] in order to investigate their miscibility properties with linear polystyrene. The unsaturated end groups of polyisobutylene were converted into anhydride termini by an ene reaction with maleic anhydride, and the product was reacted with the PPI dendrimers to generate PPI-polyisobutylene star copolymers [51]. Dendrimer-like star-branched polymers have recently appeared as a new class of hyperbranched polymers. They are recognized as nano-ordered globular macromolecules from their architectures and have many characteristic structural features, such as hierarchic hyperbranched structures, generation-based radial architectures, different branch densities between core (inside) and shell (outside), and many junction points and end-groups [36-37].

It is also possible to synthesize a variety of block copolymers with the equal branched architectures by introducing different polymer segments at each generation. Interesting morphologies and nanostructured materials have been reported by several research groups

[52-58]. Thus, dendrimer-like star-branched polymers and block copolymers are promising specialty functional materials with many possible applications to drug, vaccine, and gene encapsulated delivery devices, surface modifiers, functional nanosize spheres and micelles, surfactant, molecular recognition systems, microelectronic materials, etc. Hee-Soo Yoo e*t al.* [59] synthesized a series of dendrimer-like star-branched polystyrenes by developing an iterative methodology based on the "arm-first" divergent approach. The resulting are controlled molecular weights and compositions and narrow molecular weight distributions [59]. Dendritic copolymers are a specific group of dendrimers.

There are two different types of copolymers (Figure 2.19). Segment-block dendrimers are built with dendritic segments of different constitution. They are obtained by attaching different wedges to one polyfunctional core molecule. Layer-block dendrimers consist of concentric spheres of differing chemistry. They are the result of placing concentric layers around the central core. Hawker and Fréchet [60] synthesized a segment-block dendrimer which had one ether-linked segment and two ester-linked segments. They also synthesised a layer-block dendrimer.

Figure 2.19: Copolymers: (A) segment-block dendrimer, and (B) layer-block dendrimer.

2.9.6 Dendrimers in Electrochemical Biosensors

Dendrimers are a new class of highly branched globular polymers [259] with biocompatible properties. Thir physicochemical and biological properties make them suitable for a variety of applications including catalysis, photochemical molecular devices, electroluminescent devices, sensors and biomedical devices. The application of dendrimers in electrochemical biosensors is an emerging area of research. The structural homogeneity, biocompatibility, internal porosity, high surface area and ease of functionalization of dendrimers make them very desirable for biosensor applications. The potential applications of dendrimers in electrochemistry are imminent. Especially, the rapid advancements in the synthesis of redoxactive dendrimers along with their ability to provide a suitable microenvironment for the immobilization of biomolecules while retaining their biological activity have given great scope for their exploitation in electrochemical biosensors [260]. Over the past decade, there has been a steady and gradual development in the evaluation of the bionanocomposites of dendrimers for electrochemical sensors. PPI, typical of dendrimers, is nanoscopic in size, has highly

controllable molecular weight with large number of readily accessible terminal primary amine functional groups. It is cationic in nature and, through its nanocavities, has the ability to host anionic molecules like DNA. The use of dendrimers, dendrimer composites and metallodendrimers in biosensor and DNA microarrays is successfully emerging [261-266]. The earlier work in our research group, on dendrimer biosensors on the electrodeposition of PPI on glassy carbon electrode, resulting a stable biosensor with a good detection limit and selectivity. Cyclic voltammetry and EIS were used as the electro-analytical tools in this work [267].

CHAPTER 3

Experimental

3.1   Introduction

This chapter comprises a description of all the materials, instrumentation and experimental protocols used in this study.

3.2   Reagents

Poly(propylene imine) dendrimer from SyMO-Chem, Eindhoven, Netherlands was used as received. 2-Pyrrole carboxaldehyde (2-Py), lithium perchlorate, ammonium persulfate, dichloromethane (DCM), methanol, chloroform, hydrochloric acid ($\geq$ 32%) and sulfuric acid were all obtained from Sigma-Aldrich, South Africa. All chemicals were of analytical reagent grade and were used without further purification. The Py monomer (Aldrich) was distilled prior to use. The Buffer components disodium hydrogen phosphate (Na_2HPO_4) and potassium dihydrogen phosphate, potassium chloride, Sigma Aldrich. Ultrapure water (resistivity 18.2 MΩ cm), used as reagent water for aqueous solution preparation, was purified by a Milli-QTM system (Millipore). Analytical grade argon and nitrogen gases were purchased from Afrox, South Africa. Alumina polishing pads and powder (0.05, 0.3 and 1.0 μm) were obtained from Buehler, Illinois, USA. Platinum (Pt) wires as counter electrodes were obtained from Sigma-Aldrich.

3.3   Analytical Techniques

The following analytical techniques were employed in this study: ^{1}H NMR and FTIR, for structural analysis of the star copolymers; SEM, for morphological characterization of the star copolymers; TGA, to study the thermal stability of the prepared material; XRD analysis, to study the structural make-up of phases, crystallinity and amorphous content. Hall effect measurements were also used, to determine the electrical conductivity properties of the prepared star copolymers.

3.3.1. Proton Nuclear Magnetic Resonance Spectroscopy

^{1}H NMR spectra were recorded on a 200 MHz, Varian Gemini XR200 spectrometer, using CDCl$_3$ as the solvent, and tetramethylsilane as internal standard.

3.3.2   Fourier Transform Infrared Spectroscopy

FTIR spectra were recorded on a PerkinElmer Spectrum 100 FTIR spectrometer. The chemically prepared star copolymer material was analyzed in powder form. The electrochemically prepared star copolymer material was prepared by electrodeposition on the surface of a coated Pt electrode and then gently scraping from the electrode surface. The spectra were directly recorded in the region 400 to 4000 cm^{-1}, without mixing with KBr. The spectra obtained were used to identify the various functional groups in the star copolymer as well as those in the backbone chain of the dendrimers.

3.3.3   Thermogravimetric Analysis

Thermogravimetric analysis is a thermal analysis technique which measures the weight

change in a material, under nitrogen atmosphere, as a function of temperature and time, in a controlled environment. This can be very useful to investigate the thermal stability of a material. TGA was carried out using a PerkinElmer, Model TGA-7 instrument. The weight of each sample was less than 10 mg (usually around 7-8 mg). The most common method used in TGA is to continuously weigh a sample on a sensitive balance while heating the sample in the presence of air or an inert gas. As the temperature increases, mass loss occurs due to evaporation of water or solvent, decomposition, or reaction of the material. The mass measurements are collected over a range of temperatures and processed by a computer. A thermogram is produced, which is a plot of mass loss versus temperature. Mass loss can occur in steps, based on the temperature at which the material leaves the sample pan.
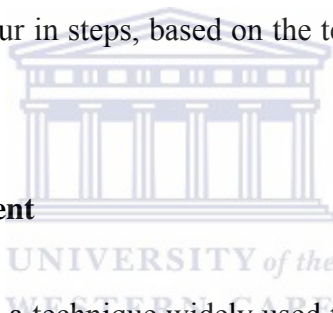
3.3.4   Hall Effect Measurement

The Hall effect measurement is a technique widely used to determine electrical properties of semiconductor materials, like conductivity, majority carrier type, resistivity and mobility. The Hall effect is based on the deflection by a magnetic field of moving charged particles. The samples were prepared by pressing a pellet (13 mm diameter) with < 6 tons pressure for 30 min at room temperature, as shown in Figure 3.3. The electronic conductivity of PPy and PPI-co-PPy chemically prepared was measured using the economical HMS-3000 Hall Measurement System.

3.3.4.1 Theory

The Hall effect's measurable phenomena have been helpful in successfully describing the

properties of electrically conducting materials. The Hall effect was discovered by Edwin Hall in 1978 [268]. When a current is travelling through a conducting material (in the absence of a magnetic field), the charge-carrying particles, which are usually electrons, travel in what is known as a "line-of-sight" path, meaning that the electrons travel in a way that takes the shortest amount of time possible.

When an electrical conductor's material is placed within a magnetic field for a constant current I flows through the conductor (x-direction) and a magnetic field B is applied perpendicularly to the current plane, a Hall voltage V_H is generated across the conductor (y-direction), which is directly proportional to the magnitude of the applied field (Figure 3.1). This effect arises due to the Lorentz force F_B and no longer travel in this straight-line path, F_B acting upon the current carriers (electrons) such that they are diverted from their original flow direction. This causes a charge build-up along the sides of the conductor, generating an electric force qE_H (where q is the electron $^-$e or hole $^+$e charge, and E_H is the electric field) that is opposite to the Lorentz force. Equilibrium state is reached when qE_H becomes equal to F_H such that the net effect becomes zero due to cancellation. At this state, the voltage potential across the conductor, due to the charge build-up, yields the Hall voltage [269].
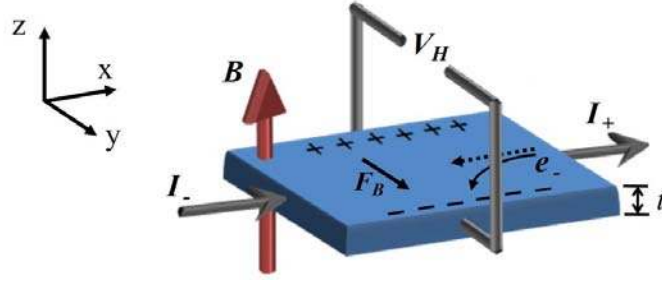
Figure 3.1: Principle of the Hall effect.

The Lorentz force (F) is described by the following equation:

$$F = q(v \times B) \tag{3.1}$$

where q is the electric charge [for a single charge quantum: $q = 1.602 \times 10^{-19}$ C], v is the velocity of the moving charge, and B is the applied magnetic field [270]. The now uneven distribution of electrons creates an electric field within the sample. The force acting on the electrons due to this electric field (E) is given as [270]:

$$F = qE \tag{3.2}$$

The electrons' velocity due to the current flow (I) is given by:

$$v = \frac{1}{nAq} \tag{3.3}$$

where n is the charge density of electrons and A is the surface area of the sample [269]. If current is still able to pass through the sample, then the Lorentz force and the force caused by the electric field have reached an equilibrium, leading to a solution for the electric field [270]:

68

$$qE_x = qv_y B_z = \frac{IB}{nA}$$

$$\therefore E = \frac{IB}{qnA} \qquad (3.4)$$

where the induced electric field only acts in the x direction, the magnetic field acts in the z direction, and the velocity of the charge-carrying particles acts in the y direction, as shown in Figure 3.2.
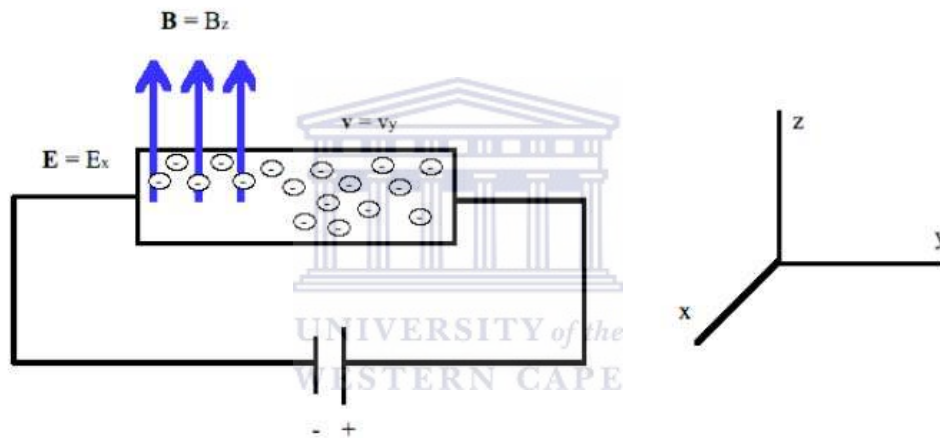
Figure 3.2: A visual description of the magnetic field, electric field, and electron velocity given in component form.

In order to measure the Hall effect, electrical contacts are arranged on a sample in a manner so as to conform to the Van der Pauw contact arrangement. The Van der Pauw technique is a method used to find the charge-carrier density, among other characteristics, using the Hall effect by measuring the Hall voltage and resistivity [271].

A thin pellet sample is prepared on a pressing pellet (13 mm diameter) with less than 6 tons of pressure for 30 min at room temperature, shown in Figure 3.3. Current is passed

between the two contacts and the potential difference is measured across the remaining two.
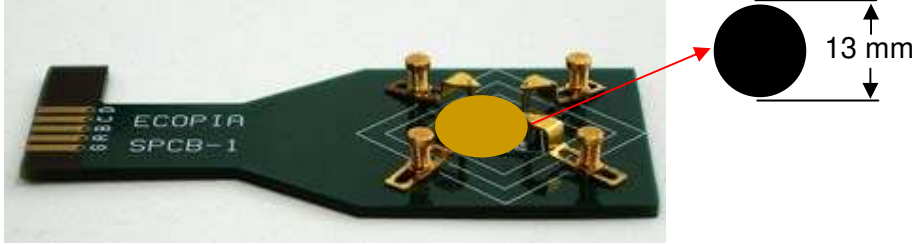
Figure 3.3: A sample with contacts attached in a Van der Pauw arrangement.

To obtain information regarding many of the more interesting properties of thin film materials, the sheet resistance (R_s) must first be determined. In order to obtain R_s, current is passed through adjacent contacts, while the potential difference is measured across the free contacts. For example, current is driven through contact A to contact B while the potential difference from contact C to contact D is measured. The R_s is given by:

$$e^{\left(\frac{-\pi R_v}{R_s}\right)} + e^{\left(\frac{-\pi R_H}{R_s}\right)} = 1 \tag{3.5}$$

where R_V is the resistivity measured across the vertical length of the sample, and R_H is the resistivity measured across the horizontal length of the sample. Both resistivities are averaged over the four possible combinations of current flow:

$$R_V = \frac{1}{4}\left(\frac{V_{CD}}{I_{AB}} + \frac{V_{AB}}{L_{CD}} + \frac{V_{DC}}{I_{BA}} + \frac{V_{BA}}{I_{DC}}\right)$$

$$R_H = \frac{1}{4}\left(\frac{V_{DA}}{I_{BC}} + \frac{V_{BC}}{L_{DA}} + \frac{V_{AD}}{I_{CB}} + \frac{V_{CB}}{I_{AD}}\right) \tag{3.6}$$

70

where V_{xy} is the potential difference measured from contact x to contact y, and, I_{xy} is the current measured by injection into contact x and out of contact y. The resistance equation given above must be solved for R_s using a numerical iterative method [272]. The Hall voltage is defined as the potential difference measured across the sample perpendicular to the direction of the current under the influence of a constant magnetic field [272]. The Hall voltage is given as follows:

$$V_H = \frac{1}{8}\left[\left(V_{AC+} + V_{CA+} + V_{BD+} + V_{DB+}\right) - \left(V_{AC-} + V_{CA-} + V_{BD-} + V_{DB-}\right)\right] \tag{3.7}$$

where V_{AC+} represents the voltage measured across probes A and C with a positive magnetic field incident perpendicular to the sample. If the resulting Hall voltage is positive, the charge-carriers are holes; likewise, if the Hall voltage is negative, the charge-carriers must be electrons. The Hall voltage may be calculated using the following expression:

$$V_H = wE = \frac{wIB}{qnA} = \frac{IB}{qnt} \tag{3.8}$$

where w is the width of the sample, I is the amplitude of the current, and t is the sample thickness. The sheet carrier concentration (n_s), or sheet density, represents the number of charge-carrying particles in a given area. It is calculated by multiplying the sample thickness (t) by the charge density (n):

$$n_s = \frac{IB}{q|V_H|} \tag{3.9}$$

The charge-carrier density (ρ), the number of charge-carrying particles within the sample volume, is found by relating the Hall voltage (V_H) and the sheet resistance (R_s) by the following expression:

$$\rho = \frac{V_H t}{IBR_S} \qquad (3.10)$$

The average drift velocity of electrons (or holes) in the presence of an electric field is known as its mobility; the mobility of a sample reveals information about the orbits of electrons within each atomic state, as well as ionization states of the compound, and may be represented by [273-274]:

$$\mu_m = \frac{1}{qn_s R_s} \qquad (3.11)$$

For a semiconductor, the sign of the mobility indicates whether the charge-carrying particles are holes (p-type) or electrons (n-type). The conductivity of a sample is given by:

$$\sigma = n_s q \mu_s \qquad (3.12)$$

and may be inverted to find the resistivity [272]. In order to properly describe the electrical properties of the materials used, an understanding of the atomic structure and behaviour of electrons in these samples is necessary. The band theory of solids provides a suitable picture to conceptualize the electrical processes at this scale [275].

The electrons contained within an atom reside in defined energy states, which could be described mathematically as a combination of wave functions used to predict the location

of an electron orbiting the atom. As many of these atoms come in close contact, the electrical energy states are split. Electrons are fermions and therefore must obey Pauli's exclusion principle, which states that no two fermions with the same set of quantum numbers may occupy the same energy state. The individual electronic energy states are separated by approximately 10^{-7} eV, allowing them to appear as though existing in a continuous energy band. There are still, however, forbidden energy levels, which appear as energy gaps between the available bands. Only valence electrons are considered when describing the conductivity of a material because the inner electrons are assumed to be tightly bound to their parent atoms. These valence electrons contribute to the valence energy band, and dictate how the material will behave. The next available energy band is known as the conduction band, which requires the presence of electrons in order to mobilize charge [11].
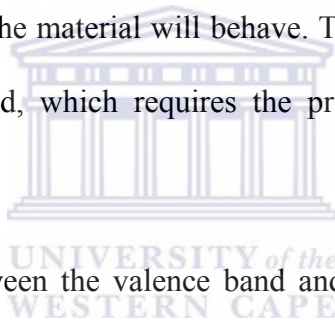
The degree of separation between the valence band and conduction band in a material defines how it will transport charge, if at all. In conducting materials, the valence and conduction bands overlap, allowing for a high conductivity. In insulators, there is a large energy gap separating the valence and conduction bands, typically > 3 eV. In semiconductors, the energy gap is small, and electrons are usually promoted to the conduction band due to thermal excitations at room temperature. The Fermi energy is the energy referring to the electron sitting in the highest occupied quantum in the sea of fermions. The Fermi function, eq 3.13, which is dependent on the Fermi energy, is used to determine the relative amount of electrons that inhabit the conduction band:

$$\int(E) = \frac{1}{1+\exp^{\left(\frac{E-E_F}{KT}\right)}}$$
(3.13)

where E is the given electron energy state, E_F is the Fermi level, k is the Boltzmann constant [$K = 8.617 \times 10^{-5} eV.K^{-1}$], and T is the temperature given in Kelvin.

3.3.5 X-ray Diffraction

X-ray diffraction is one of the most widely used material characterisation methods [276]. It is a non-destructive technique that can reveal the composition and crystallographic structure of natural and manufactured materials. In XRD analysis, X-rays of known wavelength are passed through a sample to be identified in order to identify the crystal structure. The wave nature of the X-rays means that they are diffracted by the lattice of the crystal to give a unique pattern of peaks, or 'reflections', at differing angles and of different intensity (just as light can be diffracted by a grating of suitably spaced lines).

3.3.6 Fluorescence Spectroscopy

Fluorescence spectroscopy is an important investigational tool in many areas of analytical science, due to its extremely high sensitivity and selectivity [277]. A fluorescence spectrometer from Horiba NanoLog™ 3-22-TRIAX, with double grating excitation, and emission monochromators with a slit width of 3.2 nm was used. Aqueous samples of PPI were prepared for fluorescence spectroscopy experiments by dissolving it in water. Solid samples of PPy and the star copolymer that was chemically prepared were pressed (see 3.3.4).

Fluorescence is the emission of visible light by a substance that has absorbed light of a different wavelength while spectroscopy is the study of any measurement of a quantity as a function of either wavelength or frequency. Thus, fluorescence spectroscopy can be defined as a type of electromagnetic spectroscopy which analyzes fluorescence from a sample. It involves using a beam of light, usually ultraviolet light that excites the electrons in molecules of certain compounds and causes them to emit light of a lower energy, typically, but not necessarily, visible light. Since molecules have various states called energy levels, fluorescence spectroscopy is primarily concerned with electronic and vibrational states. The species being examined are first excited, by absorbing a photon, from its ground electronic state to one of the various vibrational states in the excited electronic state. Collisions with other molecules cause the excited molecule to lose vibrational energy until it reaches the lowest vibrational state of the excited electronic state. The molecule then drops down to one of the various vibrational levels of the ground electronic state again, emitting a photon in the process. As molecules drop down into any of the several vibrational levels in the ground state, the emitted photons will have different energies, and thus frequencies. Therefore, by analyzing the different frequencies of light emitted in fluorescence spectroscopy, along with their relative intensities, the structure of the different vibrational levels can be determined. It can be noted that, in a typical experiment, the different frequencies of fluorescent light emitted by a sample are measured, holding the excitation light at a constant wavelength. This is called an emission spectrum. The emission spectrum provides information for both qualitative and quantitative analysis.

3.3.7   Scanning Electron Microscopy

A scanning electron microscope is a powerful microscope that uses electrons rather than light to form an image of objects such as fractured metal components, foreign particles and residues, polymers and biological samples, among others. It uses a focused beam of high energy electrons to generate a variety of signals at the surface of solid specimens. The signals derive from electron sample interaction and reveal information about the sample including external morphology (texture), chemical composition, crystalline structure and orientation of materials making up the sample. The advantages associated with SEM include, among others, its ability to perform analyses of selected point locations on the sample. Areas ranging from approximately 1 cm to 5 microns can also be imaged in a scanning mode using conventional SEM techniques (magnification ranging from $20\times$ to approximately $30,000\times$, and a spatial resolution of 50 to 100 nm) [278].

A SEM Gemini LEO 1525 Model microscope was used to study the morphology of the synthesised star copolymer. Powder particles were mounted onto an electrically grounded sample holder using carbon tape on a graphite support unit. Then were coated with a vapour-deposited gold layer in order to achieve good quality images and resolution. The samples were then subjected to an electron beam under vacuum to obtain micrographs of the star copolymers

3.3.8   Voltammetry

Cyclic voltammetry measurements were performed on a BAS 100B electrochemical analyzer from Bioanalytical Systems, Inc. (West Lafayette, IN).

3.3.8.1 Principles of Cyclic Voltammetry

The common characteristics of all voltammetric techniques is that they involve the application of a potential (E) to an electrode and monitoring of the resulting current (I) flowing through the electrochemical cell. In many cases, the applied potential is varied or the current is monitored over a period of time (t). Thus all voltammetric techniques can be described as some function of E, I, and t. They are considered as active techniques (as opposed to passive techniques such as potentiometry) because the applied potential forces a change in the concentration of an electroactive species at the electrode surface by electrochemically reducing or oxidizing it. Cyclic voltammetry is a widely used electroanalytical technique that uses microelectrodes and unstirred solution so that measured current is limited by the analyte diffusion at the electrode surface. It has wide applications in the study of redox processes, electrochemical properties of analyzes in solution and for understanding reaction intermediates as well as for obtaining the stability of reaction products [279]. A cyclic voltammogram is a complicated, time dependent function of a large number of physical and chemical parameters. The common experimental practice is to chose a starting potential for the working electrode E_{start}, where the analyte is electroactive, and then to change potential at a constant rate v (= dE/dt) moving from E_{start} through a potential range where oxidation or reduction of analyte can occur. A reversing potential E_{rev}, when the sweep direction is reversed (-v) and the potential usually returns to E_{start}. These steps form a single cycle, but the process can be repeated any number of times. A wide number of values of |v| have been used (0.05^{-2} × 10^6 V s^{-1}). However, multiple CV experiments can be used for variety of applications, including:

- The determination of Nernstian (reversible) or non-Nernstian (irreversible) behaviour of a redox couple

- The number of electrons transferred in an oxidation or reduction

- Formal potentials

- Rate constants

- Reaction mechanisms

- Diffusion coefficients

The initial scan can, for instance be negative to the switching potential, in which case if the scan is reversed; it runs in the positive direction. A full cycle, partial cycle or a series of cycles can be performed depending on the analysis targeted. Important parameters are usually obtained from cyclic voltammograms for analysis of redox properties and properties of an electroactive sample. These parameters include anodic and cathodic peak potentials (E_{pa} and E_{pc} respectively) as well as anodic and cathodic peak currents (i_{pa} and i_{pc} respectively). A typical cyclic voltammogram illustrating these parameters is shown in Figure 3.4.
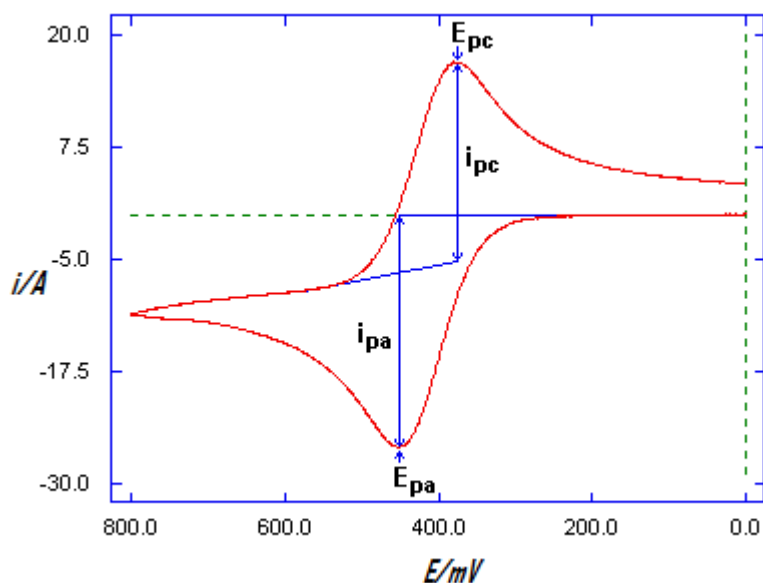
Figure 3.4: A typical cyclic voltammogram showing the basic peak parameters, E_{pa}, E_{pc}, i_{pa} and i_{pc}.

Important parameters are usually obtained from cyclic voltammograms for analysis of redox properties of an electroactive sample. These parameters include peak potentials (E_{pc}, E_{pa}) and peak currents (i_{pc}, i_{pa}) of the cathodic and anodic peaks, respectively. Consequently, important information about the sample under investigation can be obtained from the above peak parameters. This includes whether the electrochemical process displayed by the sample is reversible, irreversible or quasi-reversible. It also gives an insight into how fast the electron process is, relative to other processes such as diffusion. For instance, if the electron transfer is fast relative to the diffusion of electroactive species from the bulk solution at the surface of the electrode, the reaction is said to be electrochemically reversible and the peak separation (ΔE_p) is given by equation 3.14:

$\Delta E_p = |E_{pa} - E_{pc}| = 2.303\ RT/nF$ (3.14)

where ΔE_p is the peak separation (V), E_{pa} is the anodic peak potential (V), E_{pc} is the cathodic peak potential (V), n is the number of electrons, F is the Faraday constant (96 486,3365 C mol^{-1}), R is the gas constant (8.314 J mol^{-1} K^{-1}) and T is the absolute temperature of the system (298 K). The number of electrons (n) involved in the electrochemical process can be estimated from the above equation. Thus, for a reversible redox reaction at 25 °C (298 K) with n electrons, ΔE_p should be 0.0592/n V or about 60 mV for one electron. In practice, this value is difficult to attain because of cell resistance. Irreversibility due to slow electron transfer rate results in $\Delta E_p > 0.0592/n$ V, possibly, greater than 70 mV for a one-electron reaction [280]. The diagnostic tests for electro-reversibility are listed below.
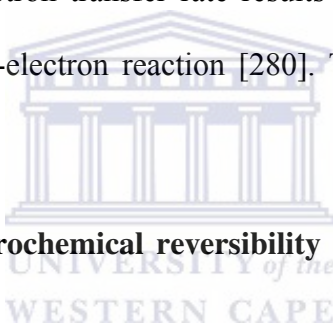
Diagnostic tests for the electrochemical reversibility of a redox couple, carried out byCV.

1. $I_{pc} = I_{pa}$

2. The peak potentials , E_{pc} and E_{pa} , are independent of the scan rate (v)

3. The formal potential ($E^{o\prime}$) is positioned mid-way between E_{pc} and E_{pa}, so $E^{o\prime} = (E_{pa} + E_{pc})/2$

4. I_p is proportional to $v^{\frac{1}{2}}$

5. The separation between E_{pc} and E_{pa} is 59 mV/n for an n-electron couple (i.e. $\Delta E_p = |E_{pa} - E_{pc}| = 0.0592/n$ V).

For reversible reaction, the concentration is related to peak current by the Randles-Sevčik

equation (at 25 °C) [279, 281]:

$$I_p = 2.69 \times 10^5 \, n^{3/2} A D^{1/2} v^{1/2} C_0$$

(3.15)

where I_p is the peak current in ampere, v is the rate at which the potential is swept in V s^{-1}, A is the electrode area (cm^2), n is the number of electrons transferred, D is the diffusion coefficient (cm^2 s^{-1}), pa is the peak anodic, pc is the peak cathodic, and C_0 is the concentration in mol cm^{-3}. Several voltammograms performed at different scan rates can lead to preparation of several linear plots whose slopes could give further information about the redox properties of the sample in question. For, instance, when the peak current is plotted against the square root of the scan rate, the slope of the linear plot can be used to estimate the diffusion coefficient according to the Randles-Sevčik (equation 3.15). When plotted, the log of peak current versus the log of scan rate gives a linear plot whose slope distinguishes between diffusion controlled peaks, adsorption peaks or even a mixture of the two. A plot of the log I_p versus log v is linear, with a slope of 0.5 for diffusion peak and a slope of 1 for an adsorption peak. Intermediate values of the slope are sometimes observed, suggesting a "mixed" diffusion-adsorption peak [280].

In some cases, the sample to be characterized may be deposited on the surface of the electrode (chemically modified electrodes). In such cases, one can estimate the surface concentration of the adsorbed material by the use of the Brown–Anson equation model:

$$I_p = \frac{n^2 F^2 \Gamma^* A v}{4RT}$$

(3.16)

where I_p, n, F, A, R, v and T are explained in equations 3.14 and 3.15 and Γ^* is the surface

81

concentration of the adsorbed species of the electrode modifier.

Although CV is very widely used for the initial redox characterization of a molecule (i.e., the redox potentials, and the stability of the different oxidation states) and for qualitative investigation of chemical reactions that accompany electron transfer, there are a number of disadvantages inherent in these techniques, which include:

i) The effects of slow heterogeneous electron transfer and chemical reactions cannot be separated if both of these effects are present, then the rate constants for these processes can only be calculated using simulations methods.

ii) There is a background charging current throughout the experiment of magnitude vC_{dl} (where C_{dl} is the capacitance of the interface at the working electrode). This restricts the detection limit to about 10^{-5} M. In addition, the ratio of the peak faradaic current to the charging current decreases with increasing v (I_p is proportional to $v^{\frac{1}{2}}$) [282].

In spite of these limitations, CV is very well suited for a wide range of applications and is one of the standard techniques used in characterization.

3.3.9   Square Wave Voltammetry

Square wave voltammetry (SWV) has received growing attention as a voltammetric technique for routine quantitative analyses. SWV was reported in 1957 by Barker [283]. This technique involves the application of square wave modulation to a constant or nearly constant dc potential, and the current generated is sampled at the end of successive half cycles of the square wave. Three currents are generated i.e. forward current from the

forward pulse (I_f), the reverse current from the reverse pulse (I_r) and that for the net current (I_d) which are then plotted against the potential on the corresponding staircase tread. The net current (I_d) is obtained by the difference between the forward and the reverse current (I_f - I_r) and is centred on the redox potential. The net current serves better analytical usage than the forward and reverse currents because it increases the discrimination against the charging current, since any residual charging current is subtracted out. Figure 3.5 shows the SWV containing the forward, reverse and net currents. The net current is larger than that of the forward and reverse current since it is the difference between them [284]. The peak height is directly proportional to the concentration of the electroactive species and detection limit as low as 10^{-8} is possible. SWV is associated with some advantages over cyclic voltammetry. These advantages include excellent sensitivity and rejection of back ground currents. The scanning speed in SWV is also high. This high speed coupled with computer control and signal averaging allows for experiments to be performed repetitively and increases the signal to noise ratio. SWV is also applied in study of electrode kinetics with regard to preceding, following or catalytic homogeneous chemical reactions and determination of some species at trace levels [285-286]. Square wave voltammetry can play very important role in the characterization of electroactive species with poor, overlapping or ill-formed redox signals in CV by producing individual sharp peaks [284]. It can also be applied in study of the electrode kinetics with regard to preceding, following or catalytic homogeneous chemical reactions and determination of some species at trace levels.
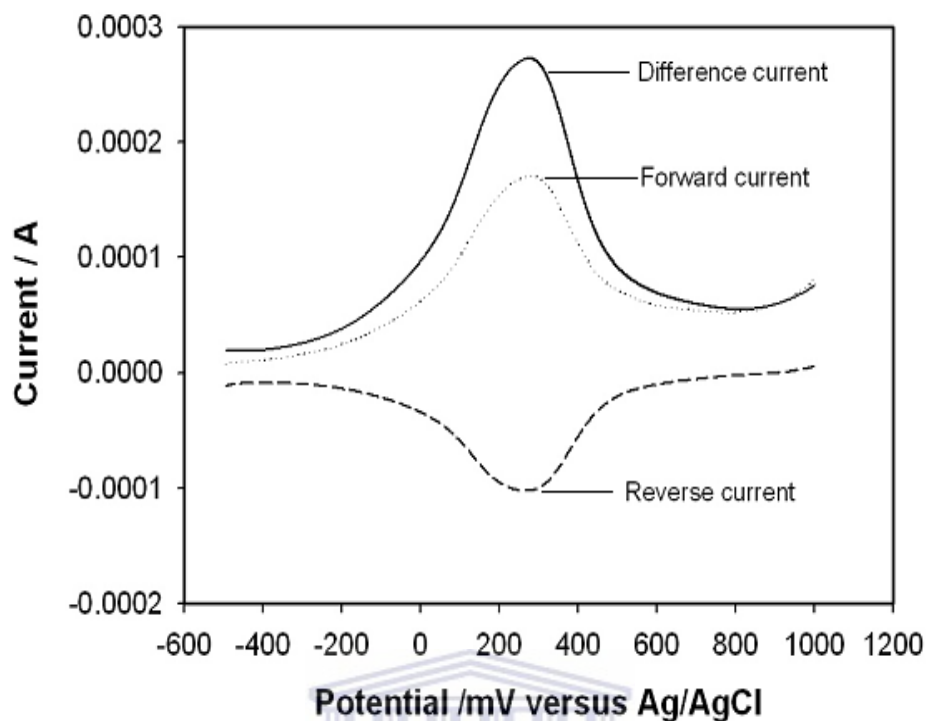
Figure 3.5: A typical SWV containing the forward, reverse and difference currents.

Consequently, the difference (I_d) is larger than each individual component in the region of the peak that is centered on the half-wave potential because I_f, and I_r have opposite signs. This difference effectively cancels the capacitive currents and thus higher scan rates are possible without background current interferences. This makes SWV a useful tool in kinetic studies.

3.3.10 Electrochemical Impedance Spectroscopy

Electrochemical impedance spectroscopy measurements were recorded with a Zahner IM6ex, Germany instrument to quantify the ionic conductivity of electrochemically prepared PPy, PPI-co-PPy, and PPI-2Py in lithium perchlorate (pH 6). At perturbation amplitude of 10 mV within the frequency range 100 kHz to 100 MHz was used. A three-

electrode electrochemical cell with argon deaerated electrolyte was used for all electrochemical measurements. The working, auxiliary and reference electrodes used were Pt, Pt wire, and Ag/AgCl (saturated 3 M NaCl), respectively.

Electrochemical Impedance Spectroscopy (EIS) or ac impedance methods have seen tremendous increase in popularity in recent years. Initially applied to the determination of the double-layer capacitance [287-288] and in ac polarography [289-290], they are now applied to the characterization of electrode processes and complex interfaces. EIS studies the system response to the application of a periodic small amplitude ac signal. These measurements are carried out at different ac frequencies and, thus, the name impedance spectroscopy was later adopted. Analysis of the system response contains information about the interface, its structure and reactions taking place there. EIS is now described in the general books on electrochemistry [291-292]. However, in impedance, a *small* perturbing potential is applied across a cell or sample and changes in a cyclic sinusoidal manner and generates a current resulting from the overpotential (η) caused by the small displacement of the potential from the equilibrium value. Over a time scale, the averaged over potential is zero. Because the potential is only perturbing, it has the advantage of minimizing the concentration change after the experiment. The induced current alternates because the voltage changes in a cyclic manner, and hence the term alternating current (AC). The term impedance is therefore a measure of the ability of a circuit to resist the flow of an AC [286]. It is synonymous to resistance (R) used in direct current (DC), which is defined by Ohm's law equation 3.17 as the ratio between voltage (E) and current (I) [279, 281].

$$R = \frac{E}{I}$$

<div align="right">3.17</div>

While this is a well known relationship, its use is limited to only one circuit element the ideal resistor.

An ideal resistor has several simplifying properties:

• It follows Ohm's Law at all current and voltage levels

• Its resistance value is independent of frequency

• AC current and voltage signals though a resistor is in phase with each other.

The real world contains circuit elements that exhibit much more complex behaviour. These elements force us to abandon the simple concept of resistance. In its place we use impedance, which is a more general circuit parameter. Like resistance, impedance is a measure of the ability of a circuit to resist the flow of electrical current. Unlike resistance, impedance is not limited by the simplifying properties listed above.

Electrochemical impedance is usually measured by applying an AC potential to an electrochemical cell and measuring the current through the cell. Assume that we apply a sinusoidal potential excitation. The response to this potential is an AC current signal. This current signal can be analyzed as a sum of sinusoidal functions (a Fourier series).

Electrochemical impedance is normally measured used a small excitation signal. This is done so that the cell's response is pseudo-linear. Linearity is described in more detail in the following section. In a linear (or pseudo-linear) system, the current response to a

sinusoidal potential will be a sinusoid at the same frequency but shifted in phase. See Figure 3.6.
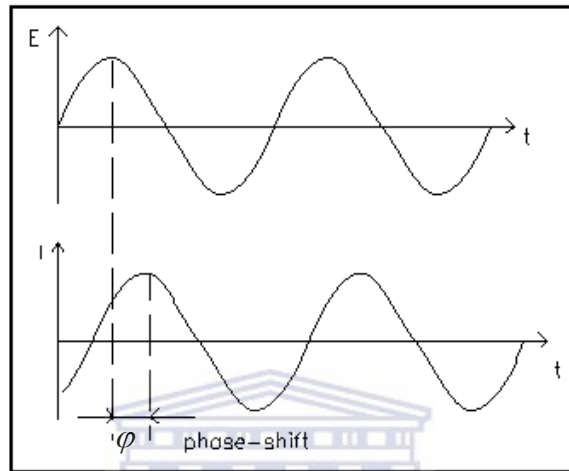
Figure 3.6: Impedance: AC plot of voltage versus current showing the shift in phase.

The system response on the application of a sinusoidal signal is described as:

$$E = E_0 \sin(\omega t) \qquad\qquad 3.18$$

$$i = I \sin(\omega t + \varphi) \qquad\qquad 3.19$$

$$i(t) = \frac{E_0}{|Z|} \sin(\omega t + \varphi) \qquad\qquad 3.20$$

where E_0 is the signal amplitude, ω = angular frequency = $2\pi f$, f is the frequency and φ is the phase angle between the current and the potential. From equation 3.20, the current and the applied potential have the same frequency but it is phase shifted by and angle φ Using

87

complex notation:

$$Z(j\omega) = Z' + jZ'' = R + \frac{1}{j\omega C} = R - j\frac{1}{\omega C}$$

3.21

The total impedance in an EIS measurement is the sum of the real impedance and imaginary impedance, while the modulus of the impedance |Z| is described as:

$$|Z| = \sqrt{(Z')^2 + (Z'')^2} = \sqrt{R^2 + (1/\omega C)^2}$$

3.22 a

$$Z^* = Z' - jZ''$$

3.22 b

The resistance R portion of the impedance is defined as the impedance to the flow of charge and it is frequency independent $Z^*(R) = Z' = R$ and $\varphi = 0$.

Z' is the real impedance which is plotted on the x axis in the Nyquist plot. The concept of double layer of charge on the electrode surface introduces another term called capacitance. The impedance of a pure capacitor is described as:

$$Z^*(C) = Z'' = \frac{1}{j\omega C}$$

3. 23

Z″ is the imaginary impedance which is a measure of the capacitance and it is frequency dependent $\varphi = -\pi/2$

While the phase angle φ is described as:

$$\tan \varphi = \frac{Z''}{Z'} = \frac{1}{\omega RC}$$

3. 24

Admittance is the inverse of impedance and it is described as:

$$Y = \frac{1}{Z}$$

3. 25

and

$$Y = jC\omega$$

3. 26

Usually data is presented in two major ways the Nyquist (complex plane) plot and the Bode plot, Nyquist plot is a plot of imaginary impedance, Z''' versus real impedance, Z'. The experimental data collected from an impedance experiment is often presented as Nyquist plot of Z' (usually positive x-axis corresponds to the real impedance), versus Z'' (usually, the positive y-axis correspond to –Z'', over a wide frequency range (normally 100 kHz to 0.1 Hz). The Nyquist plot of impedance spectra includes a semicircle portion and a linear portion, with the former at higher frequencies corresponding to the electron transfer process and the latter at lower frequencies corresponding to the diffusion process. The electron transfer resistance (R_{ct}) at the electrode surface is equal to the semicircle diameter, which can be used to describe the interface properties of the electrode [293].

Another way of presenting impedance data is a Bode plot in which the logarithm of the absolute value of Z' and the phase (φ) are plotted against the logarithm of the frequency (f) [294]. This can be plotted together or separately. Nyquist plots are more commonly displayed for historical reasons, the data is however often poorly resolved (particularly at

high frequencies), and the explicit frequency dependence is not displayed in the plot. In contrast, the Bode plot directly displays the frequency dependence; in addition, the data is well resolved at all frequencies, since a logarithmic frequency scale is used. When the frequency of the AC waveform is varied over a wide range of frequency (ca. about 10^{-4} and > 106 Hz), the impedance obtained for the system is a function of the operating frequency. Spectra of the resulting impedance at different frequencies reveal the different electrochemical kinetics involved in the system. While dipolar properties are manifest at high frequency regions, bulk and surface properties will be evident at intermediate and low frequencies respectively [294]. The total impedance of a system is determined by the impedances of the various components of the electrochemical cell; for example, electron transfer kinetics, diffusion and passivating layers. The relative contribution of the various components typically varies with frequency; for example, electron transfer kinetics may dominate at high frequencies, whereas diffusion may dominate at lower frequencies [294].

Measuring impedance over a wide frequency range allows processes with different time scales such as electron transfer, mass transport and chemical reaction to be detected within the same experiment. Impedance data is commonly analyzed by fitting it to an equivalent circuit model. The frequently used circuit, called the Randles equivalent circuit is composed of different elements such as resistors, capacitors, and inductors joined in series or in parallel. Figure 3.7 shows the impedance diagram for the real impedance (x-axis) and imaginary impedance (y-axis) with low frequency data being on the right side of the plot and higher frequencies are on the left [294].
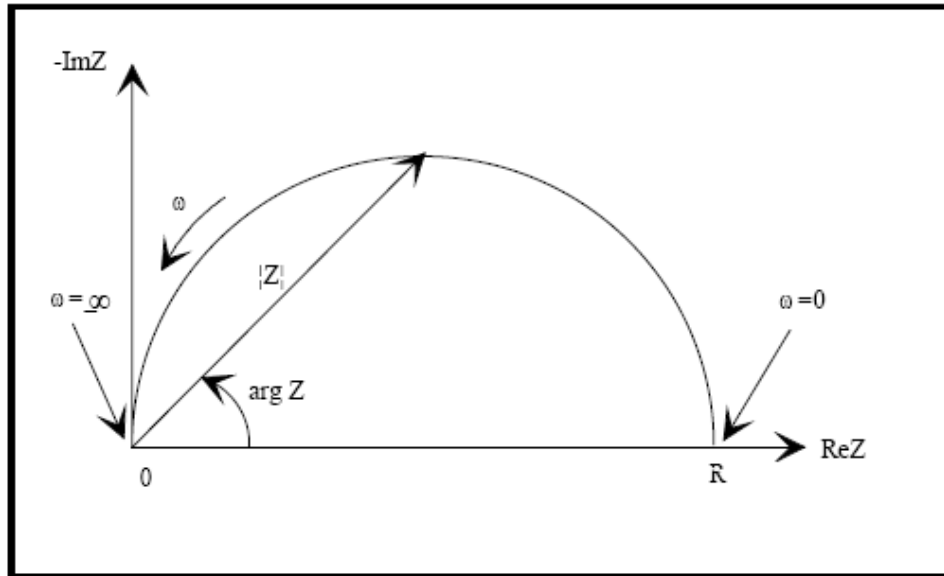
Figure 3.7: A typical impedance diagram.

A typical Nyquist plot for the impedance data is shown in Figure 3.8. The semicircular shape is characteristic of a single "time constant".
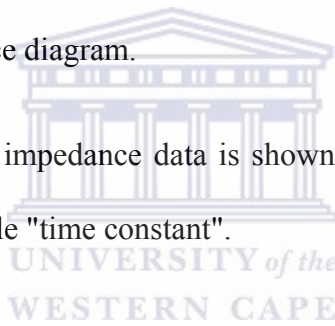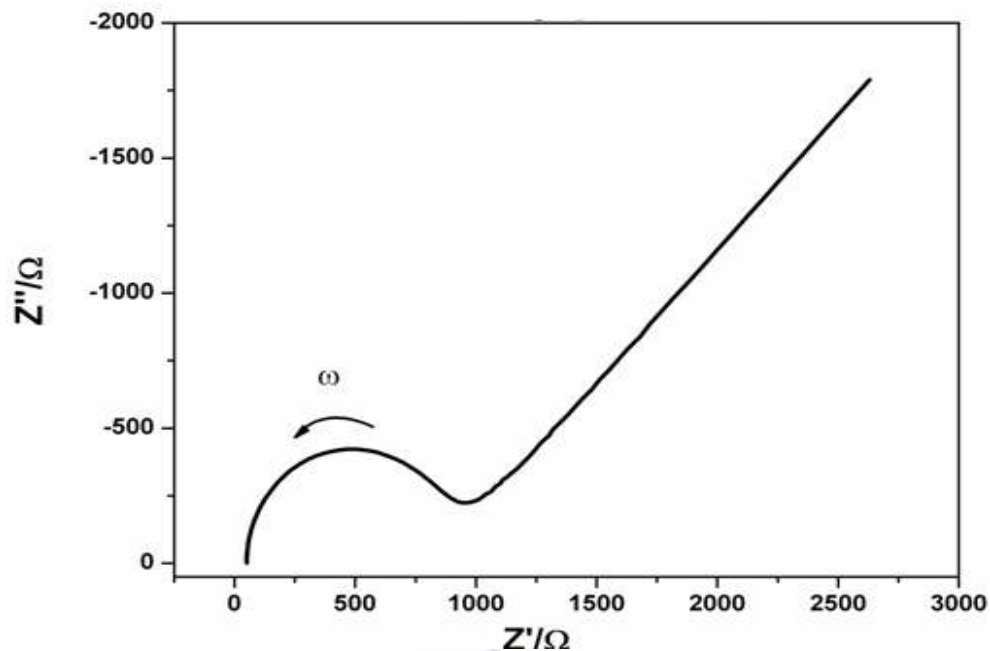
Figure 3.8: A typical Nyquist plot.

EIS is a useful tool in studying the kinetics of electrochemical reactions. Redox reactions usually involve charge transfer kinetics and mass transfer. The slower of this two determines the rate of the reaction. The mass transfer in EIS is limited to diffusion (concentration gradient) by the steady state condition. Figure 3.9 shows the Nyquist plot indicating the kinetically controlled (higher frequency) and the mass controlled (low frequency) parts of the plot.
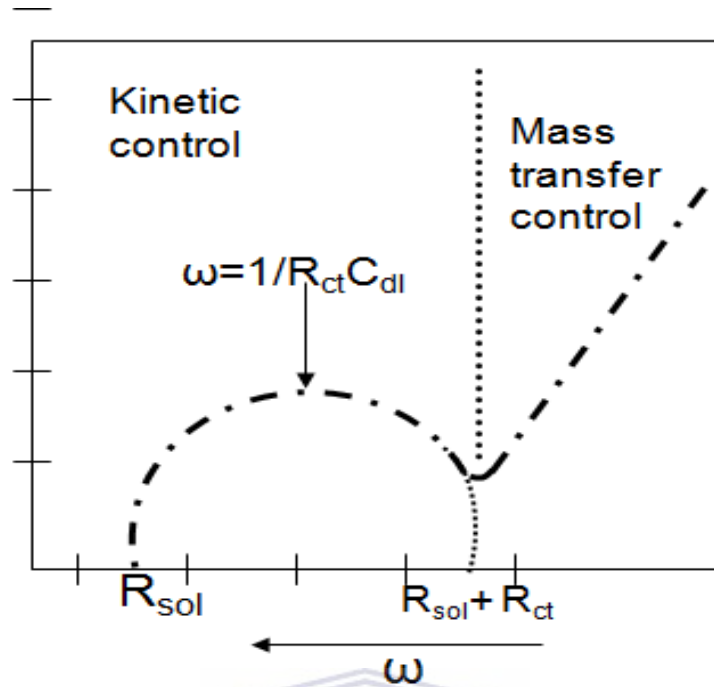
Figure 3.9: A typical Nyquist plot showing some kinetic parameters.

From ω_{max} (frequency at maximum imaginary impedance of the semicircle) useful kinetic parameters such as double layer capacitance (C_{dl}) (obtained using equation 3.27), time constant (cycle life) τ (calculated using equation 3.28), exchange current I_o (calculated using equation 3.29), and heterogeneous rate constant K_{et} (calculated using equation 3.30) can be evaluated:

$$\omega_{\text{max}} = \frac{1}{R_{\text{ct}}C_{\text{dl}}}$$
3.27

$$\tau = R_{\text{ct}}C_{\text{dl}}$$
3.28

$$I_0 = \frac{RT}{nFR_{\text{ct}}}$$
3.29

$$K_{et} = \frac{I_0}{nFAC_0}$$

3.30

where $\omega_{max} = 2\pi f$, R_s is the solution resistance, R_{ct} is the charge transfer resistance, C_{dl} is the double layer capacitance, R is the gas constant (8.314 J K^{-1} mol^{-1}), F is the Faradays constant ($96\,486$ C mol^{-1}), n is the number of electrons, τ is the time constant or cycle life (relates to the time required for the proton to completely move across the electrolyte layer from one side to the other), I_0 is the exchange current (relates to rate constant to electron transfer at zero overpotential), C_0 is the concentration (mol cm^{-3}), and K_{et} is the heterogeneous rate constant.

A representative plot of frequency as x-axis versus logarithm of real impedance as y_1-axis, and phase angle as y_2-axis called Bode plot is presented in Figures 3.10 and 3.11 A Bode plot is a plot of log magnitude of impedance and phase angle versus log of frequency [286].
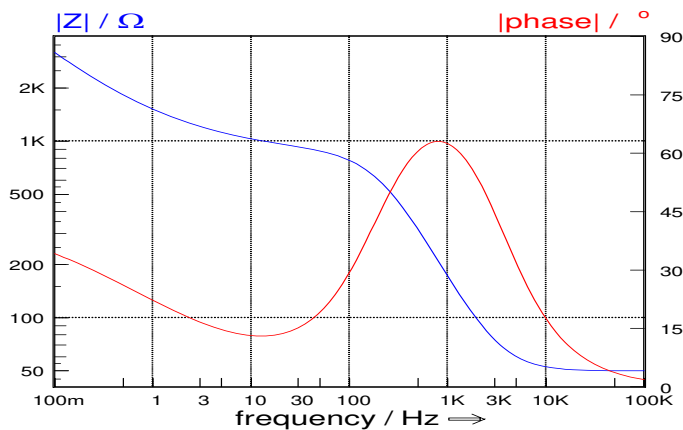
Figure 3.10: A typical Bode plot showing variation of impedance and phase angle with changes in frequency.
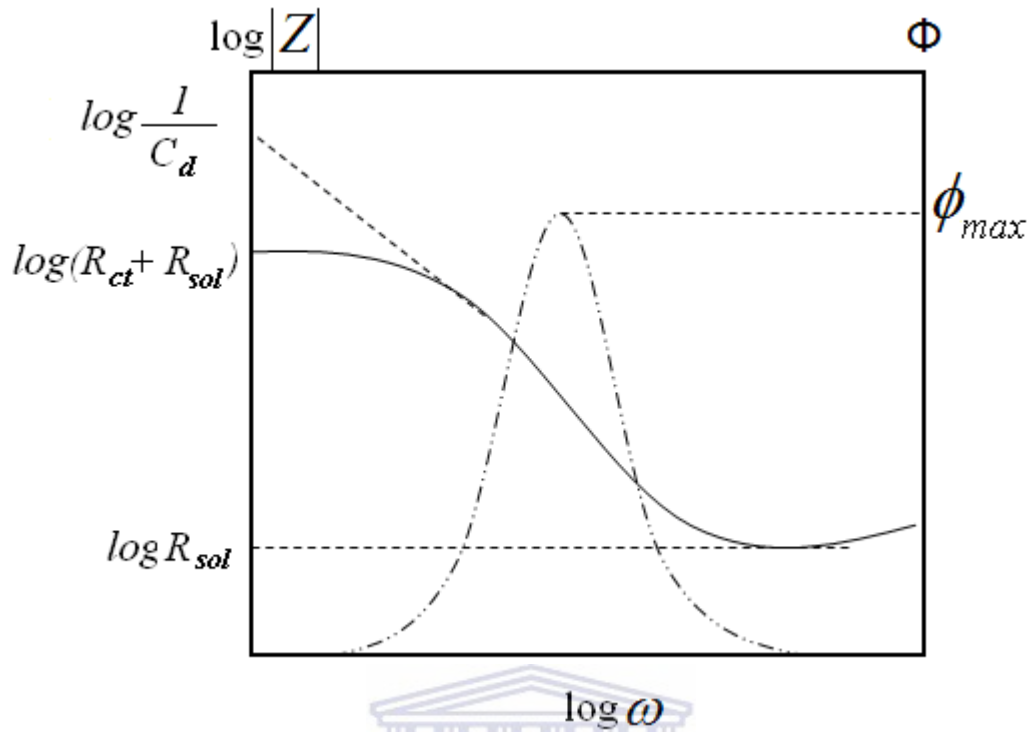
Figure 3.11: A Bode plot showing some kinetic parameters.

The Bode plot gives direct information on the frequency and phase angle. The frequency at maximum phase is a useful parameter in determining the double layer capacitance, using equation 3.31:

$$\omega_{\phi max} = \frac{(1 + R_{ct} / R_{sol})}{R_{ct} C_{dl}}$$

3.31

The commonly used Randles equivalent circuit for fitting of the impedance data is shown in Figure 3.12.
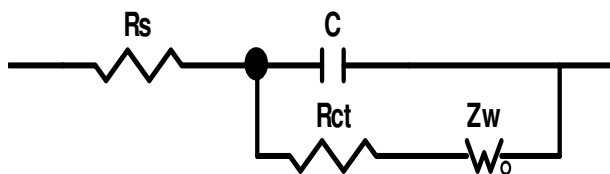
Figure 3.12: Randles equivalent circuit for a simple electrochemical cell.

C is capacitance, which is the ability of an electrochemical system to store or retain charge, and Z_w is the Warburg impedance associated with the resistance as a result of the diffusion of ions across the electrode/electrolyte interface. Thus, EIS can give useful information of the impedance changes on the electrode surface before and after modification.

3.4 Experimental Procedures

3.4.1 Synthesis of 2-Pyrrole Functionalized Poly(propylene imine) Dendrimer from G1 to G4 (PPI-2Py)

The synthesis of PPI-2Py was carried out by, first, a condensation reaction of PPI with 2-pyrrole aldehyde. A reaction mixture of PPI generation 1 (1 g, 3.15 mmol) and 2-pyrrole aldehyde (1.2 g, 12.625 mmol) in 50 mL dry methanol (50 mL) was magnetically stirred under a positive pressure of nitrogen gas for 2 days in a 100 mL three-necked round-bottom flask. The quantities used in the cases of G2 to G4 are given in Table 3.1. The methanol was removed by rotary evaporation, the residual oil was dissolved in 50 mL dichloromethane (DCM), and the organic phase was then washed with water (6 × 50 mL) to remove unreacted monomer. The DCM was removed by rotary evaporation and yielded

the desired product as an orange oil. The method used above is a slight modification of that reported by Smith *et al.* [295] and Salmon and Jutzi [296]. See Scheme 3.1. The yield was 1.65 g, 75 %.

^{1}H-NMR (CDCl$_3$ 200 MHz, ppm): 1.36 (s, br, 4H, H-1), 1.74 (t, 8H, H-2), 2.43 (m, br, 12H, H-2&3), 3.51 (t, 8H), 6.21 (t, 8H, H-8), 6.47 (d, 4H, H-7), 6.86 (s, 4H, H-9), 8.1 (s, 4H, H-6). The NMR spectrum of PPI-2Py showed a new chemical shift at 8.1 ppm for N=CH. Strong FTIR bands appeared at 1634 cm^{-1} for ν (N=C) in the dendrimer moiety and at 729 cm^{-1} for the out-of-plane bending ν(C-H) at the α position of the Py ring.

Table 3.1: Quantities of PPI dendrimer and 2-pyrrole aldehyde used during functionalization of PPI dendrimer

PPI dendrimer generations	PPI dendrimer (g, m mol)	2-Pyrrole aldehyde (g, m mol)
G1	1, 3.15	1.2, 12.625l
G2	0.5, 0.6468	0.492, 5.176
G3	0.5, 0.2965	0.2804, 4.745
G4	0.5, 0.1423	0.4325, 4.550
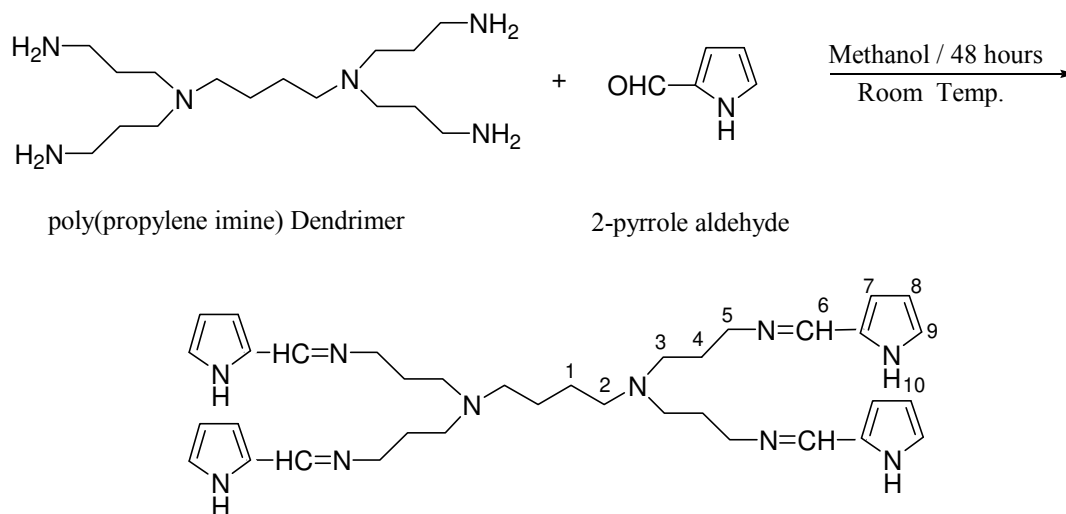
Scheme 3.1: Functionalized poly(propylene imine) dendrimer.

3.4.2 Chemical Oxidative Polymerization of Pyrrole from Functionalized Dendrimers G1-2Py–G4-2Py

The PPI-co-PPy was synthesized by reacting PPI-2Py with Py monomer using ammonium persulfate $((NH_4)_2S_2O_8)$ (APS) as an oxidant via chemical oxidative copolymerization. Conducting star copolymers with PPy side chains were obtained (see Scheme 3.2). In a typical experiment, G1PPI-2Py (0.1 g, 0.16 mmol) and Py (0.28 mL, 0.2 M) were dissolved in chloroform (20 mL), with stirring. Ammonium persulfate (0.9128 g, 0.2 M) in distilled water (20 mL) was slowly added to the above solution. The quantities used in the cases of G2PPI-2Py to G4PPI-2Py are given in Table 3.2. The polymerization reaction was carried out at room temperature for 1 hr and then terminated by pouring methanol into the reaction flask. The resultant PPI-co-PPy powder was filtered, washed several times sequentially with distilled water, methanol and acetone, filtered, and then dried in a vacuum oven at 45 °C for 12 hr. The yield was 0.145 g, 33%. This method was adapted

from literature [297], with slight modification. A similar experimental procedure was used to prepare homopolymer PPy, but here no PPI-2Py was added to the reaction mixture.

Table 3.2: Quantities of functionalized dendrimer, Py and APS used during polymerization

Functionalized dendrimer PPI-2Py	Py	APS
G1-2Py, 0.1 g, 0.1601 mmol	0.28 mL, 0.2 M	0.9128 g, 0.2 M
G2-2Py, 0.1 g, 0.0719 mmol	0.28 mL, 0.2 M	0.9128 g, 0.2 M
G3-2Py, 0.1 g,	0.28 mL, 0.2 M	0.9128 g, 0.2 M
G4-2Py, 0.1 g, 0.0167 mmol	0.28 mL, 0.2 M	0.9128 g, 0.2 M

Functionalized PPI Dendrimer (PPI-2Py)   Pyrrole
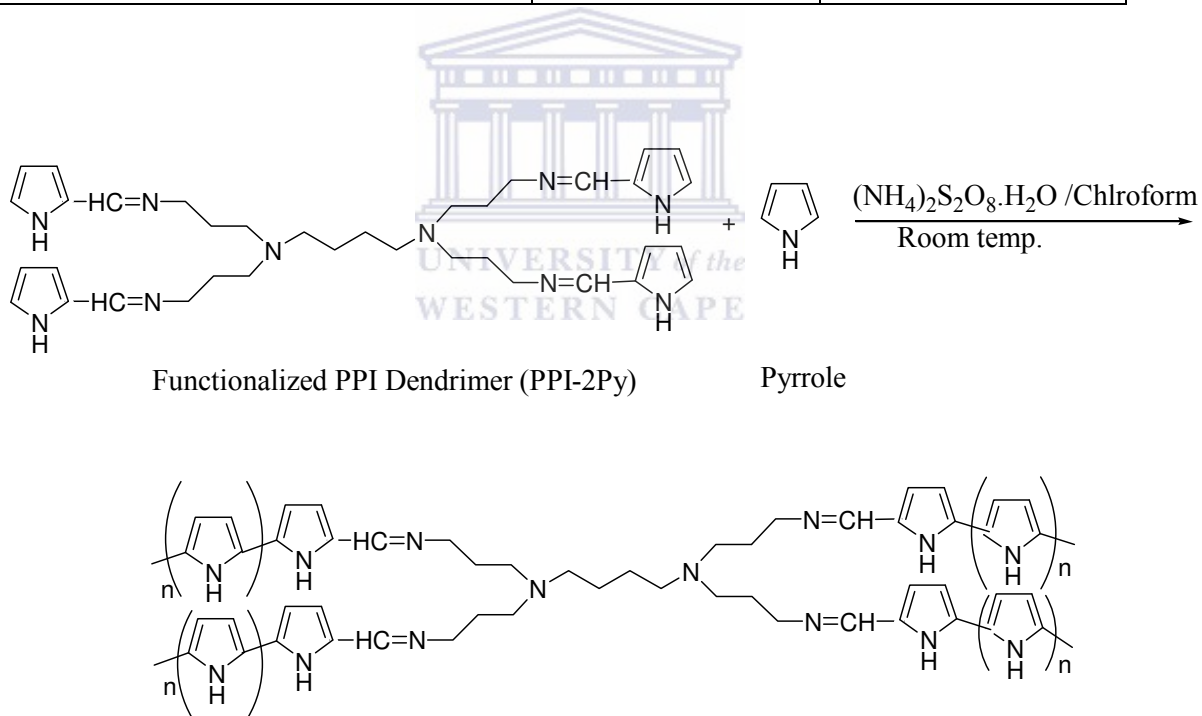
Scheme 3.2: Schematic of the synthesis of conducting star copolymers.

3.4.3 Electrodes and Solution Preparation

A Pt electrode was used throughout this study. The cleaning method commonly used for the preparation of electrodes for electrochemical measurements involves mechanical polishing. The Pt electrode was first polished repeatedly with 1.0, 0.3, and 0.05 μm alumina slurries, respectively. It was then cleaned with piranha (30% H_2O_2:H_2SO_4, 1:3) for 10 min at 80 °C in an oven, followed by sonication in ethanol and water, consecutively, for 5 min. The electrode was further cleaned electrochemically in 1 M sulfuric acid by cycling between the potentials -600 mV and +1000 mV until a reproducible cyclic voltammogram was obtained. Finally, it was thoroughly rinsed with distilled water. A small volume of PPI-2Py (5 μl) was drop coated onto, allowed to dry under a blanket of nitrogen gas, and then left to dry at room temperature. Solutions were prepared using general procedures and formulae, such as shown in equations 3.32 and 3.33, for preparation and dilution of solutions, respectively:

$$mass = \frac{molar.mass * Molarity * volume}{1000}$$

3.32

$$C_1V_1 = C_2V_2$$

3.33

3.4.4 Electrochemical Polymerization of Pyrrole on Electrodes Surfaces Coated with Pyrrole Functionalized Dendrimers G1-2Py to G4-2Py

Electrochemical polymerization of Py on Pt electrode surfaces coated with PPI-2Py was carried out in an electrochemical cell containing 5 mL of 0.1 M aqueous lithium perchlorate solution as support electrolyte and 0.177 mL of 0.5 M Py monomer.

Electrochemical polymerization was achieved by CV (+800 mV to -600 mV), performed at a scan rate of 50 mV s^{-1}, for 20 cycles. Before applying the potential to the above polymerization solution, the solution was degassed by bubbling argon gas through for 15 min, and then maintaining it oxygen-free by keeping a blanket of argon above the solution. It is during this electropolymerization process that PPy is electrodeposited on the surface of the coated electrode. The modified electrode was then removed from the solution and rinsed with water to remove any traces of monomer. A similar experimental procedure was used to prepare homopolymer PPy onto the bare polished Pt electrode surface, except that here no PPI-2Py was coated onto the Pt electrode surface.

CHAPTER 4

Results and Discussion:

Analytical Results and Electrochemistry of the Novel Conducting Star Copolymers

4.1 Introduction

This chapter presents the analytical results and electrochemistry of the novel conducting star copolymers that were prepared as described in the experimental section (3.4). A summary of the preparation methods/procedures used (chemical oxidative polymerization and electrochemical polymerization) is included here, for clarity. Novel macromolecular star copolymers based on poly(propylene imine) (PPI) dendrimer core and polypyrrole (PPy) shell were prepared. A series of dendrimeric PPy PPI star copolymers was synthesized chemically and electrochemically using generations 1 to 4 (G1 to G4) PPI dendrimer and pyrrole (Py). The synthesis procedure involved a condensation reaction between the diamino functional dendrimer and 2-Py aldehyde to afford the Py functionalized PPI dendrimer (PPI-2Py). Chemical oxidative polymerization of the PPI-2Py with additional Py monomer, using ammonium persulfate as an oxidizing agent, afforded poly(propylene imine)-co-polypyrrole (PPI-co-PPy). In an electrochemical polymerization, PPI-2Py deposited on a platinum (Pt) electrode was polymerized by cyclic voltammetry (CV) (+800 mV to -600 mV), performed at 50 mV s^{-1} in a 0.1 M LiClO$_4$ solution of 0.5M Py.

Results given and discussed in this chapter have also appeared in published form [298].

4.2   Fourier Transform Infrared Spectroscopy

The FTIR transmission spectra of PPy, PPI, PPI-2Py and PPI-co-PPy are shown in Figure 4.1 (A, B, C, D). The spectrum of PPy (Figure 4.1 A) shows absorption peaks at 3400 cm^{-1}, 1540 cm^{-1}, 1295 cm^{-1}, 1133 cm^{-1}, 1033 cm^{-1}, 890 cm^{-1}, and 777 cm^{-1}. Similar results have been reported by Depaoli *et al.* [299] and Kang *et al.* [300], namely, stretching vibration bands of the Py ring at 1543 cm^{-1} (C=C), 1295 cm^{-1} (C–C), and 1130 cm^{-1} (C–N). The peak at 3400 cm^{-1} is assigned to the N–H stretching vibration in Py. The peaks for C–H stretching and N–H bending of Py appear at 1043 cm^{-1}, while the peak for C–H bending appears at 780 cm^{-1}.

The FTIR spectra of PPI dendrimers (G1PPI to G4PPI) are shown in Figure 4.1 B. Characteristic peaks appear in the regions of 2934 and 2858 cm^{-1} (C–H stretching vibration), 1590 cm^{-1} (N–H bend), 1463 cm^{-1} (C–H bend), 1305 cm^{-1} and 1081.6 cm^{-1} (C–N stretching vibration) [301].

The spectra of PPI-2Py, from G1PPI-2Py to G4PPI-2Py (Figure 4.1 C) show out-of-plane bending of the C–H bond located at the α position in the Py ring appearing at 729 cm^{-1} [302], while the sharp band at 1634 cm^{-1} is assigned to the N=C bond stretching vibration present in the dendrimer moiety. The appearance of these two characteristic peaks confirms the functionalization of the amine groups of PPI by 2-Py.

In the PPI-co-PPy spectrum (Figure 4.1 D), the bands due to PPy appear at 1549 cm^{-1}, 1181 cm^{-1}, 1035 cm^{-1} and 899 cm^{-1}, whereas the sharp N=C band in PPI-2Py now appears

at 1671 cm^{-1}. Furthermore, most of the characteristic peaks of the PPy remained unchanged upon copolymerization with PPI-2Py The intense absorption at 729 cm^{-1}, ascribed to the out-of-plane C–H bending at the α position of the Py moiety, disappeared completely. This is an evidence of the polymerization from C–H at the α position of the Py moiety of the functionalized dendrimers, and conversion to PPI-co-PPy via α–α coupling. The sharp absorption peak at 1043 cm^{-1} corresponds to the N-H deformation [303]. The peaks at 1290 cm^{-1} and 1565 cm^{-1} are related to the C–C stretching vibration and C=C stretching mode of the Py ring, respectively [304].

(A)

(B)

Absorption (T%) vs Wavenumber (cm^{-1})

C-H   C-H   C-N

- G1PPI
- G2PPI
- G3PPI
- G4PPI

(C)

Absorption (T%) vs Wavenumber (cm^{-1})

N=C   α

- G1PPI-2Py
- G2PPI-2Py
- G3PPI-2Py
- G4PPI-2Py
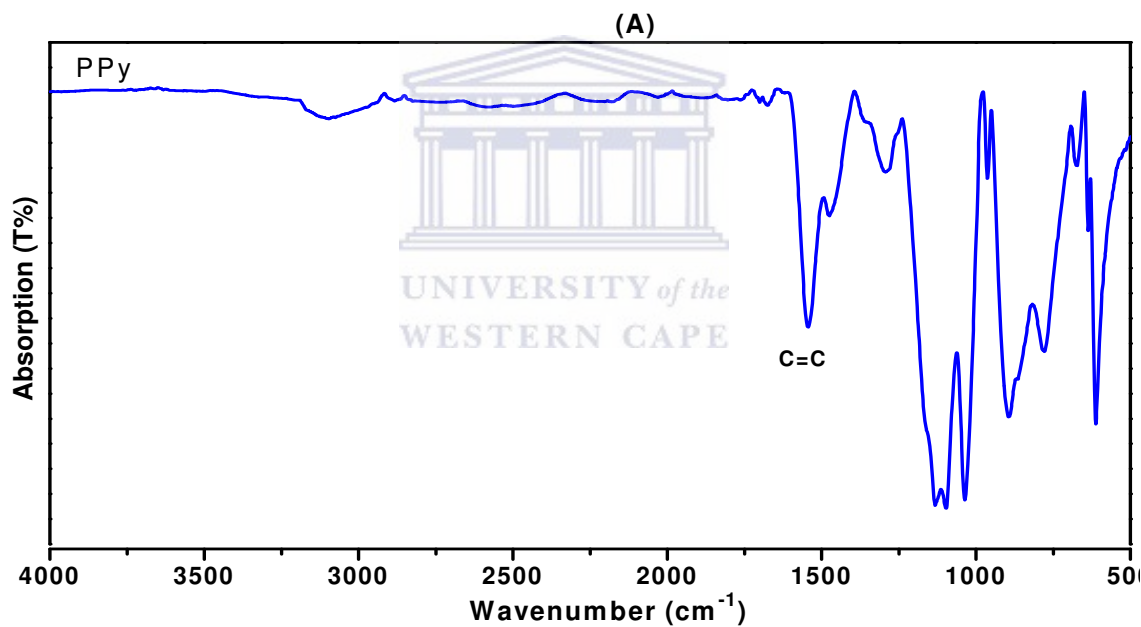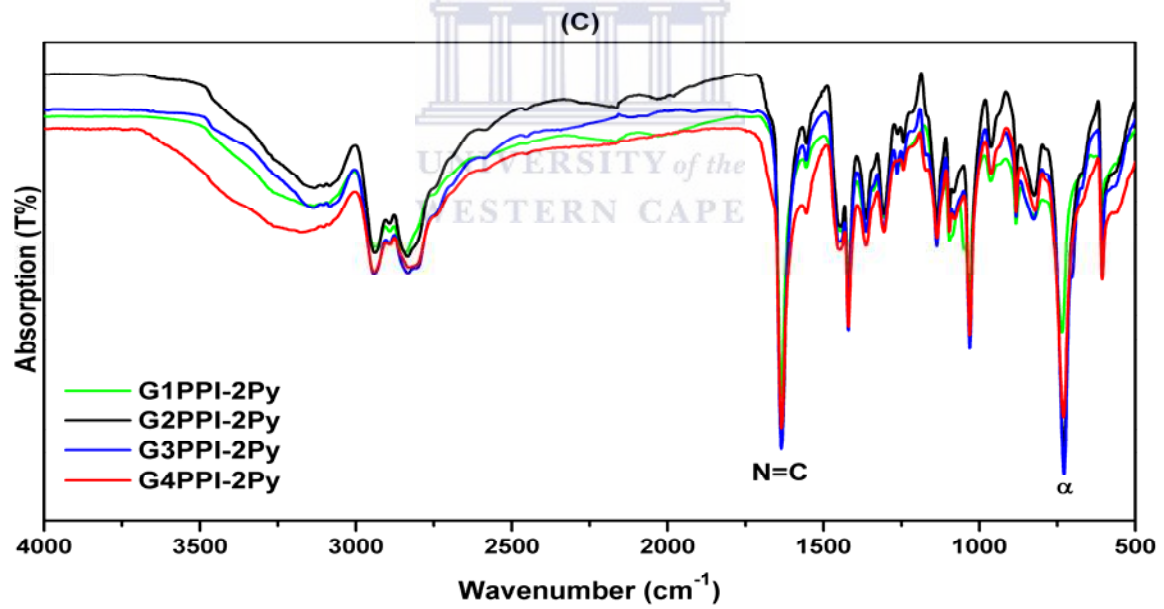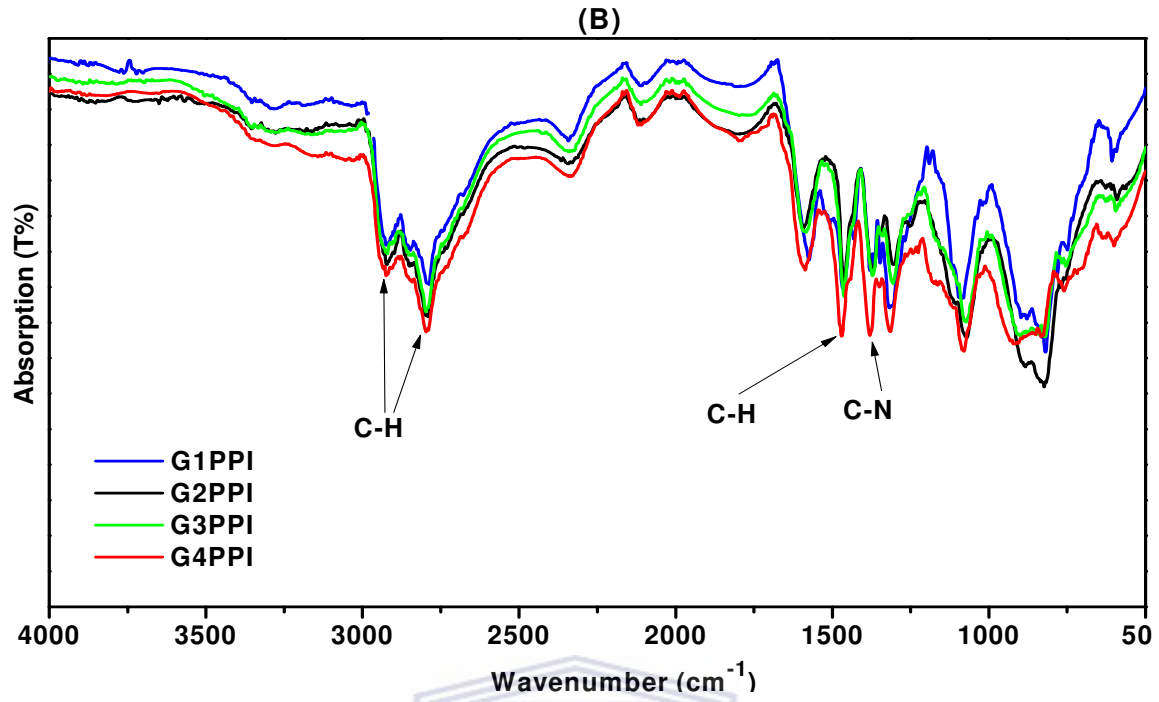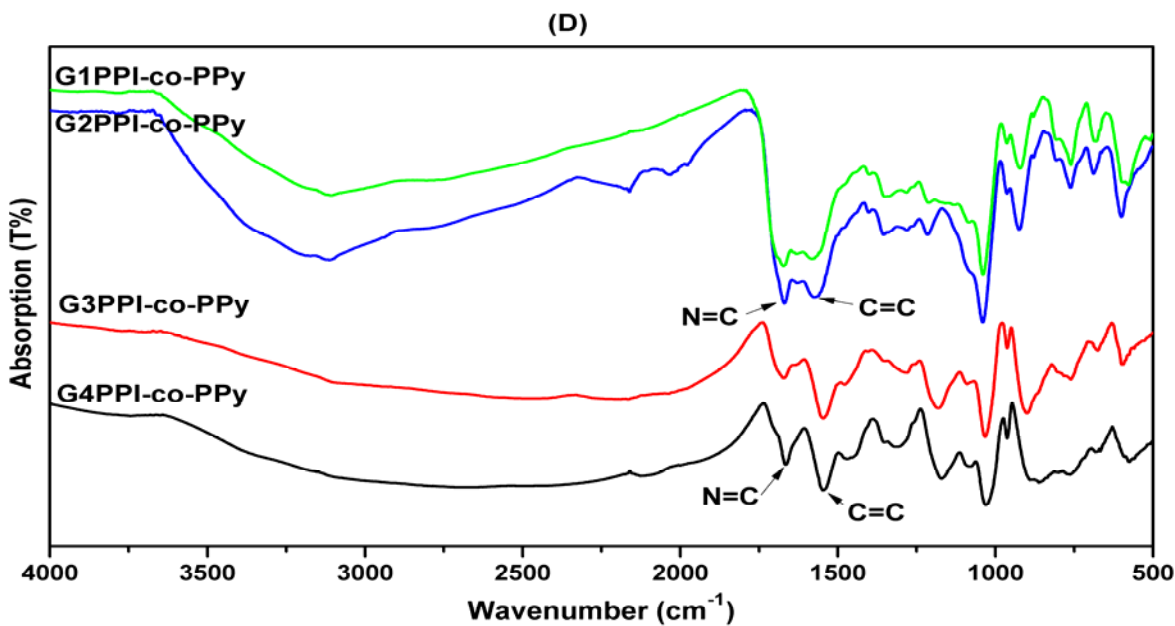
Figure 4.1: FTIR spectra of (A) polypyrrole (PPy), (B) PPI dendrimers, (C) functionalized dendrimer (PPI-2Py) and (D) star copolymer (PPI-co-PPy).

4.3   Fluorescence Spectroscopy

The G1PP1 dendrimer exhibited fluorescence properties, with excitation and emission bands at 390 and 448 nm, respectively (Figure 4.2 A). Similar results were also reported by Wang *et al*. [305]. PPy exhibited excitation and emission bands at 351 and 384 nm, respectively (Figure 4.2 B). The star copolymer exhibits fluorescence properties with excitation and emission bands at 385 and 422 nm, respectively (Figure 4.2 C). The star copolymer was excited at the wavelengths corresponding to those of PPI and PPy, to determine whether the constituents retained their individual properties. The observed emissions could not be reversed to their excitation bands upon an emission-excitation scan. In fact, the bands of the star copolymer seemed to be an average of its constituents, indicating a type of hybrid material.
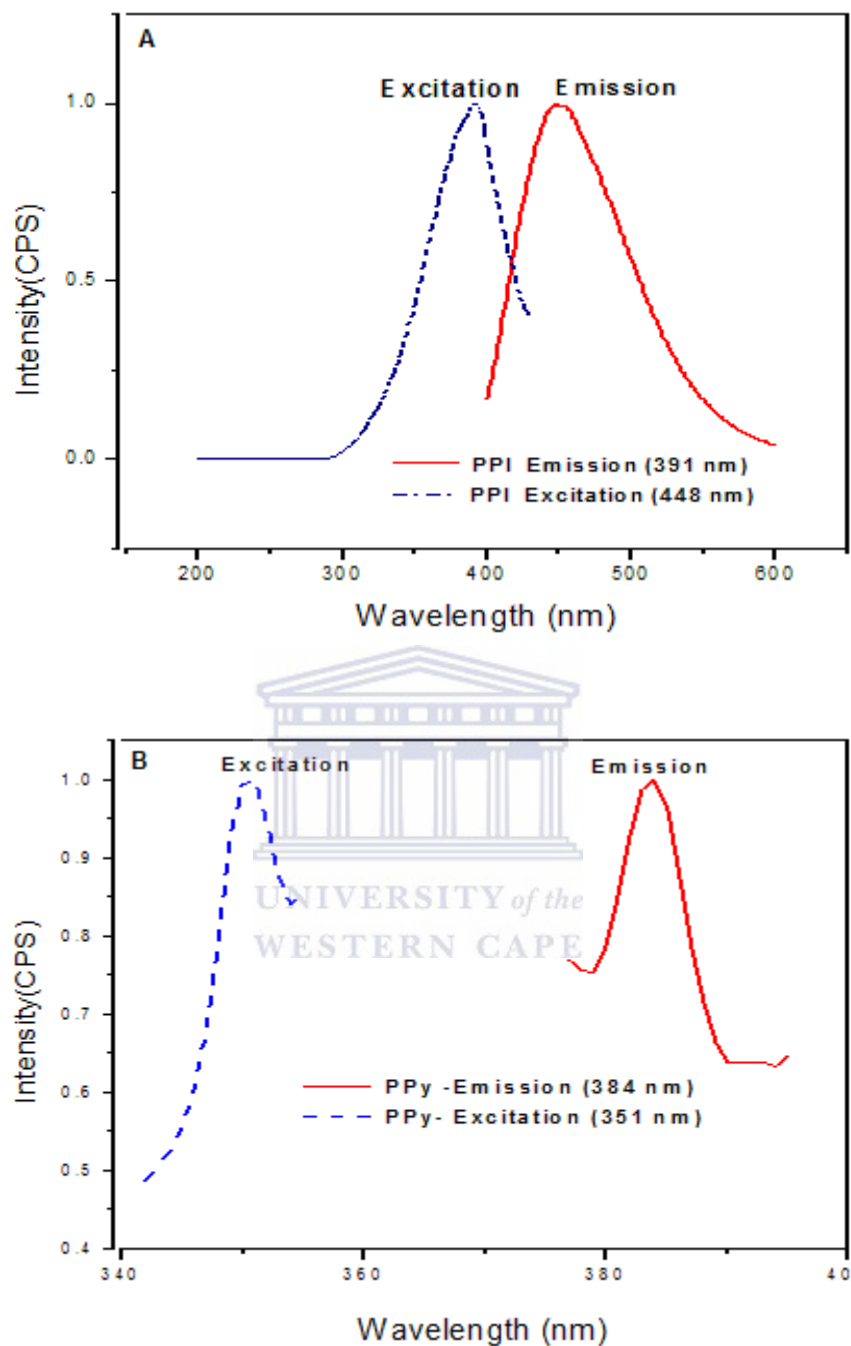
Figure 4.2 A & B: Fluorescence spectra of (A) G1PPI dendrimer, and (B) PPy
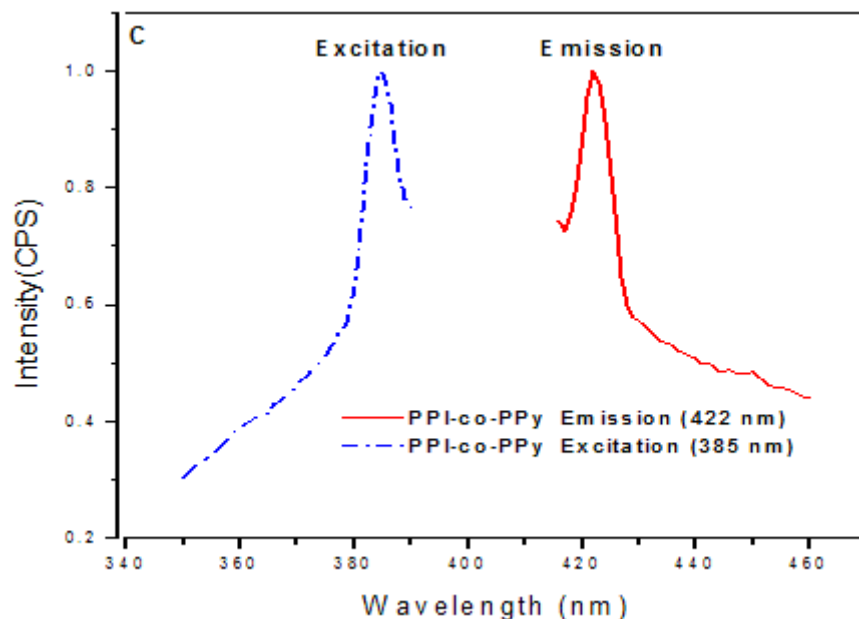
Figure 4.2 C: Fluorescence spectra of G1PPI-co-PPy dendritic star copolymer.

4.4 Scanning Electron Microscopy

The morphology of PPy differs, depending on the method of preparation, as seen in Figures 4.3 A and 4.3 B. In the case of chemically prepared PPy (4.3 A), the morphology resembles densely clustered florets, whereas the electrochemically prepared PPy (4.3 B) exhibits a dense growth of whelk-like helixes [306] initiating from the bare Pt-electrode surface, with an average base diameter of 1.0 μm. The surface of the PPI-2Py coated on a Pt electrode surface is shown in Figure 4.3 C. The morphology of the chemically prepared star copolymers resembles that of a flaky waxy material (Figure 4.3 D), in comparison to the orderly electrochemical growth of whelk-like helixes (Figure 4.3 E). At higher magnification, the whelk-like helixes of the star copolymers are hollow tubes with openings at their tapered ends, and with an average base diameter of 2.0 μm (Figure 4.3 F). Figures 4.4 G and H show the whelk-like helixes of electrochemically prepared

G2PPI-co-PPy. Figures 4.4 I and J show the whelk-like helixes of electrochemically prepared G3PPI-co-PPy star copolymers. Figures 4.4 K and L show the electrochemically prepared G4PPI-co-PPy star copolymers. These images clearly show the size difference from G1PPI-co-PPy to G4PPI-co-PPy, depending on the number of end groups on the functionalized dendrimers – the smaller the end group the bigger the size of the arms.

Chen *et al*. [306] reported the preparation of PPy whelk-like helixes on the surface of a glassy carbon electrode with an average base diameter of 1.0 μm via electrochemical polymerization of Py monomer in the presence of a surfactant. They reported that a high surface area and hydrophilicity of the PPy whelk-like helixes enhance electrocatalytic activity, as shown by an increase in the oxidation current of ascorbic acid [306]. Results of experiments carried out in the present study show that PPy whelk-like helixes can form on a bare Pt surface in the absence of surfactant as well as on a Pt surface coated with a Py-functionalized dendrimer via electropolymerization of Py in the presence of aqueous LiClO$_4$.
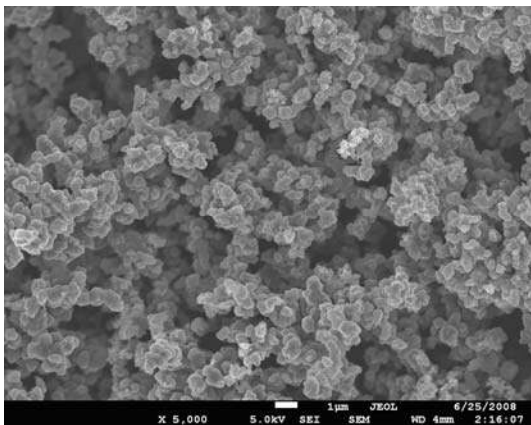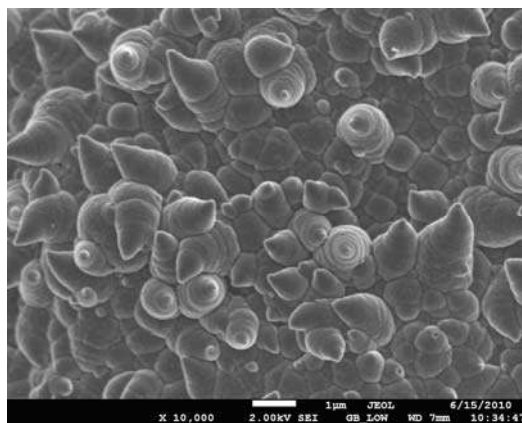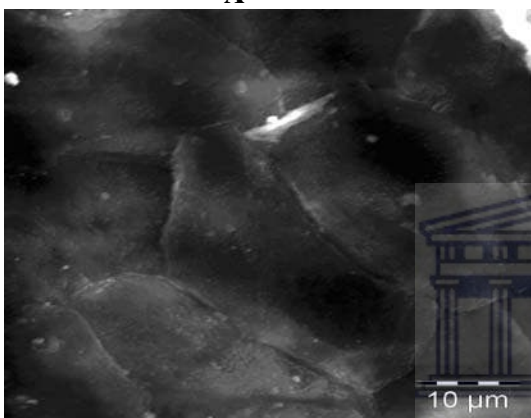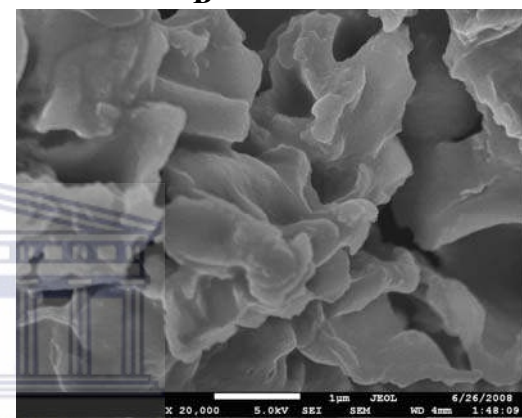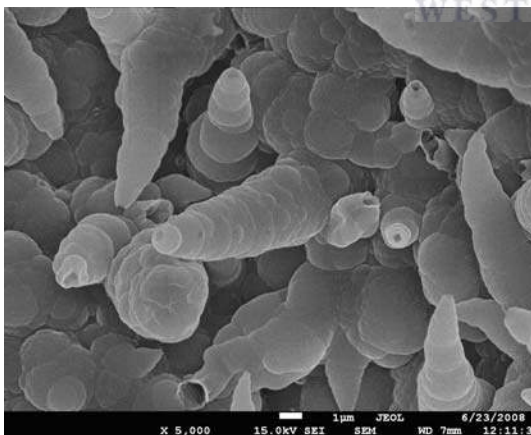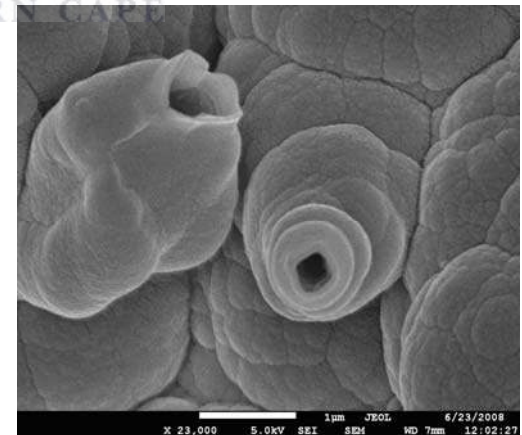
Figure 4.3: SEM images: (A) chemically synthesized PPy (×5000), (B) electrochemically synthesized PPy (×10,000), (C) functionalized dendrimer (PPI-2Py), (D) chemically synthesized G1PPI-co-PPy (×20,000), (E) electrochemically polymerized G1PPI-co-PPy (×5000), (F) electrochemically polymerized G1PPI-co-PPy (×23,000).
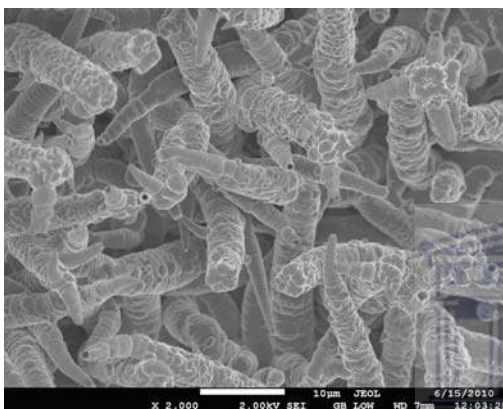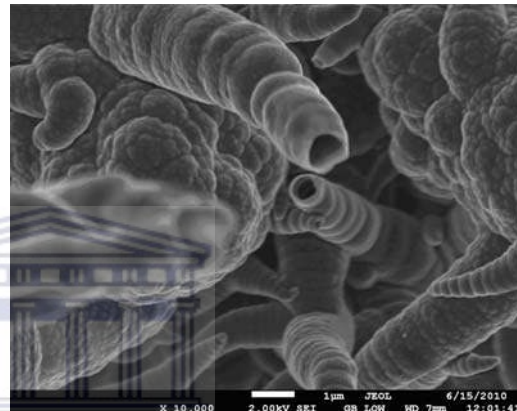
Figure 4.4: SEM images: (G) electrochemically polymerized G2PPI-co-PPy (×3500), (H) electrochemically polymerized G2PPI-co-PPy (×10,000), (I) electrochemically polymerized G3PPI-co-PPy (×2000), (J) electrochemically polymerized G3PPI-co-PPy (×10,000), (K) electrochemically polymerized G4PPI-co-PPy (×3500), and (L) electrochemically polymerized G4PPI-co-PPy (×3500).

4.5   Thermogravimetric Analysis

The thermograms of weight loss versus temperature for PPy, PPI-co-PPy, PPI-2Py and PPI were recorded at a heating rate of 10 °C min^{-1} in a nitrogen atmosphere. Results are shown in Figure 4.5. A, B and C. The weight change over the 50 to 120 °C temperature range is associated with the loss of ingress moisture present in the samples. Van Genderen *et al.* [307] have shown that the TGA of amine-terminated dendrimers is unexpectedly high, and increases with increasing molar mass. The TGA max values (temperature at which the weight loss is maximal) for G1PPI-dendrimer-(NH$_2$)$_4$ and G4PPI-dendrimer-(NH$_2$)$_{32}$ are 340 and 460 °C, respectively. For G1PPI-dendrimer-(NH$_2$)$_4$ and G4PPI-dendrimer-(NH$_2$)$_{32}$ < 10% weight loss is observed at 270 °C and 410 °C, respectively. Although nitrile-terminated dendrimers usually are not very stable at higher temperature, here it was observed that the stability increased with higher generations [308].

The thermograms for G1PPI-2Py to G4PPI-2Py showed similar thermal decomposition behaviour. The thermal decomposition behaviour of star copolymers is shown in Figures 4.5 B and 4.5 C. There was a 10% weight loss up to 250 °C, mainly due to the removal of some volatile compounds, followed by a slow and gradual decomposition of the polymer backbone up to 450 °C. The thermograms in Figure 4.5 A show a significant increase in onset temperature with increasing Py content, in the order PPI < PPI-2Py < PPI-co-PPy < PPy. In addition, the residue remaining after thermal decomposition at 700 °C was found to be in the order PPI (0%) < PPI-2Py (38%) < PPI-co-PPy (47%) < PPy (66%).

These results demonstrate that the incorporation of Py into the dendrimer increases the

thermal stability [309] and that the Py content is directly proportional to the star copolymer thermal stability. The star copolymer has thermal stability similar to that of PPy.

(A)
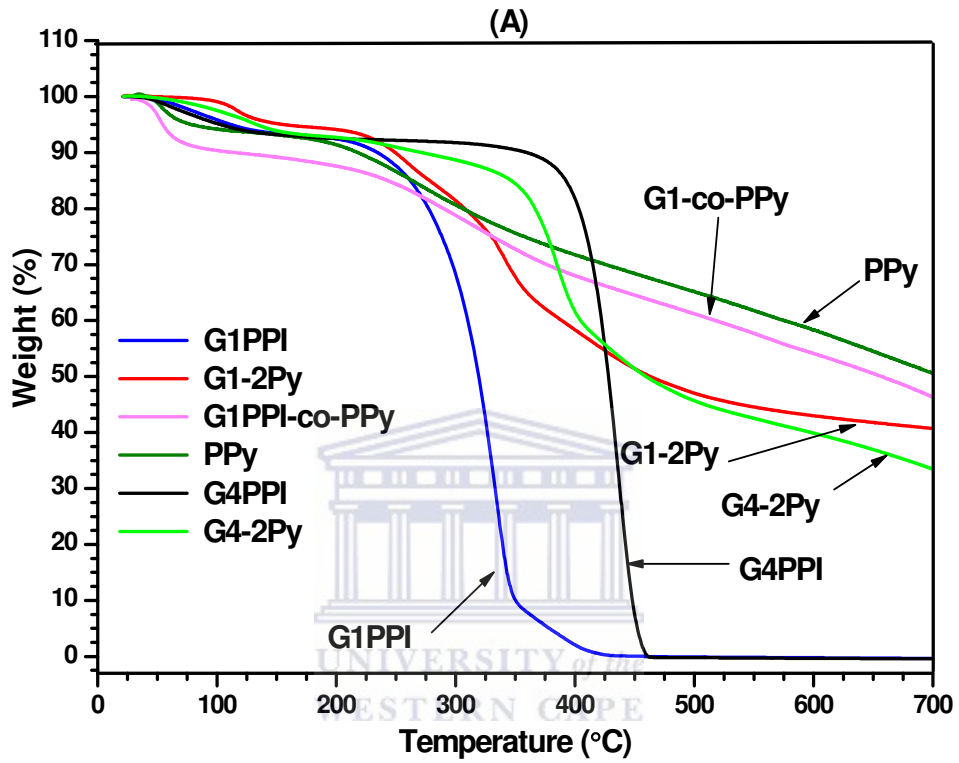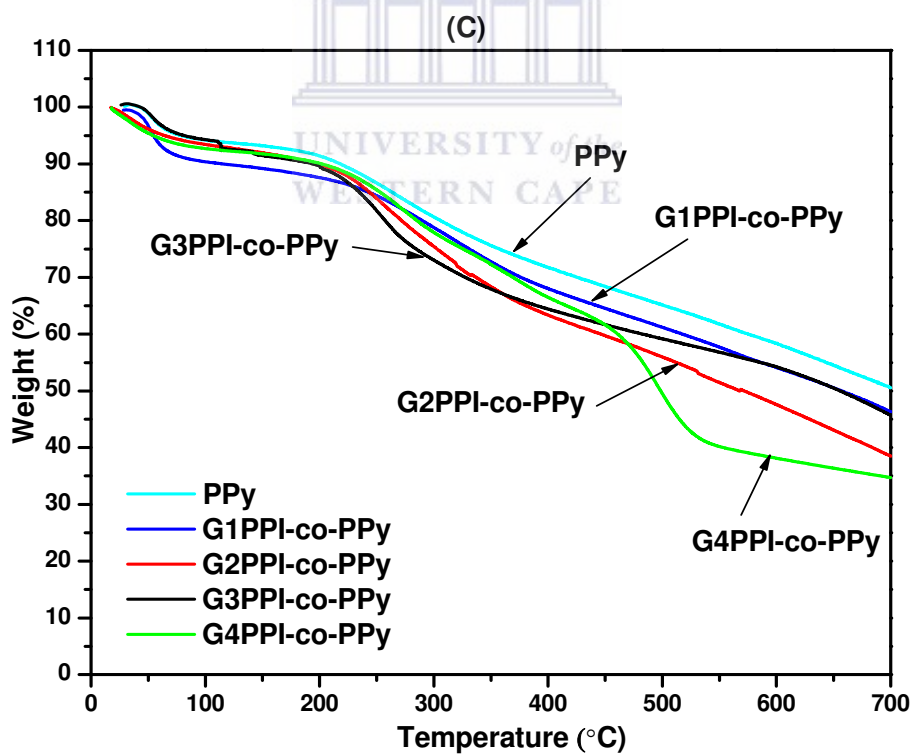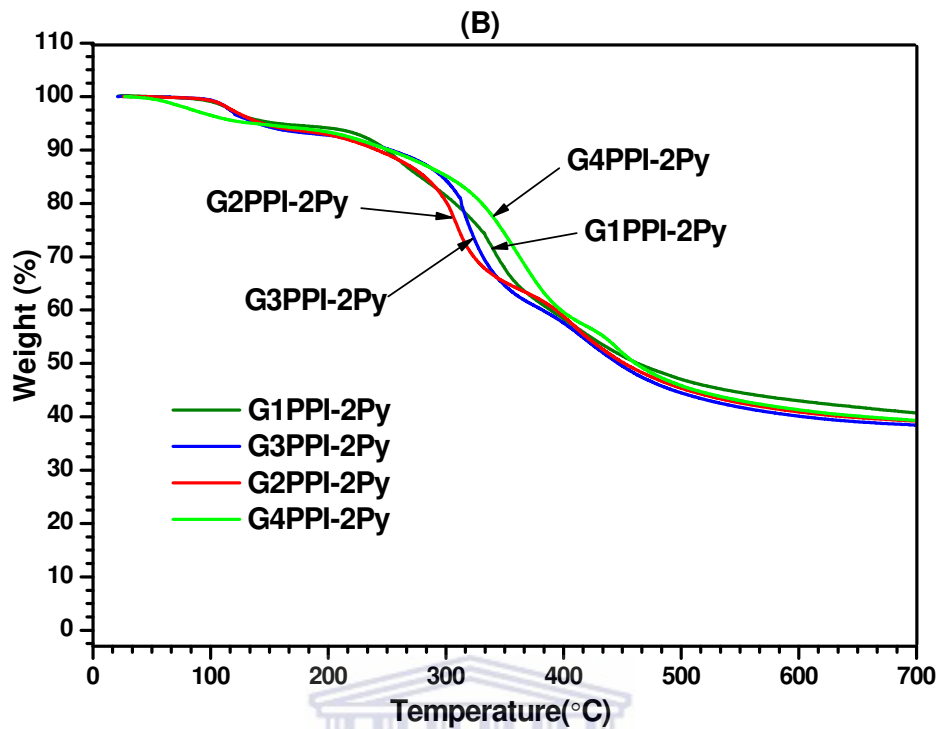
Figure 4.5: TGA data: (A) PPy, G1PPI-co-PPy, G1PPI-2Py, and PPI, (B) G1PPI-2Py to G4PPI-2Py, and (C) PPy, and G1PPI-co-PPy to G4PPI-co-PPy.

4.6   X-ray Diffraction Analysis

X-ray diffraction spectra of PPy and PPI-co-PPy are presented in Figures 4.6 a and 4.6 b, respectively. While PPy has an amorphous morphology, the copolymer showed additional crystalline peaks at 18.9°, 31.86°, 33.74°, 37.65°, 45.96°, 48.48° and 52.4°. However, between these crystalline peaks there were wide amorphous disordered regions within the star copolymers, as evident in the figure around the range $2\theta = 18°$ to 30°. The broad peak was centred at 24° and corresponded to the scattering from bare polymer chains at the interplanar spacing [310]. As PPy did not shown any crystalline peaks, the crystalline region observed in the copolymer was attributed to the presence of the dendrimer moiety in the star copolymer.
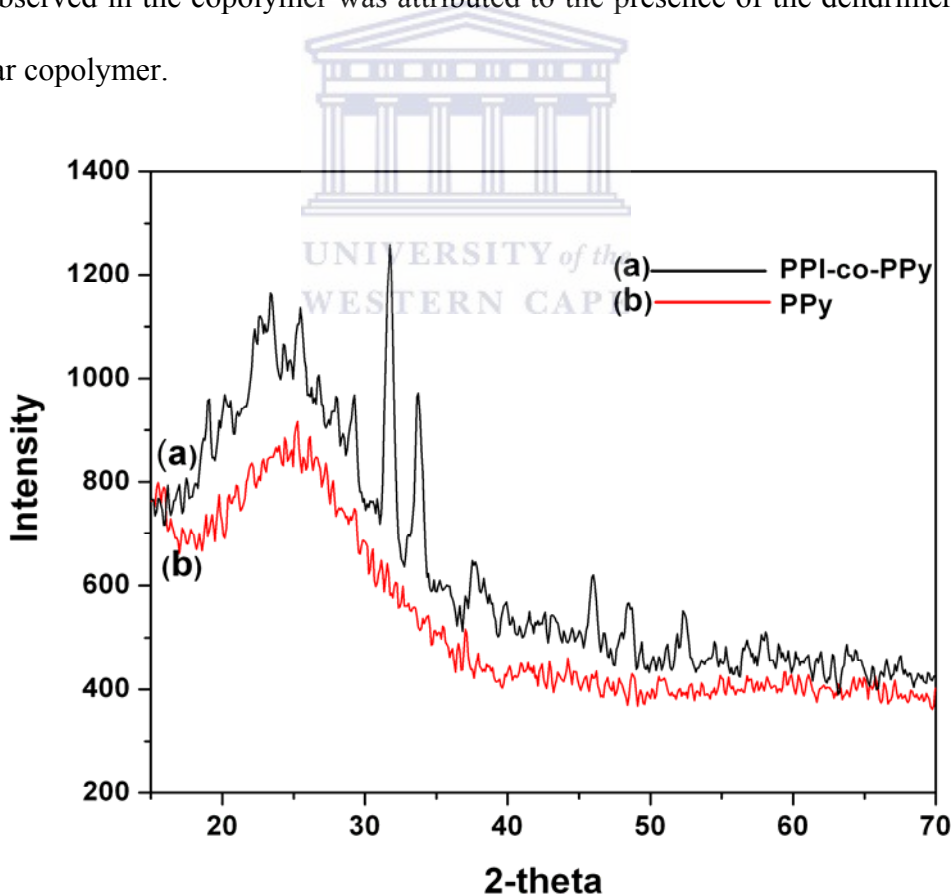
Figure 4.6: XRD data: (a) PPI-co-PPy, and (b) PPy.

4.7 Conductivity Measurements

The electronic conductivity of chemically synthesized PPy and PPI-co-PPy was determined by Hall effect measurements. The samples were prepared by pressing into pellets (13 mm diameter) at less than 6 tons of pressure for 30 min at room temperature. PPI-co-PPy is a semiconducting material. It had an electronic conductivity value of 0.7 S cm^{-1}. PPy had a value of 1.5 S cm^{-1}. The current-voltage curve for PPy and PPI-co-PPy (Figure 4.7) showed that PPI-co-PPy had higher resistance at higher voltages than PPy.
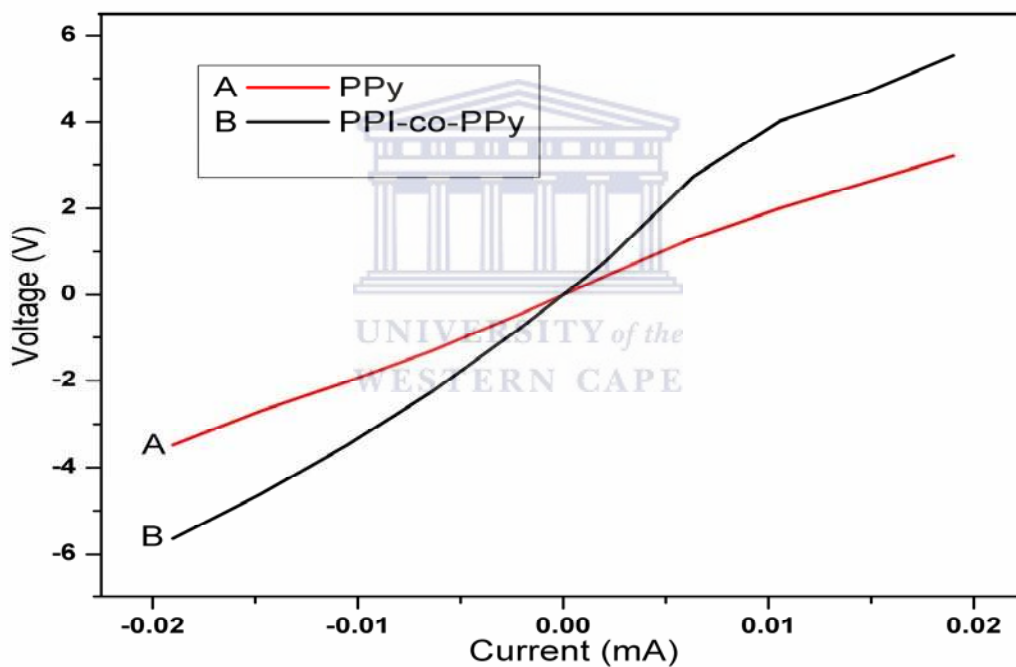
Figure 4.7: Current vs voltage curve for PPy and PPI-co-PPy star copolymers.

4.8 Electrochemical Behaviour of the G1PPI-co-PPy in PBS

Figure 4.9 shows the results of scan rate studies (2-70 mV s^{-1}) for G1PPI-co-PPy conducted in argon-degassed phosphate buffer saline (PBS) (0.1 M, pH 6.8). The (I_p) of

G1PPI-co-PPy increased linearly with increasing scan rate (v), as shown in Figure 4.9 inset, which indicates the occurrence of the electrochemistry of surface confined species. The number of electrons was calculated (n = 2) by using the Brown-Anson equation [311]. At 50 mV s^{-1} scan rate, Figure 4.8 the surface concentration of the electroactive species was determined from the Faradaic charge (Q) passed during exhaustive electrolysis of the assembly, using the same scan rate as for the electrochemical polymerization. This is based on the following equation [312].

$$\Gamma = Q/nFA \tag{4.1}$$

where n is the number of electrons transferred, F is Faraday's constant, and A is the area of the electrode. The surface concentration was calculated to be 1.0271×10^{-5} mol cm^{-2} The linear regression equations for the cathodic and anodic peaks, which are based on log peak current versus log v plots for diffusion kinetically controlled scan rates, were determined as: slope = 0.5127 ($r = 0.9984$) and slope = 0.5700 ($r = 0.9943$), respectively.
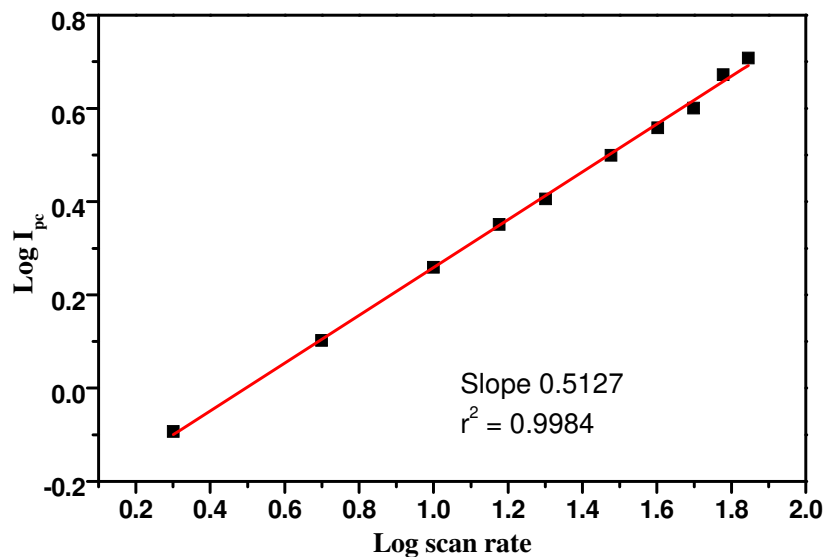
Figure 4.8: A plot of log peak current versus log scan rate.

Figure 4.10 shows cyclic voltammograms for the electrochemical polymerization (+800 mV to -650 mV) of pyrrole on G1PPI-2Py modified Pt electrode performed at a scan rate of 50 mV s^{-1}, for 20 cycles. The current was observed to increase with increasing number of cycles, implying deposition of an electroactive material on the surface of the electrode. The peak at -343 mV is due to the dendrimer on the surface of the electrode and disappears after the 5th cycle. This may be due to nucleation and self-orientation of the functionalized dendrimer on the electrode surface. Although this peak disappears after the 5th cycle, the current continues to increase with increase in cycles. Growth of PPy at this step is believed to take place at the α position of the functionalized dendrimer (Scheme 3.2), forming the G1PPI-co-PPy.
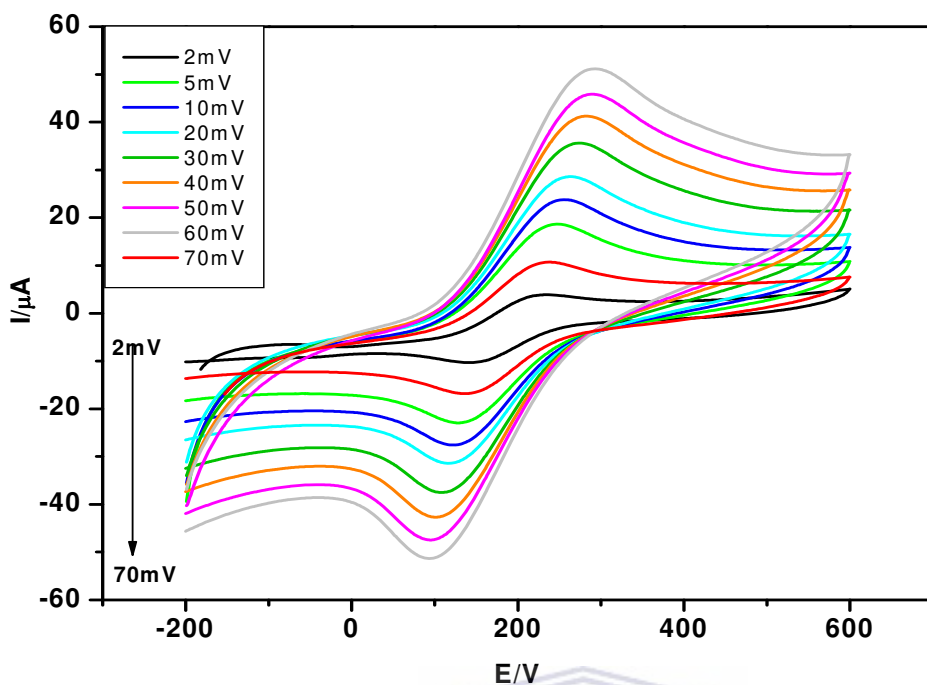
Figure 4.9: Cyclic voltammetry of G1PPI-co-PPy recorded at different scan rates.
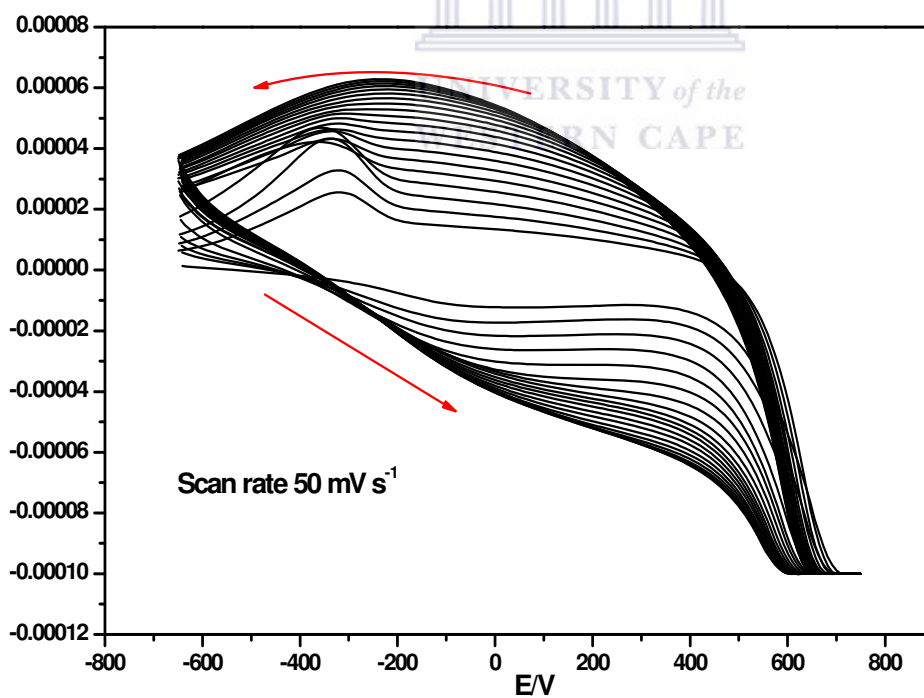
Figure 4.10: Cyclic voltammograms for the electrochemical polymerization of Py on a PPI-2Py/Pt electrode.

4.9 Electrochemical Behaviour Towards [Fe(CN$_6$)]$^{3-/4-}$ Redox Probe Surface Enhancement
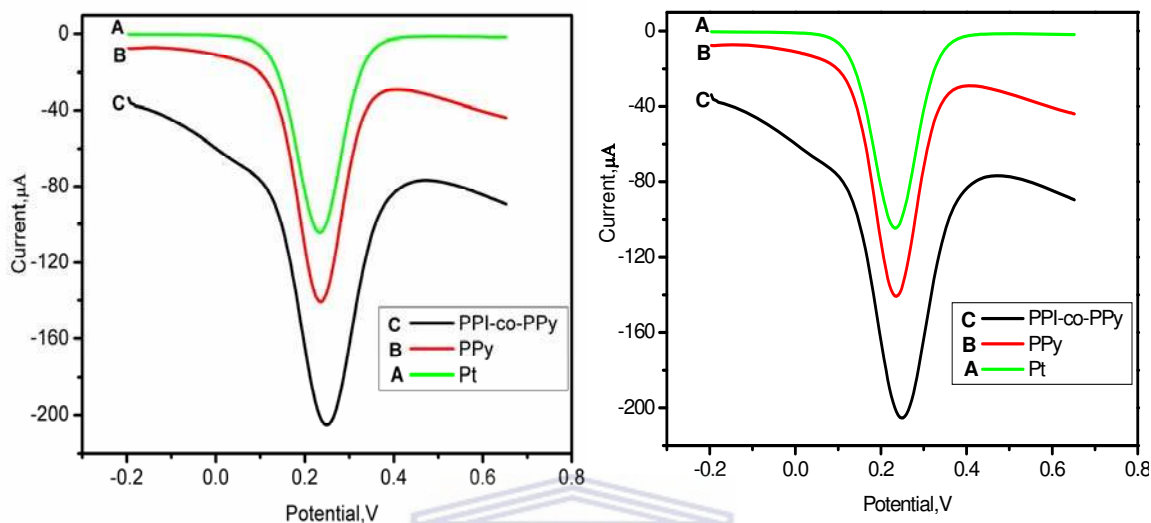
Figure 4.11: Cyclic voltammetry and square wave voltammetry of 10 mM K$_3$[Fe(CN$_6$)] in a phosphate buffer solution (pH 7.0) with KCl (0.1 M) as supporting electrolyte.

Cyclic voltammetry of the [Fe(CN$_6$)]$^{3-/4-}$ electrolyte redox probe (Figure 4.11) was carried out to compare the effect of surface enhancement or modification using pristine PPy and the star copolymer. On the bare Pt electrode, the average peak current was 26 µA. After polymerized with pristine PPy the average peak current was 63 µA. With star copolymers on the electrode the average peak current increased to 83 µA. This increase indicates that star copolymers have an enhancing effect in the redox reactions.

4.10 Electrochemical Impedance Spectroscopy

Electrochemical impedance spectroscopy was used to determine the ionic conductivity of PPy, PPI-2Py and PPI-co-PPy in lithium perchlorate (pH 6.1). (Ionic conductivity is a measure of how well a material accommodates the movement of ions carrying the current

in the solution.) The highest real impedance of 10 MΩ (not shown) was observed for PPI-2Py. The Py monomer hinders the flow of ions through the dendrimer core to the Pt electrode surface. This is expected, since Py is only conducting in its polymer state. The marked reduction in the impedance after polymerization is an indication of the Py polymerization on the dendrimer architecture. Since PPy is a conducting polymer, the PPy arm facilitates the flow of ions through the star copolymers and to the electrode surface.

The Bode plots and Nyquist plots are presented in Figures 4.12 and 4.13, respectively, compare the EIS of the star copolymer with that of the pristine PPy and bare Pt electrode. R_S models the solution resistance, R_1 and R_2 represent the resistance to the flow of the perchlorate ion through the polymer whereas the constant phase element (CPE) with an α value of between 0.8 and 0.87 was used in place of capacitance for better fitting in the Randles equivalent circuit [313]. On the bare Pt electrode, lithium perchlorate showed a two time constant behaviour as seen in the two ϕ_{max} of the phase angle in Figure 4.12 (This can also be seen in Figure 4.13 if the high frequency portion is zoomed). Since a similar two time constant is observed for the PPy and PPI-co-PPy modified electrode, it can be assumed that the impedance monitored is the charge transfer of the lithium perchlorate ions across the polymer chain. Furthermore, the relatively equal R_s value (ca 300 Ω) at a dc potential of -700 mV for all the electrodes (i.e., star copolymer, pristine polypyrrole and bare Pt electrode surface) serves as a good base for comparing the polymers. R_{ct} is the major determining parameter which relates to the ionic conductivity and kinetic behaviour which can be represented by time constant, τ. The fitting parameters using the equivalent circuit in equivalent circuit in Figure 4.12 inset for the impedance

plots are presented in Table 4.1, with fitting errors less than 5% for all the circuit elements. The phase plot at its peak maximum is characterized by frequency f_ϕ and is expressed by equation 4.2, while the maximum angle ϕ_{max} is expressed by equation 4.3 [314].

$$f_\phi = \frac{1}{4\pi RC} \sqrt{1 + \frac{R_{ct}}{R_s}} \tag{4.2}$$

$$\phi = \tan^{-1}\left(\frac{1}{1 + 2R_s/R_{ct}}\right) \tag{4.3}$$

R_{ct} and C represent charge transfer resistance (either R_1 or R_2, from Table 4.1) and capacitance, respectively. From $\tau = R_{ct} \times C_{dl}$, equation 4.2 can be rewritten as follows:

$$\tau = \frac{1}{4\pi f_\phi} \sqrt{1 + \frac{R_{ct}}{R_s}} \quad \text{or} \quad \tau = \frac{1}{2\omega_\phi} \sqrt{1 + \frac{R_{ct}}{R_s}} \tag{4.4}$$

where $\omega_\phi = 2\pi f_\phi$

These equations show that R_{ct} is inversely proportional to frequency (or τ) and directly proportional to the phase angle.

Figure 4.12 shows that the two frequency maxima for Pt|PPI-co-PPy were higher than that of Pt|PPy, while the two phase angles for Pt|PPI-co-PPy were lower than that of Pt|PPy. These observations showed that the ionic conductivity of PPI-co-PPy is higher than that of PPy (see Table 4.1). This is in an agreement with equations 4.2 and 4.3.

The time constant, τ, is taken as a kinetic index denoting the ease of transfer of ions across the polymer membrane. This kinetic parameter was calculated from the Nyquist plot (see Table 4.1). Lower time constant values for both R_1 and R_2, as expected; further depict faster kinetics of ion transfer in PPI-co-PPy than PPy. The improved ionic conductivity of the star copolymer is more evident from the Nyquist plot, which shows the least real and imaginary impedance.

Table 4.1: EIS fitted data from equivalence circuit in Figure 4.12 and calculated time constants

Kinetic parameters	Pt|bare	Pt|PPI-co-PPy	Pt|PPy
R_s (Ω)	305	300	295
R_1 (k Ω)	0.360	0.217	0.632
R_2 (k Ω)	0.1431	9.4040	419
CPE_1 (μF)	17.32	1.88	1.86
CPE_2 (μF)	549.400	0.306	1.700
Zw	16.79	2.70	-
$f_{\phi 1}$ (Hz)	-	662.0	168.5
$f_{\phi 2}$ (Hz)	-	10.03	2.24
τ_1; τ_2 (s rad^{-1})	4.76×10^{-4} ; 4.70×10^{-2}	1.2×10^{-4}; 1.58×10^{-2}	9.44×10^{-4}; 7.10×10^{-2}
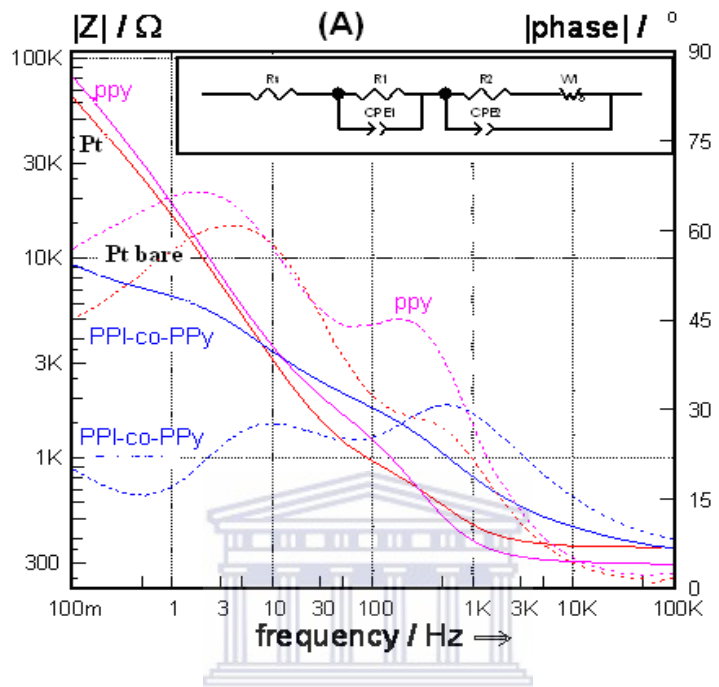
Figure 4.12: EIS Bode plots of star copolymer (PPI-co-PPy), pristine polypyrrole (PPy), and bare Pt electrode in 0.1 M LiClO$_4$ at a dc potential of -700 mV.
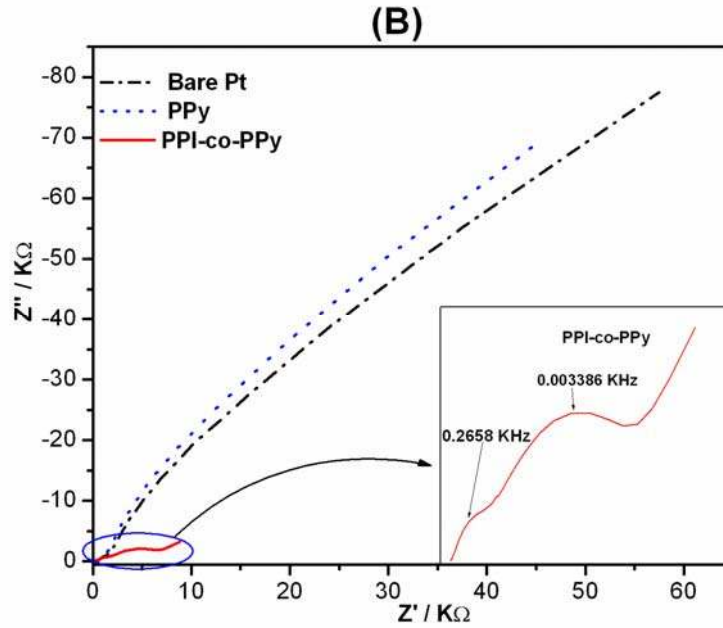
Figure 4.13: EIS Nyquist plots of star copolymer (PPI-co-PPy), pristine polypyrrole (PPy), and bare Pt electrode in 0.1 M LiClO₄ at a dc potential of -700 mV.

A surface coverage of 99% was obtained for the star copolymer on the Pt electrode. The value was determined from the R_{ct} value using the following equation:

$$\theta = 1 - \frac{R_{ct}^{\text{modified electrode}}}{R_{ct}^{\text{bare electrode}}} \tag{4.5}$$

Kinetic parameters such as heterogeneous rate constant (K_{et}) and exchange current (i_o) were also calculated, using equations 4.6, 4.7, 4.8, and 4.9 respectively.

$$\omega_{max} = \frac{1}{R_{ct} C_{dl}} \tag{4.6}$$

$$\tau = R_{ct} \times C_{dl} \tag{4.7}$$

$$i_o = \frac{RT}{nFR_{ct}} \tag{4.8}$$

$$i_o = nFAK_{et}C^* \tag{4.9}$$

where ω_{max} (frequency at the max. imaginary impedance of the semicircle) = $2\pi f$, R_{ct} is the charge transfer resistance, F is the Faraday constant, A is the area of the electrode, C_{dl} is the double layer capacitance, n is the number of electrons, and C^* is the bulk concentration of the lithium perchlorate. The values obtained for the exchange current for the electron transfer process are given in Table 4.2.

Table 4.2: Kinetic parameters of $LiClO_4$ on PPy, Pt and PPI-co-PPy modified electrodes

Kinetic para-meters	Pt|PPI-co-PPy High freq.	Pt|PPI-co-PPy Low freq.	Pt|bare High freq.	Pt|bare Low freq.	Pt|PPy High freq.	Pt|PPy Low freq.
ω_{max} (rad s^{-1})	8244.6	63.028	2098.2	21.280	65228	1058.8
τ (s rad^{-1})	1.20×10^{-4}	1.58×10^{-2}	4.76×10^{-4}	4.70×10^{-2}	9.44×10^{-4}	7.10×10^{-2}
i_0 (A)	9.868×10^{-5}	2.530×10^{-6}	7.126×10^{-5}	1.749×10^{-4}	8.637×10^{-5}	4.913×10^{-5}
k_{et} (cm s^{-1})	5.780×10^{-4}	1.480×10^{-5}	2.383×10^{-4}	2.850×10^{-4}	5.057×10^{-4}	2.876×10^{-4}

The Nyquist plot in Figure 4.13 shows improved conductivity of the star copolymer modified electrode over bare Pt electrode and polypyrrole. Impedance spectroscopy data confirmed that the star copolymer had better ionic conductivity (lower R_{ct} and τ values) at -700 mV.

CHAPTER 5

Electrochemical Impedance and Morphology of Electrochemically Synthesized G2-poly(propylene imine)-co-polypyrrole Dendritic Star Copolymer

The results discussed in this chapter stem from the experimental procedures outlined in Chapter 3 section 3.4.3 (general experimental) and section 3.4.4. The chapter presents the result of the G2-poly(propylene imine)-co-polypyrrole novel dendritic star copolymer electrochemically synthesized.

5.1   Introduction

Star copolymer materials are particularly useful for coatings because of their spherical structure and their ability to pack in three dimensions. The 3D structure with extended conjugated linear polymer chains gives star copolymer properties that are better than the typical 2D linear polymers. [23]. Star copolymers are branched macromolecules that have a central core to which multiple linear polymer chains are attached. Synthesis of conducting star, graft and block copolymerization of the conducting polymer leading to a new material with modulated properties can be employed [315-316]. Electrochemical copolymerization can produce a variety of conducting materials with different optical, electrical and morphological properties as well as control electrochromic properties [30-32].

Polypyrrole exhibits good electrical conductivity and high air stability and is a useful conducting polymer[11]. Poly(propylene imine) dendrimers are highly branched macromolecules terminated with amino groups with a number of interesting characteristics. Dendrimers, with their easily accessible multiple terminal or end functional group, are ideal for the construction of star-shaped polymers [317]. Electrochemistry and sensor application of pristine PPI, metallo-PPI and PPI-gold nanocomposites have been studied by our group [261-262, 313]. Dendrimer-star copolymers [318] are novel types of molecular architecture, in which many linear homo- or block copolymer chains are attached to a dendrimer core. Dendrimer-star copolymers combine the properties of conventional polymers with those of dendrimers [319]. Conducting star-shaped copolymers consisting of a regioregular poly(3-hexylthiophene) arm attached to a polyphenylene dendrimer core have been reported by Wang *et al*. [320]. The poly(propylene thiophenoimine)-co-poly(3,4 ethylene dioxythiophene) dendritic star copolymer was electrochemically synthesized by our group [321].

5.2   Synthesis of Pyrrole-functionalized Generation 2 Poly(propylene imine) Dendrimer (G2PPI-2Py)

The synthesis of G2PPI-2Py dendrimer was carried out by a condensation reaction of G2PPI with 2-pyrrole aldehyde following the method of Smith *et al.* [322], and Salmon and Jutzi [323] with some modifications. A reaction mixture of poly(propylene imine) generation 2 dendrimer (0.5 g, 0.6468 mmol) and 2-pyrrole aldehyde (0.4920 g, 5.174 mmol) in 50 mL dry methanol was magnetically stirred under a positive pressure of nitrogen gas for 2 days in a 100 mL three-necked round-bottom flask. The methanol was

removed by rotary evaporation and the residual oil was dissolved in 50 mL dichloromethane DCM; the organic phase was then washed with water (6 × 50 mL) to remove unreacted monomer. The DCM was removed by rotary evaporation and yielded the desired product as an orange oil. The method used above is a slight modification of that reported by Smith *et al.* [295] and Salmon and Jutzi [296]. The yield was 1.65 g, 75% (Scheme 1).

^{1}H-NMR analysis of G2PPI-2Py in (CDCl$_3$ 200 MHz, ppm): 1.36 (s, br, 4H, H-1), 1.74 (t, 8H, H-2), 2.43 (m, br, 12H, H-2&3), 3.51 (t, 8H), 6.21 (t, 8H, H-8), 6.47 (d, 4H, H-7), 6.86 (s, 4H, H-9), 8.1 (s, 4H, H-6). NMR of PPI-2Py gave a new chemical shift at 8.1 ppm for N=CH. Strong FTIR bands appeared at 1634 cm^{-1} for N=C in the dendrimer moiety, and the absorption of out-of-plane bending C–H at the α-position of the pyrrole ring at 729 cm^{-1} was observed.
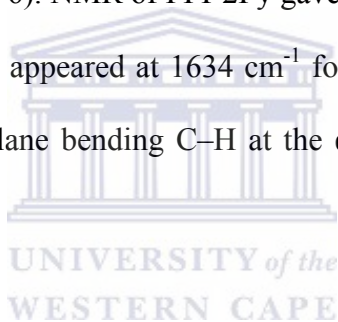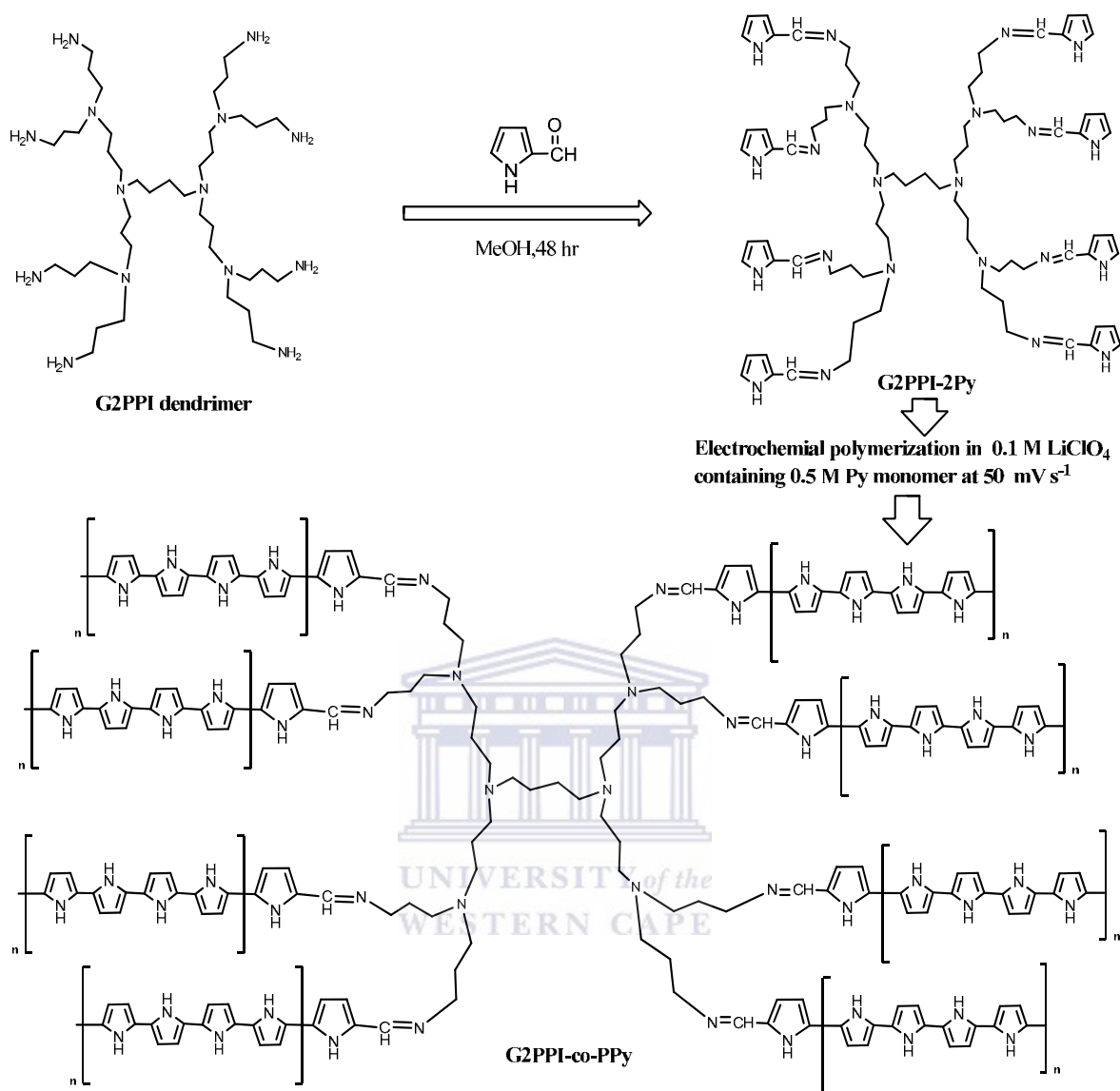
Scheme 5.1: Schematic of synthesis of G2PPI-co-PPy.

5.3 Electrochemical Synthesis of Poly(propylene imine)-co-Polypyrrole (G2PPI-co-PPy) Modified Platinum Electrode

The procedure used to prepare the G2PPI-2Py modified platinum electrode was described earlier, in Section 3.4.3. The modified electrode was then immersed in an aqueous solution of 0.1 M LiClO$_4$ (5 mL) containing 0.5 M pyrrole monomer (0.177 mL) by

cycling the potential between -600 mV and +800 mV at a scan rate of 50 mV sec^{-1} for 20 cycles to obtain G2PPI-co-PPy (see Scheme 5.1). A similar experimental procedure was used to prepare PPy homopolymer on the bare polished Pt electrode surface.

5.4   Fourier Transformed Infrared Spectroscopy

The FTIR transmission spectra of PPy, PPI-2Py, and G2PPI-co-PPy are shown in Figure 5.1. In the spectrum of PPy, the specific absorption peaks appear at 3400 cm^{-1}, 1520 cm^{-1}, 1033 cm^{-1}, 890 cm^{-1}, and 777 cm^{-1}. Similar results have been reported by Depaoli *et al.* [299] and Kang *et al.* [300, 324] for the Py ring, namely, stretching vibration bands at 1520 cm^{-1} (C=C), and 1130 cm^{-1} (C–N). The peak at 3400 cm^{-1} was assigned to the N–H stretching vibration in pyrrole. The 1100 cm^{-1} peak was broadened because of overlapping of the N-H bending vibration with the perchlorate vibrations [324]. The C–H stretching and bending of Py was observed at 780 cm^{-1}. The spectrum of PPI-2Py, showed out-of-plane bending of the C–H bond located at the α position in the Py ring at 729 cm^{-1} [302]. The sharp peak at 1634 cm^{-1} was assigned to the stretching vibration of the N=C bond present in the dendrimer moiety. In the spectrum of G2PPI-co-PPy the bands due to PPy appeared at 1590 cm^{-1}, 1416 cm^{-1}, 1015 cm^{-1}, and 799 cm^{-1}, but here the sharp N=C band in PPI-2Py now appeared at 1622 cm^{-1}. Furthermore, the absorbance at 729 cm^{-1} disappeared after the polymerization, indicating that PPI-2Py was converted to G2PPI-co-PPy via α–α coupling of the Py units. The sharp band at 1063 cm^{-1} was ascribed to the N–H in-plane deformation [303].
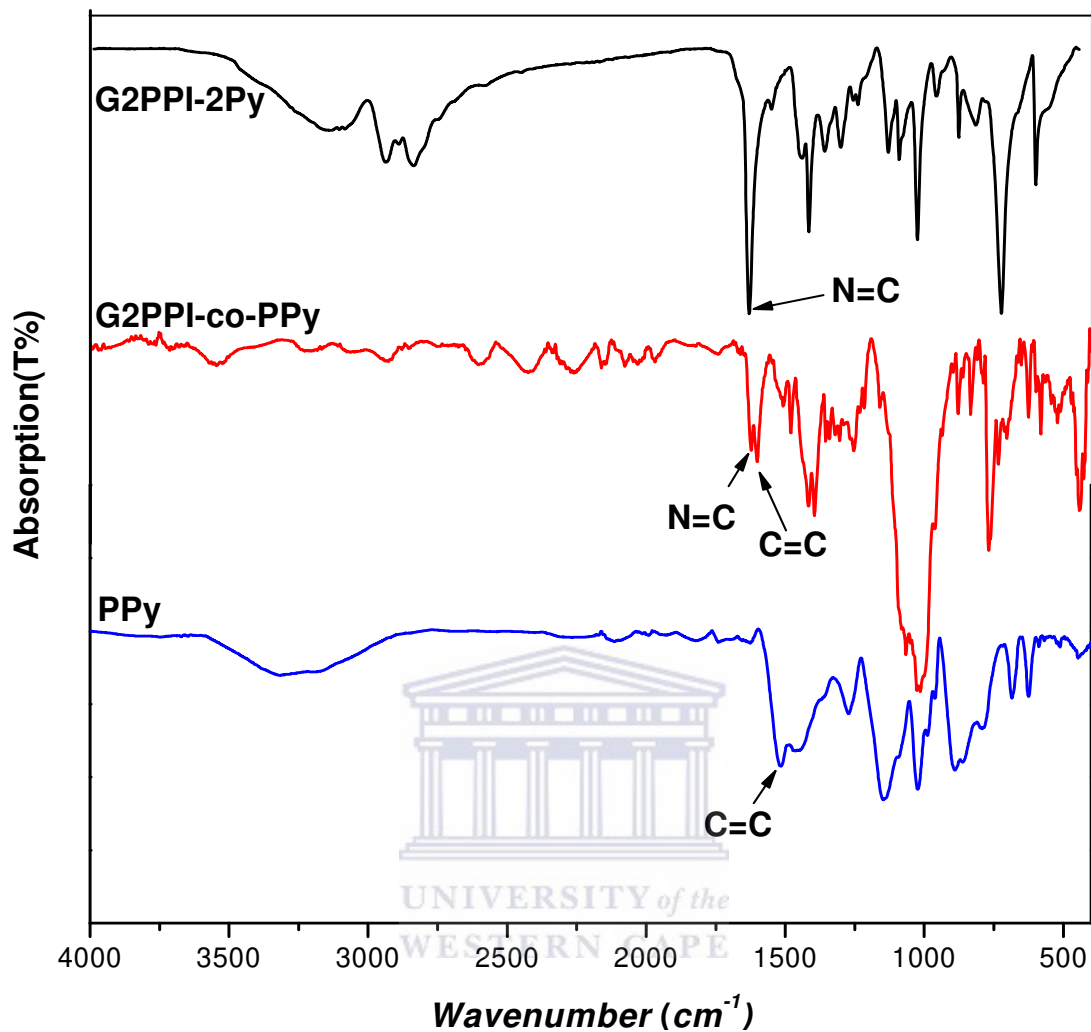
Figure 5.1: IR spectra of G2PPI-2Py, G2PPI-co-PPy and PPy.

5.5   Fluorescence Spectroscopy of G2PPI-co-PPy

The star copolymer exhibits fluorescence properties with excitation and emission, the fluorescence spectra of G2PPI, PPy and G2PPI-co-PPy were investigated and recorded as shown in the previous report [298]. Excitation and emission bands of 271 and 448 nm respectively were observed for G2PPI and this agreed with that obtained by Wang *et al*.

[325]. For the PPy 351 and 384 nm excitation and emission bands were observed respectively [298]. G2PPI-co-PPy dendritic star copolymer exhibited florescence properties with excitation at 375 nm and emission at 407 and 430 nm.

The star copolymer was excited at the wavelengths corresponding to that of the PPI and PPy to see whether the constituent retained their individual property, but the observed emission could not be reversed to their excitation bands upon an emission–excitation scan. However the fluorescence is apparently affected by the formation of G2PPI-co-PPy dendritic star copolymer via copolymerization of G2PPI-2Py modified electrode with PPy. The formation of the copolymer causes changes in the polarization of the chromophoric system. This shows that an entirely new compound was synthesized. In fact, the bands of the star copolymer seem to be an average of its constituents indicating the formation of a hybrid material. On the other hand to confirm the formation of the star copolymer, it was excited at the wavelength corresponding to G2PPI and PPy but the observed emission could not be reversed to their excitation bands upon an emission–excitation scan. This shows that an entirely new compound was synthesized.

The fluorescence intensity of G2PPI-co-PPy dendritic star copolymer is related to excitation and emission wavelength that is measured, the analysis of the excitation emission matrices (EEM). Fluorescence spectra can in addition describe the relationship among fluorescence intensity of excitation and the emission wavelength. Figure 5.2 (A, B) shows a typical three-dimensional excitation-emission matrix (EEM) fluorescence spectrum of G2PPI-co-PPy dendritic star copolymer. The fluorescence intensity of excitation wavelength in the 3D isograms ranges from 330 to 390 nm and emission

wavelength is between 400 and 460 nm. As it can be seen from Figure 5.2, A the dendritic star copolymer has the large fluorescence intensity in the emission range from 400 to 445 nm for which the maximum peak is at 433, 407 nm and excitation range from 355 to 390 nm for which the maximum peak is at 376 nm.
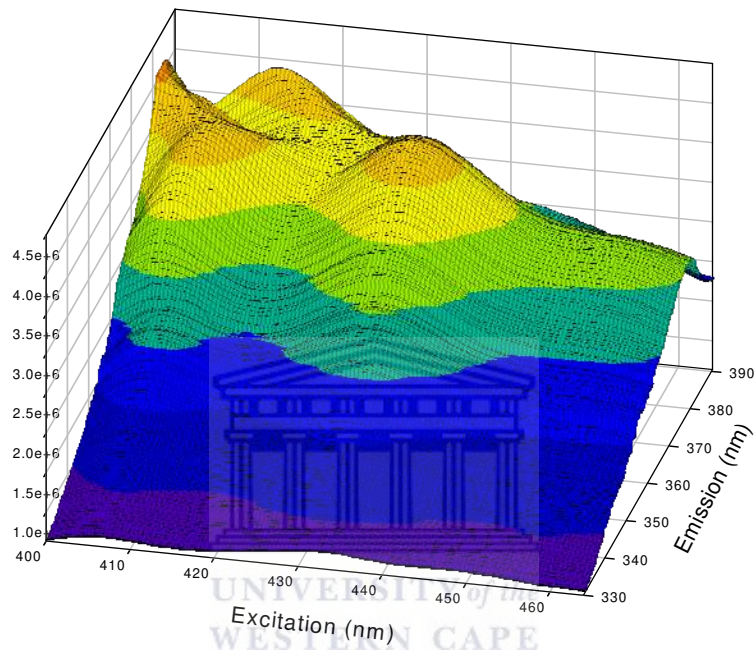
(A)
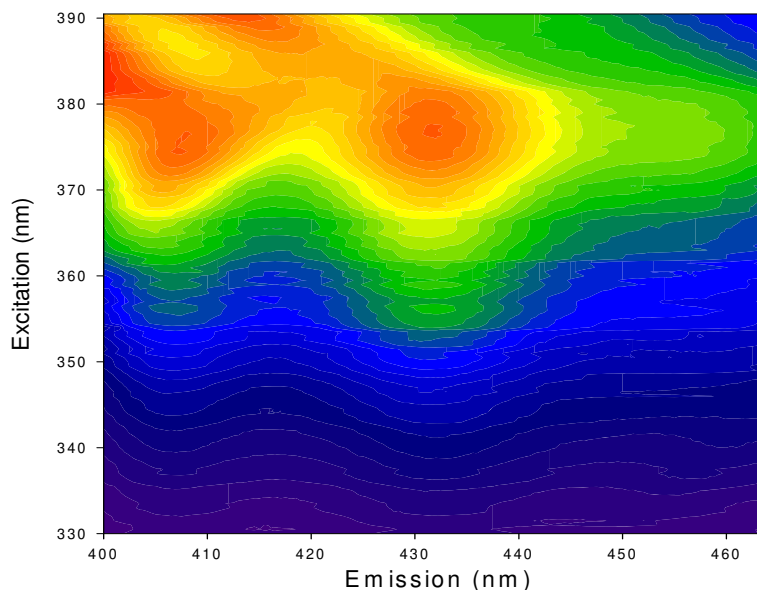
(B)

Figure 5.2: Excitation–emission matrix fluorescence of G2PPI-co-PPy dendritic star copolymer.

5.6   Scanning Electron Microscopy

The morphology of electrochemically prepared PPy (Figure 5.3 c), exhibits a dense growth of whelk-like helixes [306] initiating from the bare Pt-electrode surface with average base diameter of 1.0 µm. The surface of the G2PPI-2Py coated Pt electrode surface is shown in Figure 5.3 c. At higher magnifications (Figure 5.3 a, b) the whelk-like helixes of the star copolymers are hollow with openings at their tapered ends and with average base diameter of 0.5 µm. Chen *et al*. [306] reported the preparation of polypyrrole whelk-like helixes on the surface of a glassy carbon electrode with an average base diameter of 1.0 µm via electrochemical polymerization of pyrrole monomer in the presence of a surfactant. In addition, Chen *et al.* [306] have showed that high surface area and hydrophilicity of the polypyrrole whelk-like helixes enhances electrocatalytic activity

as shown by the increase in oxidation current of ascorbic acid. Our experiments show that polypyrrole whelk-like helices can form on a bare Pt surface, in the absence of surfactant as well as, from a Pt surface coated with a pyrrole-functionalized dendrimer via electro-polymerization of pyrrole in the presence of aqueous 0.1 M LiClO$_4$.
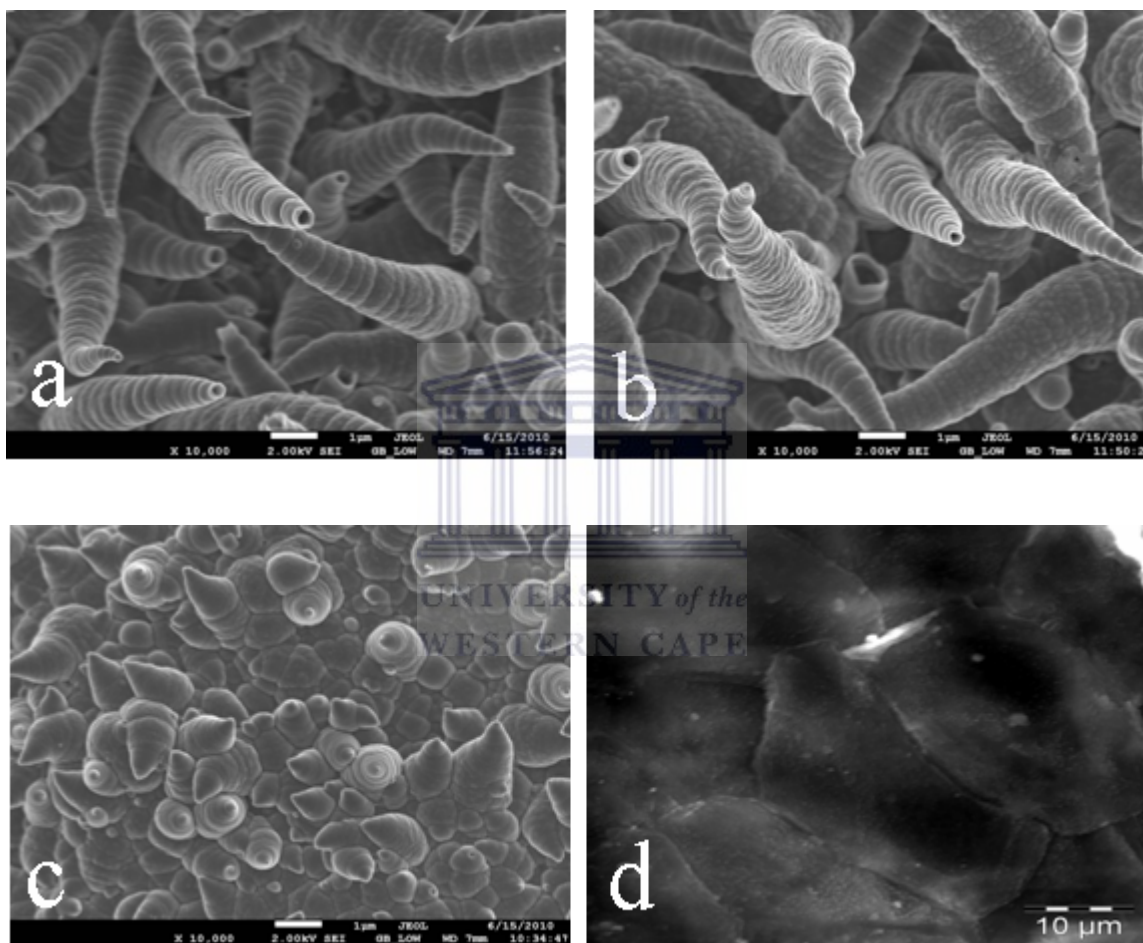
Figure 5.3: SEM images: (a, b) electrochemically polymerized G2PPI-co-PPy (×10,000), (c) electrochemically synthesized PPy on bare Pt electrode (×10,000) and, (d) functionalized dendrimer (G2PPI-2Py).

5.7 Cyclic Voltammetry of Star Copolymer Pt|G2PPI-co-PPy

Cyclic voltammograms of the Pt|G2PPI-co-PPy ranging from 20 to 100 mV sec^{-1} have been studied (Figure 5.4). It can be seen that the anodic peak currents (I_p) of Pt|G2PPI-co-PPy increased linearly with increasing scan rate (v) as shown in Figure 5.4 inset, which indicates the occurrence of the electrochemistry of surface confined species. The value of the slope of the linear plot of log v versus log I_p can be used to elucidate the nature of the processes influencing the electrochemistry of the surface confined material. Slopes with values of 1.0 and 0.5 refer to adsorption-controlled and diffusion-controlled electrochemical processes, respectively. Intermediate values for the slope indicate mixed diffusion/adsorption-controlled processes [326].

In this work, the nature of the process controlling the peak was elucidated from a plot of the log of anodic current (log I_{pa}) against the log of scan rate (log v) (not shown) which gave a slope of 0.676, r^2 = 0.99943, which confirmed the occurrence of diffusion/adsorption-controlled electrochemistry of the Pt|G2PPI-co-PPy nanoelectrode in 0.1 M LiClO$_4$ system. In order to estimate the number of electrons transferred, equation 5.1 (Laviron's equation) [327] and equation 5.2 [328] were re-expressed to give equation 5.3:

$$I_p = \frac{n^2 F^2 A \Gamma v}{4RT}$$
(5.1)

$$Q = nFA\Gamma$$
(5.2)

$$I_p = \frac{nFQv}{4RT}$$

(5.3)

where: Γ is the surface concentration of the electrode material (Pt|G2PPI-co-PPy, mol cm^{-2}), A is the electrode area (cm^2) and Q is the quantity of charge (C) calculated from the reduction peak area of the voltammogram; and n, I_p, F, R and T have their common meanings. From the plot of the anodic current (I_{pa}) against the scan rate (v) Figure 5.5, which gave a slope of 2.842×10^{-6}, $r^2 = 0.99967$, n was calculated to be 2.25 for the anodic processes. The surface concentration (Γ) of the G2PPI-co-PPy film was estimated to be 4.2733×10^{-11} mol cm^{-2}. This reveals that the electrode contains a thin electroactive surface-bound polymer film and the occurrence of electron diffusion along the conducting dendritic star copolymer chain is established.
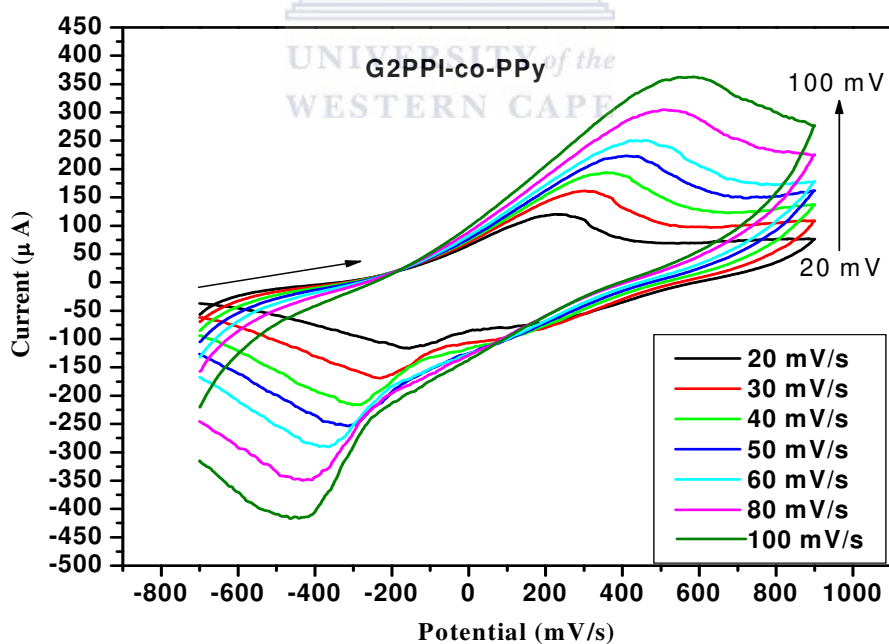
Figure 5.4: Cyclic voltammograms of star copolymer Pt|G2PPI-co-PPy at potential scan rates of 20 to 100 mV sec^{-1} in 0.1 M LiClO$_4$.
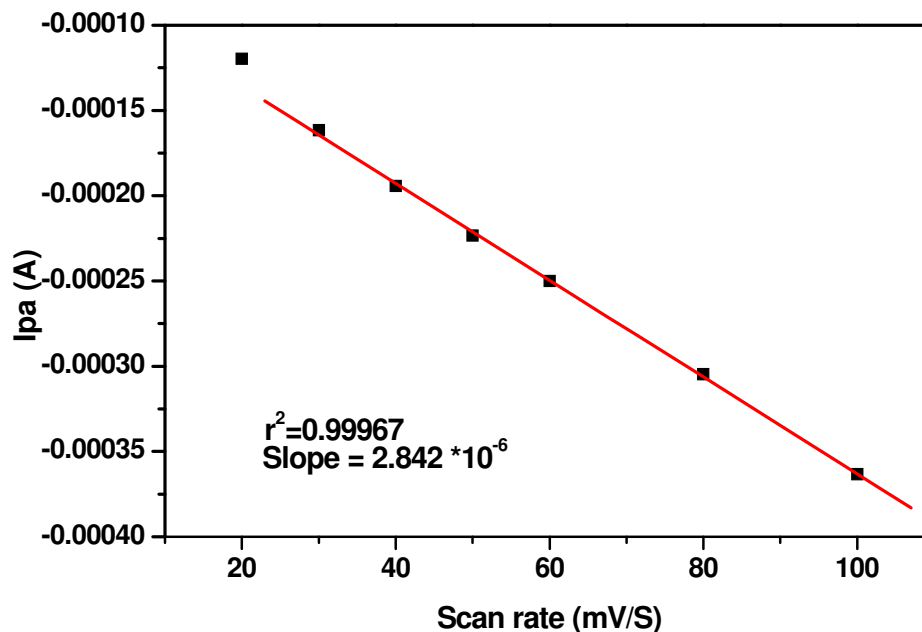
Figure 5.5: A plot of anodic current (I_{pa}) versus the scan rate (v).

5.8   Electrochemical Impedance Spectroscopy of G2PPI-co-PPy in 0.1 M LiClO$_4$

Electrochemical impedance is an effective tool for studying the interfacial properties of surface modified electrode and the mechanisms for charge transfer and ion transport in polymer film electrolyte interface. The impedance characteristics of any electrode system depends on the overall effect of several parameters which include electrolyte resistance (R_s), charge transfer resistance (R_{ct}) between the solution and the electrode surface, Warburg element (Zw) and double layer capacitance (C_{dl}) (due to the interface between the electrode surface and the solution). The use of a constant phase element instead of the capacitance is required to optimize the fit to the experiment and this is due to the nonideal nature of the electrode [329-330]. However, impedance spectroscopy also allows the detection of change in capacitance due to electrode modification. The low frequency

capacitance change (values) can be obtained from the imaginary part Z_{im} of the complex impedance part of the spectra using the following equation [331-333].

$$C_s = \frac{1}{2\pi f z_{im}}$$

(5.4)

where: f is the maximum frequency, $\pi = 3.142$, and Z_{im} is the slope of the plot of the imaginary impedance against the reciprocal of frequency.

The Nyquist plot for various modified electrodes showed a specific capacitance of 0.7415, 6.5297 and 1.9323 $\mu F\ cm^{-2}$ for bare Pt, Pt|PPy, and Pt|G2PPI-co-PPy, respectively.

EIS was used to estimate the ionic conductivity of PPy, G2PPI-2Py and G2PPI-co-PPy in lithium perchlorate (pH 6.1). Ionic conductivity is a measure of how well a material accommodates the movement of ions carrying the current in the solution. The highest real impedance to the flow of charge of ca 10 MΩ (not shown) was observed for G2PPI-2Py because the pyrrole monomer hindered the flow of ions through the dendrimer core onto the electrode. This is expected, because Py is only conducting in its polymer state. The marked reduction in the impedance after polymerization is an indication of the polymerization of the pyrrole monomer on the dendrimer architecture. Since PPy is a conducting polymer, the PPy arm facilitated the flow of ions through the star copolymers onto the electrode surface. Figure 5.6 A and B shows the Nyquist and Bode plots of Pt|G2PPI-co-PPy measured at different dc potential from -200 to -500 mV. The most conducting potential was determined by interrogating the EIS of the star copolymer at different potentials.
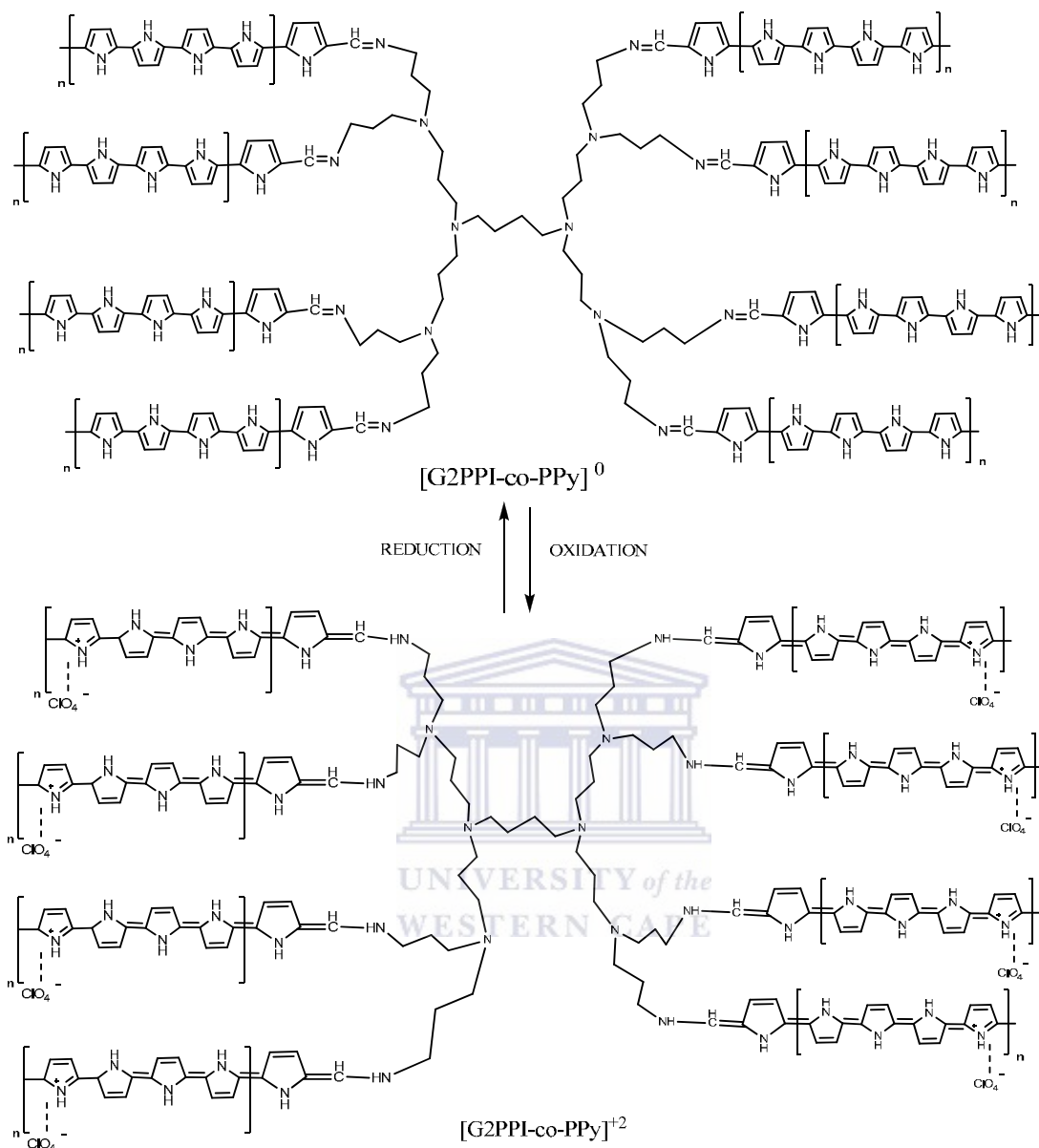
Scheme 5.2: Redox species of G2PPI-co-PPy.

As shown in Figure 5.6 A the most conducting potential was found to be -200 mV which was taken as the optimal potential. The domination of Warburg diffusion in the electrochemically prepared star copolymer was due to the holes created by the dendrimer architecture (as shown from SEM analysis) which enhanced flow of perchlorate ions.
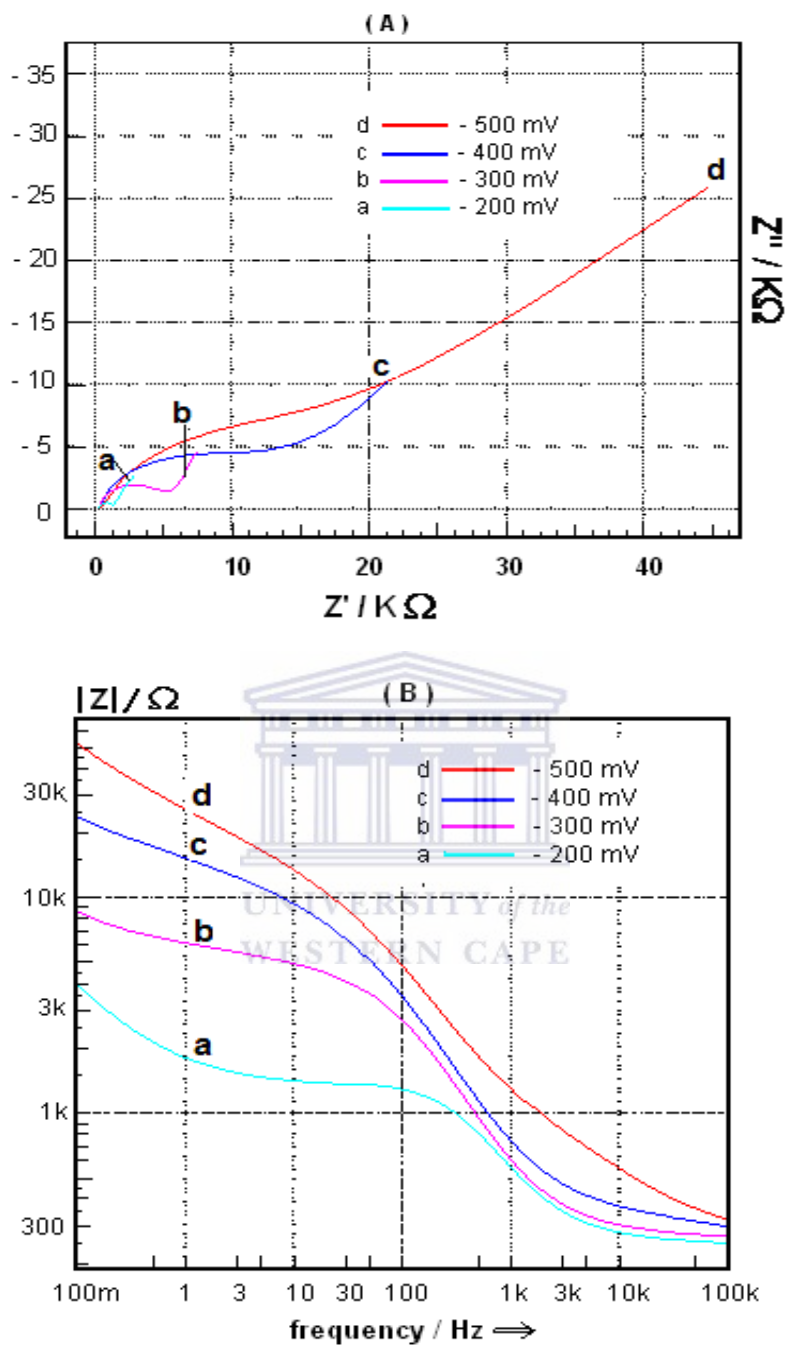
Figure 5.6: EIS: (A) Nyquist, and (B) Bode plots for Pt|G2PPI-co-PPy at different potentials from -200 to -500 mV
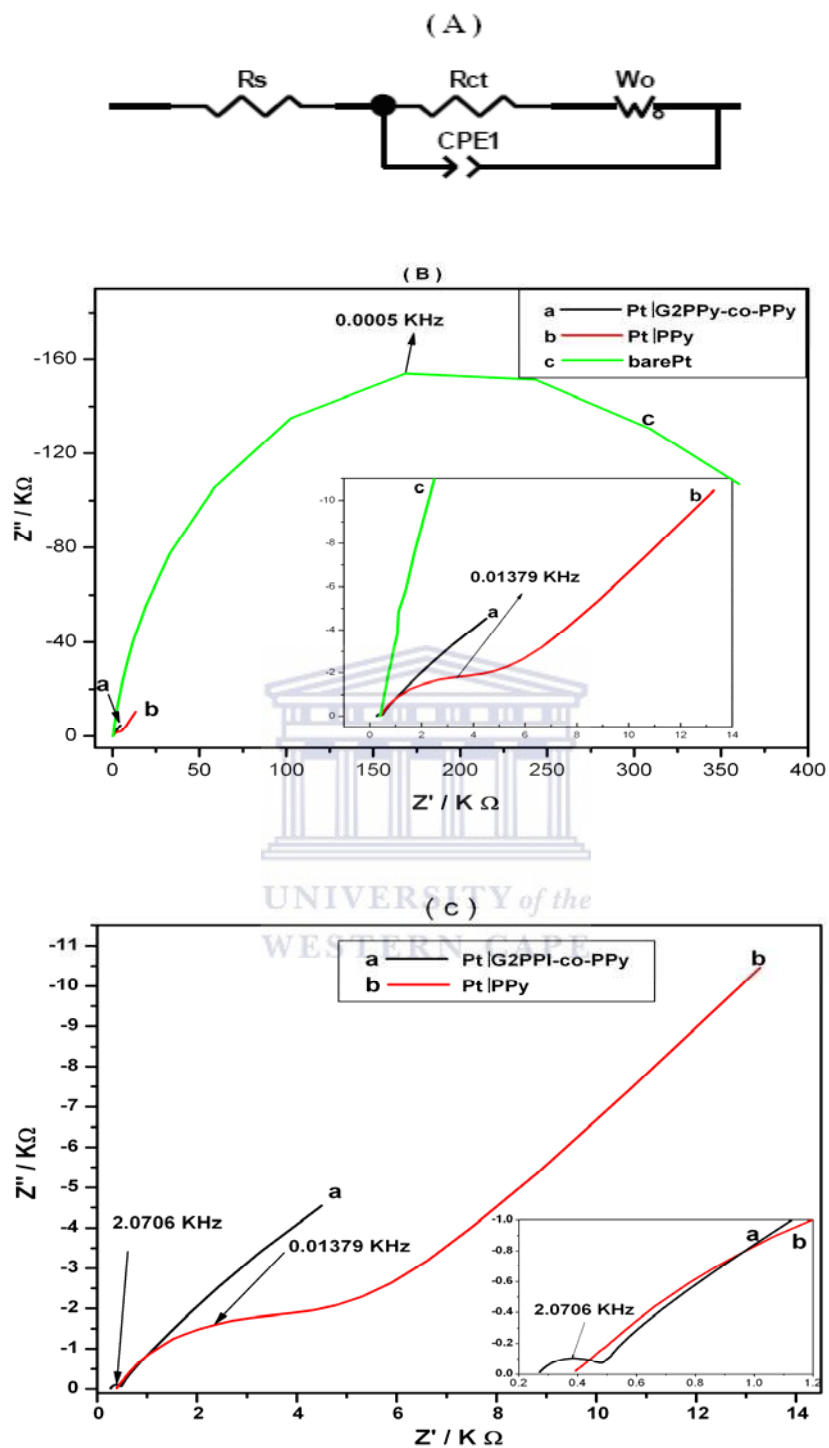
Figure 5.7: (A) Randles equivalent circuit, (B) EIS Nyquist plots of Pt, Pt|PPy, and Pt|G2PPI-co-PPy, and (C) EIS Nyquist plots of Pt|PPy, and Pt|G2PPI-co-PPy in 0.1 M LiClO$_4$ at a dc potential of -200 mV.

As shown in Figure 5.7, the diameter (i.e., charge transfer resistance, R_{ct}) of Nyquist semicircle was smaller for Pt|G2PPI-co-PPy (128.1 Ω) than for bare Pt (336.3×10^3 Ω). This shown that the conducting PPy arms of the dendrimer facilitated the flow of ions through the star copolymer onto the surface of the electrode (see Scheme 5.2). Furthermore, the PPy-modified electrode gave a Nyquist semicircle diameter of (4436 Ω), which was higher than the value of 128.1 Ω obtained for Pt|G2PPI-co-PPy. The increase in the conductivity of the dendritic star copolymer may also be ascribed to the increase in the conjugation length of the copolymer after the incorporation of the PPy arms onto the dendrimer thereby facilitating easy flow of charge through the holes created by the dendrimer architecture (as shown from SEM analysis) to the electrode surface.

The Nyquist plots shown Figure 5.7 b show that the conductivity of the star copolymer modified electrode was better than that of the bare Pt electrode and the PPy. The interfacial charge transfer resistance values, denoting either the kinetic resistance to charge transfer at the copolymer-solution boundary or electron transfer at Pt|G2PPI-co-PPy boundary, at different potentials were also plotted as shown in Figure 5.8.

The charge storage capacity, the real impedance and the charge transfer resistance of Pt|G2PPI-co-PPy varied with potential at the lowest frequency of 100 MHz as shown in Figure 5.8. The best potentials at which the dendritic star copolymer exhibited higher ionic conductivity behaviour was -200 mV with a lowest interfacial electron transfer resistance as shown in Figure 5.8.
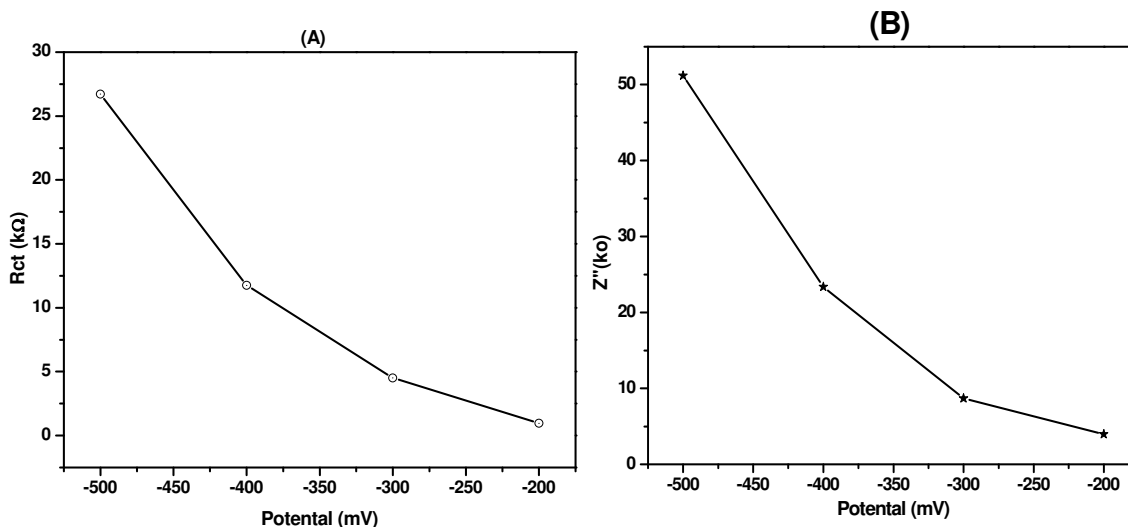
Figure 5.8: Potential dependence of (A) charge transfer resistance, and (B) real impedance for Pt|G2PPI-co-PPy at 100 MHz.

On the other hand, the same responses were observed for bare Pt and Pt electrode modified with polypyrrole (Pt|PPy) at the same potential of -200 mV used for comparing the behaviour of the three electrode platforms as illustrated by the Nyquist plots shown in Figure 5.6. Determine the effect of the platform on the kinetic parameters of the in the electrolyte solution of 0.1 M lithium perchlorate an estimate of the certain kinetic parameters such as time constant (τ), heterogeneous rate constant (K_{et}), exchange current (i_o) were carried out using the following equations, mentioned in Chapter 4 (Section 4.9): 4.6, 4.7, 4.8, and 4.9 (and repeated here for simplicity):

$$\omega_{max} = \frac{1}{R_{ct}C_{dl}}$$

$$(4.6)$$

$$\tau = R_{ct} \times C_{dl}$$

$$(4.7)$$

$$i_o = \frac{RT}{nFR_{ct}}$$

(4.8)

$$i_o = nFAK_{et}C^*$$

(4.9)

The τ values were 5.9343×10^{-7} s rad^{-1}, 0.31826 s rad^{-1} and 0.01154 s rad^{-1} for Pt|G2PPI-co-PPy, bare Pt, and Pt|PPy, respectively. The value of the exchange current calculated showed that the dendritic star copolymer exhibited a higher value (1.00226×10^{-4} A) than bare Pt (3.8177×10^{-8} A) and Pt|PPy (2.89428×10^{-6} A). These results showed that the flow of charge through the star copolymer onto the surface of the electrode was faster at the Pt|G2PPI-co-PPy modified electrode than the bare electrode.

The heterogeneous rate constant is a measure of the rate of electron transfer at the surface of the electrode. Hence, an increase in K_{et} value from 1.1177×10^{-7} cm s^{-1} for the bare Pt electrode to 2.9343×10^{-4} cm s^{-1} for the dendritic star copolymer modified electrode also corroborated the facile flow of charge through the copolymer platform [298]. Furthermore, the time constant obtained from equation 4.7 for the star copolymer platform was lower than that for the bare Pt electrode (see Table 5.1). This is in agreement with earlier reports for modified electrodes [267]. The impedance parameters in Table 5.1 were obtained by fitting the equivalent circuit shown in Figure 5.7 A, where the fitting error was less than 5%.

Table 5.1: Kinetics parameters of $LiClO_4$ on bare Pt, and Pt|PPy and Pt|G2PPI-co-PPy modified electrodes at -200 mV

Kinetic parameters	Pt|bare	Pt|PPy	Pt|G2PPI-co-PPy
ω_{max} (rad s^{-1})	3.142	86.650	13011.650
τ (s rad^{-1})	0.318260	0.01154	5.9343×10^{-7}
i_0 (A)	3.8177×10^{-8}	2.89428×10^{-6}	1.00226×10^{-4}
K_{et} (cm s^{-1})	1.1177×10^{-7}	8.4737×10^{-6}	2.9343×10^{-4}

Surface coverage of 99% was obtained for the star copolymer on the Pt electrode. The value was determined from the R_{ct} value using the equation 4.5

In summary, as seen in Table 5.1, the star copolymer had better ionic conductivity than polypyrrole and bare Pt (lower R_{ct} and τ values) at -200 mV.

This impedance behaviour suggests that this material can be tuned, based on the applied potential, for desired performance-one of the characteristics of a smart material. Moreover, impedance changes were also observed in the phase angle values after the Pt electrode was modified with PPy, and G2PPI-co-PPy. Figure 5.9 shows the plots of phase angle changes with frequency for the bare Pt, PPy, and G2PPI-co-PPy. Bode plots demonstrated significant differences in the electronics of bare Pt, PPy, and G2PPI-co-PPy interfaces. On the other hand, the EIS spectra showed that at low frequency (100 MHz), when the electronic of the electrode system are minimally perturbed, the Pt|G2PPI-co-PPy exhibited semiconductor behaviour (phase angle value 45.3°). The Pt|PPy and Pt electrode had phase angle values of 38.2°and 16.5°, respectively.
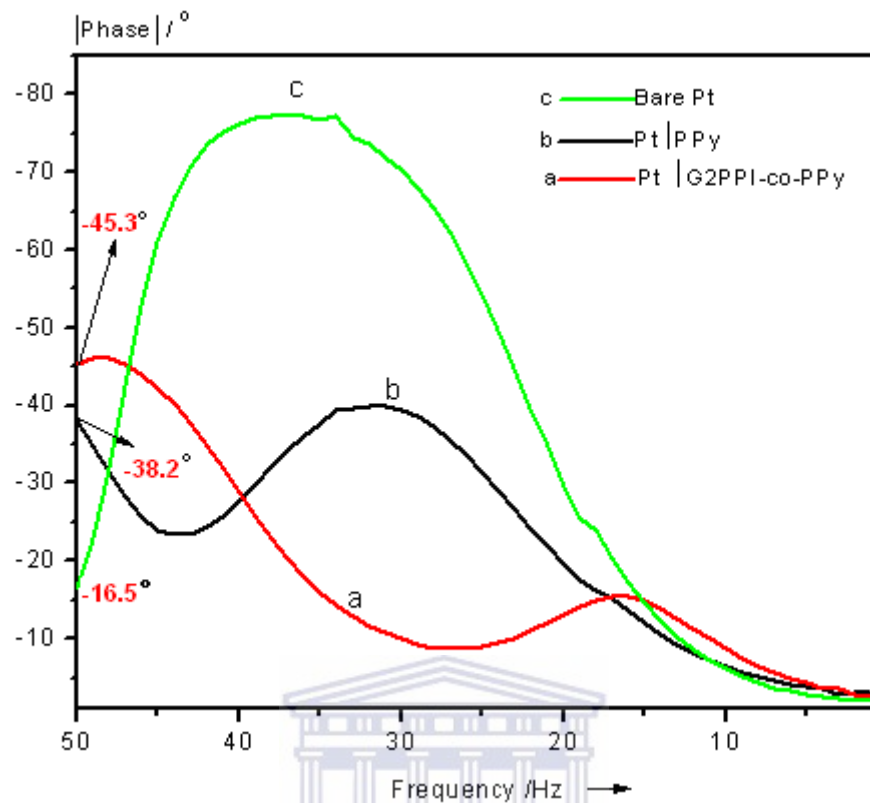
Figure 5.9: EIS Bode phase angle plots at a dc potential of -200 mV: star copolymer Pt|G2PPI-co-PPy, pristine PPy, and bare Pt in 0.1 M LiClO$_4$.

5.9. Sub Conclusions

A novel dendritic conducting star copolymer, G2PPI-co-PPy, was successfully synthesized electrochemically. It exhibited high ionic conductivity, which facilitated the free flow of charge through the holes created by the PPy arms in the conducting star copolymer. Morphological characterization of G2PPI-co-PPy revealed hollow whelk-like helixes of the star copolymers, with an open structure, which explains the ease of charge transportation through the copolymer film. The nanoelectrode exhibited a two-electron electrochemistry process. The Bode phase angle analysis of EIS data confirmed that the star copolymer is a highly semiconductor material.

CHAPTER 6

CONCLUSIONS AND RECOMMENDATIONS

6.1 Conclusions

Novel dendritic conducting star copolymers with polypyrrole arms and a poly(propylene imine) (PPI) dendrimer core of generations 1 to 4 (G1 to G4) was successfully synthesized, by making use of both chemical, as well as electrochemically-based experimental protocols. The Proton Nuclear Magnetic Resonance (^{1}H NMR) of PPI-2Py gave a new chemical shift at 8.1 ppm for N=CH, which confirmed the incorporation of 2-pyrrole aldehyde into the PPI dendrimer structure and Fourier transform infrared spectroscopy (FTIR) showed that strong bands appeared at 1630 cm^{-1} for N=C in the dendrimer moiety, and at 729 cm^{-1} for C-H at the α-position of the PPy ring, while the Thermogravimetric analysis (TGA) for chemical prepared star copolymer exhibited improved of thermal stability than pyrrole functionalized PPI dendrimer. X-ray diffraction (XRD) analysis of first generation chemical prepared star copolymer (G1PPI-co-PPy) revealed a broadly amorphous structure associated with PPy, and crystalline peaks for PPI at 2θ values equal to 18.9°, 31.86°, 33.74°, 37.65°, 45.96°, 48.48° and 52.4°. The electrical conductivity of the chemical prepared star copolymer have been analyzed along with the Hall effect measurements, which has been performed that the conducting star copolymers are a semiconductor N-type having electronic conductivity of 0.7 S cm^{-1} in comparison to the 1.5 S cm^{-1}. The IV curve measurements of Voltage to Current for polypyrrole and star copolymer showed high resistance and the high voltage in the star

copolymer than that of polypyrrole. This shows that polypyrrole has higher electronic conductivity than the star copolymer

Scanning electron microscopy (SEM) results shows that the electrochemically prepared star copolymer has interesting morphological surface (whelk-like helixes), the results showed changes in the surface morphology from functionalized dendrimer to the star copolymer the morphology; In fact, while the morphology of the chemically prepared copolymers resembles that of flaky wax material, at higher magnifications, it became apparent that the electrochemically grown star copolymers actually consist of hollow open tubes (with openings at their tapered ends) having an average base diameter of 2.0 μm. In this regard, it is anticipated that these holes will in fact give the conducting star copolymers higher Ionic conductivity, resulting from the flow of ions from the solution electrolytes to the surface of the modified electrode through the star copolymer.

Electrochemical impedance spectroscopy (EIS) showed that the first generation conducting star copolymers G1PPI-co-PPy exhibited slightly higher ionic conductivity than pristine PPy in lithium perchlorate the Z'/kΩ values are 500, 2.5 and 1.75 for G1PPI-2Py, PPy and G1PPI-co-PPy, respectively.

The research work also focused on the electrochemical study of a second generation conducting star copolymers G2PPI-co-PPy on platinum electrode at dc potential applied of -200 mV, decreased the electrochemical charge transfer resistance when compared to electrodeposited polypyrrole (PPy) on platinum electrode as well as the bare Pt. The decrease in charge transfer resistance may attribute to an increase in the conjugation length of the polymer as result of the linking of the highly conjugated PPy to the PPI

dendrimer. Bode impedimetric analysis indicates that G2PPI-co-PPI is a semiconductor with a maximum phase angle shift of 45.3° at 100 mHz.

The Electrochemical impedance spectroscopy (EIS) showed phase angle Bode plots of forth generation conducting star copolymers G4PPI-co-PPy on platinum electrode observes that impedance changed with change dc potential applied. At -700 mV, the star copolymer and PPy show two times constant as depicted in the two ϕ_{max} of the phase angle (two semi circles on the Nyquist plot) and one time constant at 100 mV, depicts that the interfacial kinetics of these material strongly depends on the applied potential. The star copolymer exhibited a 2-electron electrochemistry and a surface coverage of 99%, the conducting star copolymer film was found to have excellent electrochemical properties, such as improved electron transfer ability, and good stability. That we believed to particularly useful for electroanalytical application.

The conducting star copolymers are novel and have not been reported to the best of my Knowledge elsewhere. Related to this, it was considered that the study and exploration of these compounds properties such as semi-conductivity, potential tenability, fluorescence, biocompatible nature of the dendrimer core and interstitial voids, in conducting and/or electroactive film configuration settings could contribute to the knowledge of very useful materials for enzymatic biosensor applications and super-capacitive material.

6.2 Recommendation:

My thesis open an entirely new view of the electrochemistry of conducting dendrimeric star copolymers on poly(propylene imine) dendrimer core polypyrrole from generation G1

to G4. These conducting star copolymers have been synthesized for the first time. In order to tailor these materials for future applications such as super capacitance material, rechargeable batteries, sensor and biosensor applications, as well as optical power limiting materials, new and versatile synthetic tools must be developed. Moreover, the structure property relationship of these materials must be further understood.

I recommend more surface studies such scanning electrochemical spectroscopy and X-ray photoelectron spectroscopy should be investigated so as to have better clue to the surface chemistry of the electrosynthetic poly(propylene imine) dendrimer core polypyrrole dendrimeric conducting star copolymer. For chemically prepared dendrimeric conducting star copolymer need more conductivity study and the effect of metal nanoparticles insertion on the conductivity using Hall effect measurement.

Future work to establish further the electrochemistry of chemically and electrochemically prepared of these dendrimeric conducting star copolymers will be worthwhile. Electrochemistry of star copolymer has been shown good electrochemistry results; the application of the dendrimeric conducting star copolymer as enzymatic biosensor platforms is worth investing.

References

1. Skotheim, T. A., *Handbook of conducting polymers*. Vol. 2. 1986, New York: Marcel Dekker.

2. Fei Wang, R. D. R., and Timothy L. Rose, *An electrically conducting starpolymer.* Journal of the American Chemical Society, 1997. **119**: 11106-11107.

3. Gubbels, F., Jerome R., Vanlathem E., Deltour R., Blacher S., and Brouers F., *Kinetic and thermodynamic control of the selective localization of carbon black at the interface of immiscible polymer blends*. Chemistry of Materials, 1998. **10**(5): 1227-1235.

4. Zhang, C., Yi X.-S., Yui H., Asai S., and Sumita M., *Morphology and electrical properties of short carbon fiber-filled polymer blends: High-density polyethylene/poly(methyl methacrylate)*. Journal of Applied Polymer Science, 1998. **69**(9): 1813-1819.

5. Lagrève, C., Feller J. F., Linossier I., and Levesque G., *Poly(butylene terephthalate)/ poly(ethylene-co-alkyl acrylate)/ carbon black conductive composites: Influence of composition and morphology on electrical properties.* Polymer Engineering & Science, 2001. **41**(7): 1124-1132.

6. El-Tantawy, F., Kamada K., and Ohnabe H., *A novel way of enhancing the electrical and thermal stability of conductive epoxy resin–carbon black composites via the Joule heating effect for heating-element applications.* Journal of Applied Polymer Science, 2003. **87**(2): 97-109.

7. F.O.Toribio, and T.C.Maria, *Soft and wet conducting polymers for artificial muscles.* Advanced Materials, 2003. **15**: 279-282.

153

8.   Lee, J.-W., Serna F., Nickels J., and Schmidt C. E., *Carboxylic acid-functionalized conductive polypyrrole as a bioactive platform for cell adhesion.* Biomacromolecules, 2006. **7**(6): 1692-1695.

9.   Kotwal, A.Schmidt C. E., *Electrical stimulation alters protein adsorption and nerve cell interactions with electrically conducting biomaterials.* Biomaterials, 2001. **22**(10): 1055-1064.

10.   Heeger, A. J., *Semiconducting and metallic polymers: the fourth generation of polymeric materials.* Synthetic Metals, 2001. **125**(1): 23-42.

11.   Shimizu, A., Yamaka K., and Kohno M., *Rechargeable lithium batteries using polypyrrole-poly(styrenesulfonate) composite as the cathode-active material.* Bulletin of the Chemical Society of Japan, 1988. **61**: 4401-4406.

12.   Sotzing, G., Reynolds J. R., and Steel P., *Electrochromic conducting polymers via electrochemical polymerization of bis(2-(3,4-ethylenedioxy)thienyl) monomers.* Journal Chemistry of Materials, 1996. **8**: 882-889.

13.   Braun, D.Heeger A., *Visible light emission from semiconducting polymer diodes* Applied Physics Letters, 1991. **58**(18): 1982-1984.

14.   Larmat, F.Reynolds J. R., Synth Met, 1996. **79**: 229-223.

15.   Selampinar, F., Toppare L., Akbulut U., Yalcin T., and Suzer S., Synth Met, 1995. **68**: 109-116.

16.   Martin, R., Liang W., Menon V., Parthasarathy R., and Parthasarathy A., Synth Met 1993. **55**: 3766-3773.

17.   Selampinar, F., Akbulut U., Ozden M. Y., and Toppare L., Biomaterials, 1997. 64.

18.   Singh, R., Tandon R. P., Panwar V. S., and Chandra S., *Low frequency ac conduction in lightly doped polypyrrole films.* J Appl Phys, 1991. **69**: 2504-2508.

19.   Qian, R. Y., Qiu J. J., and Shen D. Y., Synth Met 1987. **18**: 13-18.

20.   Ak, M.Toppare L., Materials Chemistry and physics, 2009. **114**: 789-794.

21.   Chronakis, I. S., Grapenson S., and Jakob A., Polymer, 2006. **47**: 1597-1603.

22.   Brahim, S.Guiseppi-Elie A., Electroanalysis, 2005. **17**: 556-570.

23.   Wang, F.Rauh R. D., *Reflective and conductive star polymers*. 2000 EIC Laboratories, Inc. (Norwood, MA) US.

24.   McCullough, R. D.Lowe R. D., *Enhanced electrical conductivity in regioselectively synthesized poly(3-alkylthiophenes).* Journal of the Chemical Society, Chemical Communications, 1992(1): 70-72.

25.   McCullough, R. D., Tristram-Nagle S., Williams S. P., Lowe R. D., and Jayaraman M., *Self-orienting head-to-tail poly(3-alkylthiophenes): new insights on structure-property relationships in conducting polymers.* Journal of the American Chemical Society, 1993. **115**(11): 4910-4911.

26.   Chen, T.-A., Wu X., and Rieke R. D., *Regiocontrolled synthesis of poly(3-alkylthiophenes) mediated by rieke zinc: Their characterization and solid-state properties.* Journal of the American Chemical Society, 1995. **117**(1): 233-244.

27. Risch, B. G., Wilkes G. L., and Warakomski J. M., *Crystallization kinetics and morphological features of star-branched nylon-6: effect of branch-point functionality.* Polymer, 1993. **34**(11): 2330-2343.

28. Sotzing, G. A., Reynolds J. R., and Steel P. J., *Electrochromic conducting polymers via electrochemical polymerization of bis(2-(3,4-ethylenedioxy)thienyl) monomers.* Chemistry of Materials, 1996. **8**(4): 882-889.

29. MacDiarmid, A. G.Epstein A. J., *Conducting polymers: past, present and future.* Materials Research Society Symposium Proceeding, 1994. **328**: 133-144.

30. Bulut, U., Yilmaz F., Yagci Y., and Toppare L., *Synthesis, characterization and electrochromic properties of conducting copolymers of 3-[(3-thienylcarbonyl)oxy]-2,2-bis{[(3-thienylcarbonyl)oxy]}propyl 3-thiophene carboxylate with thiophene and pyrrole.* Reactive & Functional Polymers, (2004) **61**: 63-70

31. Sahin, E., Camurlu P., Toppare L., Mercore V. M., Cianga I., and YagcI Y., *Conducting copolymers of thiophene functionalized polystyrenes with thiophene.* Journal of Electroanalytical Chemistry, 2005. **579**(2): 189-197.

32. Xu, J., Nie G., Zhang S., Han X., Hou J., and Pu S., *Electrochemical copolymerization of indole and 3,4-ethylenedioxythiophene.* Journal of Materials Science, 2005. **40**(11): 2867-2873.

33. Miyashita, K., Kamigaito M., Sawamoto M., and Higashimura T., *Synthesis of end-functionalized polystyrenes with organosilicon end-capping reagents via living cationic polymerization.* Journal of Polymer Science Part A: Polymer Chemistry, 1994. **32**(13): 2531-2542.

34.   Schenning, A. P. H. J., Peeters E., and Meijer E. W., *Energy transfer in supramolecular assemblies of oligo(p-phenylene vinylene)s terminated poly(propylene imine) dendrimers.* Journal of the American Chemical Society, 2000. **122**(18): 4489-4495

35.   Schenning, A. P. H. J., Jonkheijm P., Hofkens J., Feyter S. D., Asavei T., Cotlet M., Schryver F. C. D., and Meijer E. W., *Formation and manipulation of supramolecular structures of oligo(p-phenylenevinylene) terminated poly(propylene imine) dendrimers.* Chemical Communications, 2002(12).

36.   Hirao, A., Sugiyama K., Tsunoda Y., Matsuo A., and Watanabe T., *Precise synthesis of well-defined dendrimer-like star-branched polymers by iterative methodology based on living anionic polymerization.* Journal of Polymer Science Part A: Polymer Chemistry, 2006. **44**(23): 6659-6687.

37.   Trollsås, M., Kelly M. A., Claesson H., Siemens R., and Hedrick J. L., *Highly branched block copolymers: design, synthesis, and morphology.* Macromolecules, 1999. **32**(15): 4917-4924.

38.   Hedrick, J. L., Trollsås M., Hawker C. J., Atthoff B., Claesson H., Heise A., Miller R. D., Mecerreyes D., Jérôme R., and Dubois P., *Dendrimer-like star block and amphiphilic copolymers by combination of ring opening and atom transfer radical polymerization.* Macromolecules, 1998. **31**(25): 8691-8705.

39.   Roovers, J., Zhou L. L., Toporowski P. M., Zwan M. v. d., Iatrou H., and Hadjichristidis N., *Regular star polymers with 64 and 128 arms. Models for polymeric micelles.* Macromolecules, 1993. **26**(16): 4324-4331.

40.   Roovers, J.Comanita B., *Dendrimers and dendrimer-polymer hybrids*, in *Branched Polymers I*, J. Roovers, Editor. 1999, Springer, Berlin / Heidelberg. p. 179-228.

41.   Kimura, M., Kato M., Muto T., Hanabusa K., and Shirai H., *Temperature-sensitive dendritic hosts:□ synthesis, characterization, and control of catalytic activity.* Macromolecules, 2000. **33**(4): 1117-1119.

42.   Cooper, A., Londono J., Wignall G., McClain J., Samulski E., Lin J., Dobrynin A., Rubinstein M., Burke A., Frechet J., and DeSimone J., *Extraction of a hydrophilic compound from water into liquid CO2 using dendritic surfactants.* Nature, 1997. **389**(6649): 368-371.

43.   Hedden, R. C., Bauer B. J., Paul Smith A., Gröhn F., and Amis E., *Templating of inorganic nanoparticles by PAMAM/PEG dendrimer-star polymers.* Polymer, 2002. **43**(20): 5473-5481.

44.   Luo, D., Haverstick K., Belcheva N., Han E., and Saltzman W. M., *Poly(ethylene glycol)-conjugated PAMAM dendrimer for biocompatible, high-efficiency DNA delivery.* Macromolecules, 2002. **35**(9): 3456-3462.

45.   Hedden, R. C.Bauer B. J., *Structure and dimensions of PAMAM/PEG dendrimer−star polymers.* Macromolecules, 2003. **36**(6): 1829-1835.

46.   Comanita, B., Noren B., and Roovers J., *Star poly(ethylene oxide)s from carbosilane dendrimers.* Macromolecules, 1999. **32**(4): 1069-1072.

47.   Zhao, Y., Shuai X., Chen C., and Xi F., *Synthesis and characterization of star-shaped poly(l-lactide)s initiated with hydroxyl-terminated poly(Amidoamine) (PAMAM-OH) dendrimers.* Chemistry of Materials, 2003. **15**(14): 2836-2843.

48.   Heise, A., Diamanti S., Hedrick J. L., Frank C. W., and Miller R. D., *Investigation of the initiation behavior of a dendritic 12-arm initiator in atom transfer radical*

polymerization. Macromolecules, 2001. **34**(11): 3798-3801.

49.   H.A.M. van Aert, Genderen M. H. P. v., and Meijer E. W., *Star-shaped poly(2,6-dimethyl-1,4-phenylene ether).* Polymer Bulletin, 1996. **37**: 273-280.

50.   van Aert, H. A. M., Burkard M. E. M., Jansen J. F. G. A., van Genderen M. H. P., Meijer E. W., Oevering H., and Buning G. H. W., *Functional oligomers, telechelics, and graft and star-shaped poly(2,6-dimethyl-1,4-phenylene ether)s prepared by redistribution.* Macromolecules, 1995. **28**(23): 7967-7969.

51.   Liu, M., Petro M., Fréchet J. M. J., Haque S. A., and Wang H. C., *Preparation of hydrophobic poly(isobutylene) star polymer with hydrophilic poly(propylene imine) dendritic cores.* Polymer Bulletin, 1999. **43**: 51-58.

52.   Francis, R., Taton D., Logan J. L., Masse P., Gnanou Y., and Duran R. S., *Synthesis and surface properties of amphiphilic star-Sshaped and dendrimer-like copolymers based on polystyrene core and poly(ethylene oxide) corona.* Macromolecules, 2003. **36**(22): 8253-8259.

53.   Trollsås, M., Atthoff B., Claesson H., and Hedrick J. L., *Dendritic homopolymers and block copolymers: Tuning the morphology and properties.* Journal of Polymer Science Part A: Polymer Chemistry, 2004. **42**(5): 1174-1188.

54.   Urbani, C. N., Lonsdale D. E., Bell C. A., Whittaker M. R., and Monteiro M. J., *Divergent synthesis and self-assembly of amphiphilic polymeric dendrons with selective degradable linkages.* Journal of Polymer Science Part A: Polymer Chemistry, 2008. **46**(5): 1533-1547.

55.   Stancik, C. M., Pople J. A., Trollsås M., Lindner P., Hedrick J. L., and Gast A. P., *Impact of core architecture on solution properties of dendrimer-like star*

159

copolymers. Macromolecules, 2003. **36**(15): 5765-5775.

56.   Urbani, C. N., Bell C. A., Lonsdale D., Whittaker M. R., and Monteiro M. J., *Self-assembly of amphiphilic polymeric dendrimers synthesized with selective degradable linkages.* Macromolecules, 2007. **41**(1): 76-86.

57.   Matmour, R., Lepoittevin B., Joncheray T. J., El-khouri R. J., Taton D., Duran R. S., and Gnanou Y., *Synthesis and investigation of surface properties of dendrimer-like copolymers based on polystyrene and poly(tert-butylacrylate).* Macromolecules, 2005. **38**(13): 5459-5467.

58.   van Ruymbeke, E., Orfanou K., Kapnistos M., Iatrou H., Pitsikalis M., Hadjichristidis N., Lohse D. J., and Vlassopoulos D., *Entangled dendritic polymers and beyond:□ rheology of symmetric cayley-tree polymers and macromolecular self-assemblies.* Macromolecules, 2007. **40**(16): 5941-5952.

59.   Yoo, H.-S., Watanabe T., and Hirao A., *Precise synthesis of dendrimer-like star-branched polystyrenes and block copolymers composed of polystyrene and poly(methyl methacrylate) segments by an iterative methodology using living anionic polymerization.* Macromolecules, 2009. **42**(13): 4558-4570.

60.   Hawker, C. J.Fréchet J. M. J., *Unusual macromolecular architectures: The convergent growth approach to dendritic polyesters and novel block copolymers.* Journal of the American Chemical Society, 1992. **114**: 8405-8413.

61.   Heinze, J., *Electrochemistry of conducting polymers.* Synthetic Metals, 1991. **41-43**: 2805-2823.

62.   Wang, F., Rauh R. D., and Rose T. L., *An electrically conducting star polymer.* Journal of the American Chemical Society, 1997. **119**(45): 11106-11107.

63.   Yamamoto, H., Oshimia M., Fukuda M., Isa I., and Yoshino K., *Characteristics of aluminum solid electrolyte capacitors using a conducting polymer.* Journal of Power Sources, 1996. **60**: 173-177.

64.   Liu, Y.-C.Chung K.-C., *Characteristics of conductivity-improved polypyrrole films via different procedures.* Synthetic Metals, 2003. **139**: 277-281.

65.   Sung, J.-H., Kim S.-J., and Lee K.-H., *Fabrication of microcapacitors using conducting polymer microelectrodes.* Journal of Power Sources, 2003. **124**(1): 343-350.

66.   Xue, H.Shen Z., *A highly stable biosensor for phenols prepared by immobilizing polyphenol oxidase into polyaniline-polyacrylonitrile composite matrix.* Talanta, 2002. **57**(2): 289-295.

67.   Kanazawa, K. K., Diaz A. F., Geiss R. H., Gill W. D., Kwak J. F., Logan J. A., Rabolt J. F., and Street G. B., *'Organic metals': polypyrrole, a stable synthetic 'metallic' polymer.* Journal of the Chemical Society, Chemical Communications, 1979(19): 854-855.

68.   Gerard, M., Chaubey A., and Malhotra B. D., *Application of conducting polymers to biosensors.* Biosensors and Bioelectronics, 2002. **17**(5): 345-359.

69.   Saxena, V.Malhotra B. D., *Prospects of conducting polymers in molecular electronics.* Current Applied Physics, 2003. **3**(2-3): 293-305.

70.   Huang, L.-M., Wen T.-C., Gopalan A., and Ren F., *Structural influence on the electronic properties of methoxy substituted polyaniline/aluminum Schottky barrier diodes.* Materials Science and Engineering B, 2003. **104**(1-2): 88-95.

71. Brahim, S., Wilson A. M., Narinesingh D., Iwuoha E., and Guiseppi-Elie A., *Chemical and biological sensors based on electrochemical detection using conducting electroactive polymers.* Microchimica Acta, 2003. **143**(2): 123-137.

72. Groenendaal, L., Zotti G., Aubert P. H., Waybright S. M., and Reynolds J. R., *Electrochemistry of poly(3,4-alkylenedioxythiophene) derivatives.* Advanced Materials, 2003. **15**(11): 855-879.

73. Feast, W. J., *In Handbook of conducting polymers*, ed. T.A. Skotheim. 1986, New York: Marcel Dekker.

74. Riande, E.Diaz-Calleja R., *Electrical properties of polymers* 2004: Marcel Dekker, Inc., New York.

75. Soos, Z. G., in *Handbook of conductive polymers*, T.A. Skotheim, Editor. 1986, Marcel Dekker: New York. p. 165-196.

76. Masuda, H.Asano D. K., *Preparation and properties of polypyrrole.* Synthetic Metals, 2003. **135-136**: 43-44.

77. Rehwald, W.Kiess H. G., *charge transport in polymers*, in *Conjugated conducting polymers*, H.G. Kiess, Editor. 1992, Springer-Verlag: New York. p. 135-173.

78. Kim, S. W., Bae Y. H., and Okano T., *Hydrogels: swelling, drug loading, and release.* Pharmaceutical Research, 1992. **9**: 283-290.

79. Langer, R., *New methods of drug delivery.* Science, 1990. **249**: 1527-1533.

80. Salzner, U., Lagowski J. B., Pickup P. G., and Poirier R. A., *Comparison of*

geometries and electronic structures of polyacetylene, polyborole, polycyclopentadiene, polypyrrole, polyfuran, polysilole, polyphosphole, polythiophene, polyselenophene and polytellurophene. Synthetic Metals, 1998. **96**(3): 177-189.

81. Walczak, R. M., *Synthetic methodology as a basis for conducting polymer design* 2006, Dissertation, University of Florida.

82. Kang, E. T., Neoh K. G., and Tan K. L., *Polyaniline: a polymer with many interesting intrinsic redox states.* Progress in Polymer Science, 1998. **23**: 277-324.

83. Teasdale, P., *Properties of polypyrroles*, in *Conductive Electroactive Polymers*. 2002, CRC Press.

84. Nashat, A.Langer R., *Temporal characteristics of activation, deactivation, and restimulation of signal transduction following depolarization in the pheochromocytoma cell line PC- 12.* Molecular and Cellular Biology, 2003. **23**: 4788-4795.

85. Schmidt, C. E., Shastri V. R., Vacanti J. P., and Langer R., *Stimulation of neurite outgrowth using an electrically conducting polymer.* Proceedings of the National Academy of Sciences, 1997. **USA 94**: 8948-8953.

86. Cui, X., Hetke J. F., Wiler J. A., Anderson D. J., and Martin D. C., *Electrochemical deposition and characterization of conducting polymer polypyrrole/PSS on multichannel neural probes.* Sensors and Actuators A, 2001. **93**: 8-18.

87. Reut, J., Reut N., and Opik A., *Preparation and characterization of multilayer systems consisting of the soluble and electrochemically synthesized polypyrrole*

films. Synthetic Metals, 2001. **119**: 81-82.

88.   Freund, M. S., Karp C., and Lewis N. S., *Growth of thin processale films of poly(pyrrole) using phosphomolybdate clusters.* Inorganica Chimica Acta, 1995. **240**: 447-451.

89.   Street, G. B., in *Handbook of conductive polymers* T.A. Skotheim, Editor. 1986, Marcel Dekker: New York. p. 265-292.

90.   Lunn, B. A., Unsworth J., Booth N. G., and Innis P. C., *Determination of the thermal conductivity of polypyrrole over the temperature range 280-335K.* Journal of Materials Science, 1993. **28**: 5092-5098.

91.   Mott, N. F.Davis E. A., *Electronic processes in non-crystalline materials*, Clarendon Press, Oxford, 1979.

92.   Mott, N., F, *Electronc in glass.* Nobel Lecture, 8 December 1977.

93.   Kumar, D.Sharma R. C., *Advances in conductive polymers.* European Polymer Journal, 1998. **34**(8): 1053-1060.

94.   Sun, X., Lu D., Fu R., Li X. S., Lin D. L., and George T. F., *Gap states of charged solitons in polyacetylene.* Physical Review B, 1989. **40**(18): 12446.

95.   Larsson, S.Rodriguez-Monge L., *Conductivity in polyacetylene. II. Ab initio and tight-binding calculations of soliton structure and reorganization energy in ordered and disordered structures.* International Journal of Quantum Chemistry, 1996. **58**(5): 517-532.

96.   Li, X., Jiao Y., and Li S., *The syntheses, properties and application of new*

conducting polymers. European Polymer Journal, 1991. **27**(12): 1345-1351.

97.   Pichler, K., Halliday D. A., Bradley D. D. C., Burn P. L., Friend R. H., and Holmes A. B., *Optical spectroscopy of highly ordered poly(p-phenylene vinylene)* Journal of Physics: Condensed Matter, 1993. **5**: 7155-7172.

98.   Margolis, J. M., *Conductive polymers and plastics.* 1989: Chapman and Hall, 2-11

99.   Shirakawa, H., Louis E. J., MacDiarmid A. G., Chiang C. K., EDWIN J. LOUIS, and Heeger A. J., *Synthesis of electrically conducting organic polymers: halogen derivatives of polyacetylene, (CH)x.* Journal of the Chemical Society, Chemical Communications, 1977: 578-580.

100.   Čík, G., Šeršeň F., and Dlháň L., *Thermally induced transitions of polarons to bipolarons in poly(3-dodecylthiophene).* Synthetic Metals, 2005. **151**(2): 124-130.

101.   Kaufman, J. H., Colaneri N., Scott J. C., and Street G. B., *Evolution of polaron states into bipolarons in polypyrrole.* Physical Review Letters, 1984. **53**(10): 1005.

102.   Farias, G. A., da Costa W. B., and Peeters F. M., *Acoustical polarons and bipolarons in two dimensions.* Physical Review B, 1996. **54**(18): 12835-12840.

103.   Irle, S.Lischka H., *Combined ab initio and density functional study on polaron to bipolaron transitions in oligophenyls and oligothiophenes* Journal of Chemical Physics, 1997. **107**(8): 3021-3032.

104.   Fernandes, M. R., Garcia J. R., Schultz M. S., and Nart F. C., *Polaron and bipolaron transitions in doped poly(p-phenylene vinylene) films.* Thin Solid Films, 2005. **474**(1-2): 279-284.

105. Verbist, G., Peeters F. M., and Devreese J. T., *Large bipolarons in two and three dimensions.* Physical Review B, 1991. **43**(4): 2712-2720.

106. Shimidzu, T., Ohtani A., Iyoda T., and Honda K., *A novel type of polymer battery using a pyrrole-polyanion composite electrode.* Journal of the Chemical Society, Chemical Communications, 1987(5): 327-328.

107. Peres, R. C. D., De Paoli M.-A., Panero S., and Scrosati B., *A new electrode for a poly(pyrrole)-based rechargeable battery.* Journal of Power Sources, 1992. **40**(3): 299-305.

108. Tarkuc, S., Sahin E., Toppare L., Colak D., Cianga I., and Yagci Y., *Synthesis, characterization and electrochromic properties of a conducting copolymer of pyrrole functionalized polystyrene with pyrrole.* Polymer, 2006. **47**(6): 2001-2009.

109. Mermillod, M., Tanguy J., and Petiot F., *A Study of chemically synthesized polypyrrole as electrode material for battery applications.* Journal of The Electrochemical Society, 1986. **133**(6): 1073-1079.

110. Diaz, A. F., Castillo J. I., Logan J. A., and Lee W. Y., *Electrochemistry of conducting polypyrrole films.* Journal of Electroanalytical Chemistry, 1981. **129**(1-2): 115-132.

111. Burroughes, J. H., Bradley D. D. C., Brown A. R., Marks R. N., Mackay K., Friend R. H., Burns P. L., and Holmes A. B., *Light-emitting diodes based on conjugated polymers.* Nature, 1990. **347**(6293): 539-541.

112. Larmat, F., Reynolds J. R., and Qiu Y. J., *Polypyrrole as a solid electrolyte for tantalum capacitors.* Synthetic Metals, 1996. **79**(3): 229-233.

113. Rudge, A., Raistrick I., Gottesfeld S., and Ferraris J. P., *A study of the electrochemical properties of conducting polymers for application in electrochemical capacitors.* Electrochimica Acta, 1994. **39**(2): 273-287.

114. Selampinar, F., Toppare L., Akbulut U., Yalçin T., and Süzer S., *A conducting composite of polypyrrole II. As a gas sensor.* Synthetic Metals, 1995. **68**(2): 109-116.

115. Miasik, J. J., Hooper A., and Tofield B. C., *Conducting polymer gas sensors.* Journal of the Chemical Society, Faraday Transactions 1: Physical Chemistry in Condensed Phases, 1986. **82**(4): 1117-1126.

116. Bartlett, P. N., Archer P. B. M., and Ling-Chung S. K., *Conducting polymer gas sensors part I: fabrication and characterization.* Sensors and Actuators, 1989. **19**(2): 125-140.

117. Hwang, L. S., Ko J. M., Rhee H. W., and Kim C. Y., *A polymer humidity sensor.* Synthetic Metals, 1993. **57**(1): 3671-3676.

118. Martin, C. R., Liang W., Menon V., Parthasarathy R., and Parthasarathy A., *Electronically conductive polymers as chemically-selective layers for membrane-based separations.* Synthetic Metals, 1993. **57**(1): 3766-3773.

119. Schuhmann, W., Kranz C., Huber J., and Wohlschläger H., *Conducting polymer-based amperometric enzyme electrodes. Towards the development of miniaturized reagentless biosensors.* Synthetic Metals, 1993. **61**(1-2): 31-35.

120. Schuhmann, W., *Functionalized polypyrrole. A new material for the construction of biosensors.* Synthetic Metals, 1991. **41**(1-2): 429-432.

121. Selampinar, F., Akbulut U., Özden M. Y., and Toppare L., *Immobilization of invertase in conducting polymer matrices.* Biomaterials, 1997. **18**(17): 1163-1168.

122. Kivelson, S., *Electron hopping conduction in the soliton model of polyacetylene.* Physical Review Letters, 1981. **46**(20): 1344-1348.

123. Kudoh, Y., Akami K., and Matsuya Y., *Properties of chemically prepared polypyrrole with an aqueous solution containing Fe2(SO4)3, a sulfonic surfactant and a phenol derivative.* Synthetic Metals, 1998. **95**: 191-196.

124. Rodriguez, J., Grande H.-J., and Otero T. F., *Conductive polymers: synthesis and electrical properties*, in *Handbook of Organic Conductive Molecules and Polymers*, H.S. Nalwa, Editor. 1997, Wiley Sons: Chichester.

125. Tüken, T., YazIcI B., and Erbil M., *The use of polyindole for prevention of copper corrosion.* Surface and Coatings Technology, 2006. **200**(16-17): 4802-4809.

126. Bazzaoui, M., Martins J. I., Bazzaoui E. A., Martins L., and Machnikova E., *Sweet aqueous solution for electrochemical synthesis of polypyrrole part 1B: On copper and its alloys.* Electrochimica Acta, 2007. **52**(11): 3568-3581.

127. Lehr, I. L.Saidman S. B., *Corrosion protection of iron by polypyrrole coatings electrosynthesised from a surfactant solution.* Corrosion Science, 2007. **49**(5): 2210-2225.

128. Kiefer, R., Chu S. Y., Kilmartin P. A., Bowmaker G. A., Cooney R. P., and Travas-Sejdic J., *Mixed-ion linear actuation behaviour of polypyrrole.* Electrochimica Acta, 2007. **52**(7): 2386-2391.

129. Scheller, F. W., Wollenberger U., Warsinke A., and Lisdat F., *Research and*

development in biosensors. Current Opinion in Biotechnology, 2001. **12**: 35-40.

130.   Sabouraud, G., Sadki S., and Brodie N., *The mechanisms of pyrrole electropolymerization.* Chemical Society Reviews, 2000. **29**: 283-293.

131.   Zelikin, A. N., Lynn D., Farhadi J., Martin I., Shastri V., and Langer R., *Erodible conducting polymers for potential biomedical applications.* Angewandte Chemie International Edition, 2002. **41**: 141-144.

132.   George, P. M., *Novel polypyrrole derivatives to enhance conductive polymer-tissue interactions*, in *Medical and Electrical Engineering.* 2005, Massachusetts Insititute of MIT: America.

133.   Liu, Y., Cui, T Varahramyan K., *All-polymer capacitor fabricated with inkjetprinting technique.* Solid-State Electronics, 2003. **47**: 1543-1548.

134.   Furukawa, Y., Tazawa S., Fujii Y., and Harada I., *Raman spectra of polypyrrole and its 2,5-13C-substituted and C-deuterated analogues in doped and undoped states.* Synthetic Metals, 1988. **24**(4): 329-341.

135.   Somani, P.Radhakrishnan S., *Electrochromic response in polypyrrole sensitized by prussian blue.* Chemical Physics Letters, 1998. **292**(1-2): 218-222.

136.   Girotto, E. M.de Paoli M.-A., *Polypyrrole color modulation and electrochromic contrast enhancement by doping with a dye.* Advanced Materials, 1998. **10**(10): 790-793.

137.   Alkan, S., Toppare L., Hepuzer Y., and Yagci Y., *Block copolymers of thiophene-capped poly(methyl methacrylate) with pyrrole.* Journal of Polymer Science Part A: Polymer Chemistry, 1999. **37**(22): 4218-4225.

138.   Kizilyar, N., Toppare L., Önen A., and Yağci Y., *Synthesis of conducting PPy/pTHF copolymers.* Journal of Applied Polymer Science, 1999. **71**(5): 713-720.

139.   Kalaycioglu, E., Toppare L., Yagci Y., Harabagiu V., Pintela M., Ardelean R., and Simionescu B. C., *Synthesis of conducting H-type polysiloxane-polypyrrole block copolymers.* Synthetic Metals, 1998. **97**(1): 7-12.

140.   Bengü, B., Toppare L., and Kalaycioglu E., *Synthesis of conducting graft copolymers of 2-(N-pyrrolyl)ethylvinyl ether with pyrrole.* Designed Monomers & Polymers, 2001. **4**(1): 53-65.

141.   Tourillon, G., *Polythiophene and its derivatives*, in *Handbook of conducting polymers*, T. Skotheim, Editor. 1986: New York: Marcel Dekker. p. 293-350.

142.   Yueqiang, S., Carneiro K., Ping W., and Renyuan Q., in *Electronic Properties of Conjugated Polymers*, H. Kuzmany, M. Mehring, and S. Roth, Editors, International Winter School: Springer-Verlag, Kirchberg, Tirol, 1987.

143.   Cioffi, N., Torsi L., Losito I., Di Franco C., De Bari I., Chiavarone L., Scamarcio G., Tsakova V., Sabbatini L., and Zambonin P. G., *Electrosynthesis and analytical characterisation of polypyrrole thin films with copper nanoparticles.* Journal of Materials Chemistry, 2001. **11**: 1434-1440.

144.   Reynolds, J. R., Baker C. K., Jolly C. A., Poropatic P. A., and Ruiz J. P., in *Conductive polymers and plastics* J.M. Margolis, Editor, Chapman and Hall,: New York, 1989. p. 1-40.

145.   Riande, E.Diaz-Calleja R., *Electrical properties of polymers.* 2004, New York:

Marcel Dekker.

146.   Meikap, A. K., Das A., Chatterjee S., Digar M., and Bhattacharyya S. N., *Electrical transport in doped polypyrrole films at low temperature* Physical Review B, 1993 **47**(3): 1340-1345.

147.   Ansari, R., *Polypyrrole conducting electroactive polymers: synthesis and stability studies.* E-Journal of Chemistry, 2006. **3**(13): 186-201.

148.   K.Dodlhofer and K. Rajeshwar, *Handbook of conducting polymers, 2nd edition , .* ed. T.A. Skotheim, R.L. Elsenbaumer and J.R.Reynolds,Marcel Dekker, New York , , 1998,. **531.**

149.   Lyons, M. E. G., *Advances in Chemical Physics,Polymeric systems, ed.   I. Prigogine and S.A. Rice, .* John Wiley Sons New York, , 1997. **94**: 297.

150.   Said Sadki, P. S., Nancy Brodie and Guillaume Sabouraud *The mechanism of pyrrole polymerization.* Royal society of Chemistry, 2000. **29**: 283-293.

151.   Kuang-Hsuan Yang, Y.-C. L., Chung-Chin Yu, *Temperature effect of electrochemically roughened gold substrates on polymerization electrocatalysts of polypyrrole.* Analytica Chimica Acta, 2009. **631**: 40-46.

152.   Vork, F. T. A., Schuermans B. C. A. M., and Barendrecht E., *Influence of inserted anions on the properties of polypyrrole.* Electrochimica Acta, 1990. **35**(2): 567-575.

153.   Yoshino, K., Tabata M., Satoh M., Kaneto K., and Ohsawa T., Technology Reports of the Osaka University, 1985. **35**(1807): 231-236.

154.	Sun, B., Jones J. J., Burford R. P., and Skyllas-Kazacos M., *Stability and mechanical properties of electrochemically prepared conducting polypyrrole films.* Journal of Materials Science, 1989. **24**(11): 4024-4029.

155.	Ko, J. M., Rhee H. W., Park S.-M., and Kim C. Y., *Morphology and electrochemical properties of polypyrrole films prepared in aqueous and nonaqueous solvents.* Journal of The Electrochemical Society, 1990. **137**(3): 905-909.

156.	Vernitskaya, T. V. E., O.N., *Polypyrrole: a conducting polymer; its synthesis, properties and applications.* Russian Chemical Reviews,, 1997. **66**(5): 443-457.

157.	Kaplin, D. A.Qutubuddin S., *Electrochemically synthesized polypyrrole films: effects of polymerization potential and electrolyte type.* Polymer, 1995. **36**(6): 1275-1286.

158.	Sadik, O. A., *Bioaffinity sensors based on conducting polymers: a short review.* Electroanalysis, 1999. **11**(12): 839-844.

159.	Santhanam, K. S. V., *Conducting polymers for biosensors: Rationale based on models.* Pure and Applied Chemistry, 1998. **70**(6): 1259-1262.

160.	Ngamna, O., Morrin A., Moulton S. E., Killard A. J., Smyth M. R., and Wallace G. G., *An HRP based biosensor using sulphonated polyaniline.* Synthetic Metals, 2005. **153**(1-3): 185-188.

161.	Vidal, J.-C., Garcia-Ruiz E., and Castillo J.-R., *Recent advances in electropolymerized eonducting polymers in amperometric biosensors.* Microchimica Acta, 2003. **143**(2): 93-111.

162. Malhotra, B.Singhal R., *Conducting polymer based biomolecular electronic devices.* Pramana, 2003. **61**(2): 331-343.

163. Borole, D. D., Kapadi U. R., Mahulikar P. P., and Hundiwale D. G., *Conducting polymers: an emerging field of biosensors.* Designed Monomers & Polymers, 2006. **9**(1): 1-11.

164. Lyons, M. E. G., Bannon T., Hinds G., and Rebouillat S., *Reaction/diffusion with michaelis-menten kinetics in electroactive polymer films Part 2. The transient amperometric response.* Analyst, 1998. **123**: 1947-1959.

165. Jiang, X., Xu Q., Dertinger S. K. W., Stroock A. D., Fu T.-m., and Whitesides G. M., *A general method for patterning gradients of biomolecules on surfaces using microfluidic networks.* Analytical Chemistry, 2005. **77**(8): 2338-2347.

166. Morrin, A., Ngamna O., Killard A. J., Moulton S. E., Smyth M. R., and Wallace G. G., *An amperometric enzyme biosensor fabricated from Ppolyaniline nanoparticles.* Electroanalysis, 2005. **17**(5-6): 423-430.

167. Henry, A. C., Tutt T. J., Galloway M., Davidson Y. Y., McWhorter C. S., Soper S. A., and McCarley R. L., *Surface modification of poly(methyl methacrylate) used in the fabrication of microanalytical devices.* Analytical Chemistry, 2000. **72**(21): 5331-5337.

168. Cosnier, S., Galland B., Gondran C., and Le Pellec A., *Electrogeneration of biotinylated functionalized polypyrroles for the simple immobilization of enzymes.* Electroanalysis, 1998. **10**(12): 808-813.

169. Ionescu, R. E., Gondran C., Gheber L. A., Cosnier S., and Marks R. S., *Construction of amperometric immunosensors based on the electrogeneration of a*

permeable biotinylated polypyrrole film. Analytical Chemistry, 2004. **76**(22): 6808-6813.

170.   Minett, A. I., Barisci J. N., and Wallace G. G., *Immobilisation of anti-Listeria in a polypyrrole film.* Reactive and Functional Polymers, 2002. **53**(2-3): 217-227.

171.   Lvov, Y., *Interfacing molecular assemblies and immobilisation technology*, in *Protein Architecture*, Y. LvovH. Möhwald, Editors. 2000: Marcel Dekker, New York. p. 193.

172.   Rusling, J. F.Forster R. J., *Electrochemical catalysis with redox polymer and polyion-protein films.* Journal of Colloid and Interface Science, 2003. **262**(1): 1-15.

173.   Ugo, P., Moretto L. M., Mazzocchin G. A., Guerriero P., and Martin C. R., *Electrochemical preparation and characterization of an anion-permselective composite membrane for sensor technology.* Electroanalysis, 1998. **10**(17): 1168-1173.

174.   Okahata, Y., Tsuruta T., Ijiro K., and Ariga K., *Preparations of Langmuir-Blodgett films of enzyme-lipid complexes: A glucose sensor membrane.* Thin Solid Films, 1989. **180**(1-2): 65-72.

175.   Tatsuma, T., Ogawa T., Sato R., and Oyama N., *Peroxidase-incorporated sulfonated polyaniline-polycation complexes for electrochemical sensing of H2O2.* Journal of Electroanalytical Chemistry, 2001. **501**(1-2): 180-185.

176.   Georganopoulou, D. G., Carley R., Jones D. A., and Boutelle M. G., *Development and comparison of biosensors for in-vivo applications.* Faraday Discussions, 2000. **116**: 291-303.

177.   Bartlett, P. N.Caruana D. J., *Electrochemical immobilization of enzymes. Part V. Microelectrodes for the detection of glucose based on glucose oxidase immobilized in a poly(phenol) film.* Analyst, 1992. **117**: 1287-1292.

178.   Barlett, P. N.Cooper J. M., *A review of the immobilization of enzymes in electropolymerized films.* Journal of Electroanalytical Chemistry, 1993. **362**(1-2): 1-12.

179.   Cooper, J. C.Hall E. A. H., *Electrochemical response of an enzyme-loaded polyaniline film.* Biosensors and Bioelectronics, 1992. **7**(7): 473-485.

180.   Iwakura, C., Kajiya Y., and Yoneyama H., *Simultaneous immobilization of glucose oxidase and a mediator in conducting polymer films.* Journal of the Chemical Society, Chemical Communications, 1988(15): 1019-1020.

181.   Bartlett, P. N.Whitaker R. G., *Electrochemical immobilisation of enzymes: Part II. Glucose oxidase immobilised in poly-N-methylpyrrole.* Journal of Electroanalytical Chemistry and Interfacial Electrochemistry, 1987. **224**(1-2): 37-48.

182.   Martínez, R. C., Domínguez F. B., García I. M. S., Méndez J. H., Orellana R. C., and Guzmán R. S., *Electrochemical response of a polypyrrole-dodecylsulphate electrode with multicharged cations and vitamins B1 and B6. Application as a microsensor in flow-injection analysis.* Analytica Chimica Acta, 1996. **336**(1-3): 47-56.

183.   Vidal, J. C., García E., and Castillo J. R., *In situ preparation of a cholesterol biosensor: entrapment of cholesterol oxidase in an overoxidized polypyrrole film electrodeposited in a flow system: Determination of total cholesterol in serum.* Analytica Chimica Acta, 1999. **385**(1-3): 213-222.

184. Cooper, J. C., Hämmerle M., Schuhmann W., and Schmidt H. L., *Selectivity of conducting polymer electrodes and their application in flow injection analysis of amino acids.* Biosensors and Bioelectronics, 1993. **8**(1): 65-74.

185. Schuhmann, W., *Amperometric substrate determination in flow-injection systems with polypyrrole-enzyme electrodes.* Sensors and Actuators B: Chemical, 1991. **4**(1-2): 41-49.

186. Astruc, D., Boisselier E., and Ornelas C., *Dendrimers designed for functions: from physical, photophysical, and supramolecular properties to applications in sensing, catalysis, molecular electronics, and nanomedicine.* Chemical Reviews, 2010. **110**: 1857-1959.

187. Vögtle, F., Gestermann S., Hesse R., Schwierz H., and Windisch B., *Functional dendrimers.* Progress in Polymer Science, 2000. **25**(7): 987-1041.

188. Breitenbach, J., Spektrum der Wissenschaft/Digest: Moderne Chemie, 1998.

189. Newkome, G. R., Yao Z., Baker G. R., and Gupta V. K., *Micelles. Part 1. Cascade molecules: a new approach to micelles. A [27]-arborol.* The Journal of Organic Chemistry, 1985. **50**(11): 2003-2004.

190. Tomalia, D. A., Baker H., Dewald J., Hall M., Kallos G., Martin S., Roeck J., Ryder J., and Smith P., *A new class of polymers: Starburst dendritic macromolecules.* Polymer, 1985. **17**(1): 117-132.

191. Esfand, R.Tomalia D. A., *Poly(amidoamine) (PAMAM) dendrimers: From biomimicry to drug delivery and biomedical applications, Drug Discovery* Today, 2001. **6**: 427-436.

192.	Dunham, T. H., Ward B. B., and Jr J. R. B., *General carriers for drug delivery*, in *DENDRIMER-BASED NANOMEDICINE*, I.J. MajorosJ.R.B. Jr, Editors. 2008, Pan Stanford Publishing Pte. Ltd. p. 25.

193.	*Dendrimers -Novel Drug Delivery System/ http://www.doyouknow.in/Articles/Pharmaceutical/Dendrimers-Novel-Drug-Delivery-System.aspx.*[cited 2011 18-july].

194.	Buhleier, E., Wehner W., and Vogtle F., *Cascade - and nonskid-chain-like synthesis of molecular cavity topologies.* Synthesis, 1978. **55**: 155-158.

195.	Maciejewski, M., *Concepts of trapping topologically by shell molecules.* Journal of Macromolecular Science, Part A: Pure and Applied Chemistry, 1982. **17**(4): 689-703.

196.	Tomalia, D. A., Baker H., Dewald J., Hall M., Kallos G., Martin S., Roeck J., Ryder J., and Smith P., *A New class of polymers: starburst-dendritic macromolecules.* polymer Journal, 1985. **17**: 117-132.

197.	Esfand, R.Tomalia D. A., *Poly(amidoamine) (PAMAM) dendrimers: from biomimicry to drug delivery and biomedical applications.* Drug Discovery Today, 2001. **6**(8): 427-436.

198.	Hahn, U., Gorka M., Vogtle F., Vicinelli V., Ceroni P., Maestri M., and Balzani V., *Light-harvesting dendrimers: Efficient intra- and intermolecular energy-transfer processes in a species containing 65 chromophoric groups of four different types.* Angewandte Chemie International Edition, 2002. **41**: 3595.

199.	Wells, M.Crooks R. M., *Interactions between organized, surfaceconfined*

monolayers and vapor-phase probe molecules 10. Preparation and properties of chemically sensitive dendrimer surfaces. Journal of the American Chemical Society, 1996. **118**: 3988-3689.

200.   Bu, J., Judeh Z. M. A., Ching C. B., and Kawi S., *Epoxidation of olefins catalyzed by Mn(II) salen complex anchored on PAMAMSiO2 dendrimer.* Catalysis Letters, 2003. **85**: 183-187.

201.   Viers, B. D., Bauer B. J., Akpalu Y., Groehn F., Liu D., and Kim G., *Hydrogels formed by end-linking peg to dendrimer cross-link agents.* Polymer Preprints, 2000. **41**(1): 728-729.

202.   Majoros, I., Thomas T., Mehta C., and Jr J. B., *PAMAM dendrimerbased multi-functional engineered nanodevice for cancer therapy.* Journal of Medicinal Chemistry, 2005. **48**(19): 5892-5899.

203.   Poxon, S. W., Mitchell P. M., Liang E., and Hughes J. A., *Dendrimer delivery of oligonucleotides.* Drug Delivery, 1996. **3**(4): 255-261.

204.   Majoros, I., Myc A., Thomas T., Mehta C., and Jr J. B., *PAMAM dendrimer-based multi-functional engineered nano-device for cancer therapy II: Synthesis, characterization, and functionality.* Biomacromolecules, 2006. **7**(2): 579-579.

205.   Eichman, J. D., Bielinska A. U., Kukowska-Latallo J. F., and Baker J. R., *The use of PAMAM dendrimers in the efficient transfer of genetic material into cells.* Pharmaceutical Science & Technology Today, 2000. **3**(7): 232-245.

206.   Kukowska-Latallo, J. F., Bielinska A., Johnson J., Spindler R., Tomalia D. A., and Jr J. B., *Efficient transfer of genetic material into mammalian cells using Starburst polyamidoamine dendrimers.* Proceedings of the National Academy of Sciences,

1996. **93**(10): 4897-4902.

207. Kobayashi, H., Kawamoto S., Saga T., Sato N., Hiraga A., Ishimori T., Akita Y., Mamede M. H., Konishi J., Togashi K., and Brechbiel M. W., *Novel liver macro-molecular MR contrast agent with a polypropylenimine diaminobutyl dendrimer core: Comparison to the vascular MR contrast agent with the polyamidoamine dendrimer core.* Magnetic Resonance in Medicine, 2001. **46**(4): 795-802.

208. Tomalia, D. A., Naylor A. M., and III W. A. G., *Starburst dendrimers: molecular-level control of size, shape, surface chemistry, topology, and flexibility from atoms to macroscopic matter.* Angewandte Chemie International Edition. English, 1990. **29**: 138-175.

209. Tomalia, D. A., Hedstrand D. M., and Wilson L. R., *Encyclopedia of polymer science and engineering.* 2nd ed, ed. J.I. Kroschwitz. Vol. Index 1990, New York: Wiley.

210. Gudat, D., *Inorganic cauliflower: Functional main group element dendrimers constructed from phosphorus- and silicon-based building blocks.* Angewandte Chemie International Edition in English, 1997. **36**(18): 1951-1955.

211. FrechetJ J. M., *Functional polymers and dendrimers: reactivity, molecular architecture, and interfacial energy.* Science, 1994. **263**(5154): 1710-1715.

212. Fréchet, J. M. J., Hawker C. J., Gitsov I., and Leon J. W., *Dendrimers and hyperbranched polymers: two families of three-dimensional macromolecules with similar but clearly distinct properties.* Journal of Macromolecular Science, Part A: Pure and Applied Chemistry, 1996. **33**(10): 1399 - 1425.

213. Tomalia, D. A., Baker H., Dewald J., Hall M., Kallos G., Martin S., Roeck J.,

Ryder J., and Smith P., *A New class of polymers: starburst-dendritic macromolecules.* polymer Journal, 1985. **17**(1): 117-132.

214.   Tomalia, D. A., Dewald J. R., Hall M. R., Martin S. J., and Smith P. B., in *1st SPSJ International Polymer Conference, Society of Polymer Science Japan, Kyoto*. 1984. p. 65.

215.   Rutt, J. S., *Dendrimers and nanotechnology: A patent explosion, foley and larner paper presented at the national nanotechnology initiative conference, washington DC.* 2002. **29**.

216.   Hult, A., Johansson M., and Malmström E., *Hyperbranched polymers*, in *Branched Polymers II*, J. Roovers, Editor. 1999, Springer Berlin / Heidelberg. p. 1-34.

217.   Fréchet, J. M. J., Hawker C. J., Gitsov I., and Leon J. W., *Dendrimers and Hyperbranched Polymers: Two families of Three Dimensional Macromolecules with Similar but Clearly Distinct Properties.* Journal of Macromolecular Science, Part A Pure and Applied Chemistry, 1996. **33**: 1399-1425.

218.   Tomalia, D. A., *Starburst/Cascade Dendrimers: Fundamental building blocks for a new nanoscopic chemistry set.* Advanced Materials, 1994. **6**(7-8): 529-539.

219.   Witvrouw, M., Fikkert V., Pluymers W., Matthews B., Mardel K., Schols D., Raff J., Debyser Z., Clercq E. D., Holan G., and Pannecouque C., *Polyanionic (i.e. polysulfonate) dendrimers can inhibit the replication of human immunodeficiency virus (HIV) by interfering with both virus absorption and later steps (reverse transcriptase/ integrase) in the virus replication cycle.* Molecular Pharmacology, 2000. **58**(5): 1100-1108.

220. Shaunak, S., Thomas S., Gianasi E., Godwin A., Jones E., Teo I., Mireskandari K., Luthert P., Duncan R., Patterson S., Khaw P., and Brocchini S., *Polyvalent dendrimer glucosamine conjugates prevent scar tissue formation.* Nature Biotechnology, 2004. **22**(8): 977-984.

221. Svenson, S.Tomalia D. A., *Dendrimers in biomedical applications--reflections on the field.* Advanced Drug Delivery Reviews, 2005. **57**(15): 2106-2129.

222. Caminade, A. M., Laurent R., and Majoral J. P., *Characterization of dendrimers.* Advanced Drug Delivery Reviews, 2005. **57**: 2130-2146.

223. Hodge, P., *Polymer science branches out.* Nature, 1993. **362**: 18-19.

224. Fischer, M.Vogtle F., *Dendrimers: From design to application - a progress report.* Angewandte Chemie International Edition, 1999. **38**: 885-905.

225. Hummelen, J. C., van Dongen J. L. J., and Meijer E. W., *Electrospray mass spectrometry of poly(propylene imine) dendrimers; the issue of dendritic purity or polydispersity.* Chemistry - A European Journal, 1997. **3**(9): 1489-1493.

226. Hawker, C.Frechet J. M. J., *A New convergent approach to monodisperse dendritic macromoleucles.* Journal of the Chemical Society, Chemical Communications, 1990: 1010-1013.

227. Ramzi, A., Scherrenberg R., Brackman J., Joosten J., and Mortensen K., *Intermolecular Interactions between dendrimer molecules in solution studied by small-angle neutron scattering.* Macromolecules, 1998. **31**: 1621-1626.

228. Welch, C., FHoagland D. A., *The electrophoretic mobility of PPI dendrimers: do charged dendrimers behave as linear polyelectrolytes or charged spheres.*

Langmuir, 2003. **19**: 1082-1088.

229.   Naylor, A. M., Goddard W. A. I., Kiefer G. E., and Tomalia D. A., *Starburst dendrimers. 5. molecular shape control.* Journal of the American Chemical Society, 1989. **111**: 2339-2341.

230.   Jansen, J. F. G. A., Meijer E. W., and de Brabander-van den Berg E. M. M., *The dendritic box: shape-selective liberation of encapsulated guests.* Journal of the American Chemical Society, 1995. **117**: 4417-4418.

231.   Hawker, C. J., Wooley K. L., and Frechet J. M. J., *Unimolecular micelles and globular amphiphiles: dendritic macromolecules as novel recyclable solubilization agents.* Journal of the Chemical Society, Perkin Transactions 1, 1993(12): 1287-1297.

232.   Gohel, M. C.Parikh r., *"Dendrimer: An overview,"* Targeted Drug Delivery. Systems, 2009. **7**(3).

233.   Watanabe, S.Regen S. L., *Dendrimers as building blocks for multilayer construction.* Journal of the American Chemical Society, 1994. **116**(19): 8855-8856.

234.   Percec, V., Chu P., and Kawasumi M., *Toward "Willowlike" Thermotropic Dendrimers.* Macromolecules, 1994. **27**(16): 4441-4453.

235.   Matthews, O. A., Shipway A. N., and Stoddart J. F., *Dendrimers branching out from curiosities into new technologies.* Progress in Polymer Science, 1998. **23**: 1-56.

236.   Zimmerman, S. C., Zeng F., Reichert D. E. C., and Kolotuchin S. V., *Self-*

assembling dendrimers. Science, 1996. **271**(5252): 1095-1098.

237. Huck, W. T. S., van Veggel F. C. J. M., and Reinhoudt D. N., *Controlled assembly of nanosized metallodendrimers.* Angewandte Chemie International Edition in English, 1996. **35**(11): 1213-1215.

238. Burchard, W., Kajiwara K., and Nerger D., *Static and dynamic scattering behavior of regularly branched chains: a model of soft-sphere microgels.* J Polym Sci Polym Phys Ed, 1982. **20**: 157-171.

239. Alexander, S.Orbach R., *Density of states on fractals:"fractons".* Journal de Physique Letttres (Paris), 1982. **43**: 625-631.

240. Wooley, K. L., Hawker C. J., Pochan J. M., and Frechet J. M. J., *Physical properties of dendritic macromolecules: a study of glass transition temperature.* Macromolecules, 1993. **26**(7): 1514-1519.

241. Gennes, P. G. d.Hervet H., *Statistics of « starburst » polymers.* Journal de physique. Lettres, 1983. **44**(9): 351-360.

242. Tomalia, D.Dewald J., *Dense star polymer and dendrimers.* May 6,1986: U.S.Patent 4587329.

243. Miller, L. L., Duan R. G., Tully D. C., and Tomalia D. A., *Electrically conducting dendrimers.* Journal of the American Chemical Society, 1997. **119**(5): 1005-1010.

244. Hawker, C. J., Malmstrom E. E., Frank C. W., and Kampf J. P., *Exact linear analogs of dendritic polyether macromolecules: Design, synthesis, and unique properties.* Journal of the American Chemical Society, 1997. **119**: 9903-9904.

245. Welch, P.Muthukumar M., *Tuning the density profile of dendritic polyelectrolytes.* Macromolecules, 1998. **31**: 5892-5897.

246. Stiriba, S. E., Frey H., and Haag R., *Dendritic polymers in biomedical applications: From potential to clinical use in diagnostics and therapy.* Angewandte Chemie International Edition in English, 2002. **41**: 1329-1334.

247. *http://www.symo-chem.nl/dendrimer.htm* Dendrimer Chemistry [cited 2011 25 july].

248. Brabander, E. M. M. d.Put J. A., *Proceedings of the american chemical society division of polymeric materials.* Science and Engineering, 1995. **73**: 79.

249. Service, R. F., *Dendrimers: Dream molecules approach real applications* Science, 1995. **267**(5197): 458-459.

250. Hawker, C. J., Wooley K. L., and Frechet J. M. J., *Unimolecular micelles and globular amphiphiles: dendritic macromolecules as novel recyclable solubilization agents* Journal of the Chemical Society Perkin Transactions 1, 1993(12): 1287-1297.

251. Robert, S. F., *Dendrimers: Dream Molecules Approach Real Applications.* Science, 27 January 1995. **267**(5197): 458-459

252. Donald, A. T., Donald A. K., William J. K. J., Roberta C. C., Ian A. T., Michael J. F., David M. H., and Larry R. W., *Starburst conjugates.* 1994, The Dow Chemical Company (Midland, MI): US Patene 5338532.

253. Wiener, E. C., Brechbiel M. W., Brothers H., Magin R. L., Gansow O. A., Tomalia D. A., and Lauterbur P. C., *Dendrimer-based metal chelates: a new class of*

magnetic resonance imaging contrast agents. Magnetic Resonance in Medicine, 1994. **31**: 1-8.

254.	Newkome, G. R.Shreiner C. D., *Poly(amidoamine), polypropylenimine, and related dendrimers and dendrons possessing different 1/2 branching motifs: An overview of the divergent procedures.* Polymer, 2008. **49**(1): 1-173.

255.	Ardoin, N.Astruc D., *The molecular trees : from syntheses towards applications.* Bulletin de la Societe Chimique de France, 1995. **132**: 875-909.

256.	Huskens, J., and M. A. D., and Reinhoudt D. N., *Attachment of molecules at a molecular printboard by multiple host-guest interactions.* Angewandte Chemie International Edition, 2002. **41**: 4467-4471.

257.	Bruinink, C. M., Nijhuis C. A., Peter M., Dordi B., Crespo-Biel O., Auletta T., Mulder A., Schonherr H., Vancso G. J., Huskens J., and Reinhoudt D. N., *Supramolecular microcontact printing and Dip-pen nanolithography on molecular printboards.* Chemistry - A European Journal, 2005. **11**: 3988-3996.

258.	Tanghe, L.Goethals E., *Grafting of living poly(tetrahydrofuran) onto amino-dendrimers.* e-Polymers, 2001. **1**: 1-11.

259.	Frechet, J., *Functional polymers and dendrimers: reactivity, molecular architecture, and interfacial energy.* Science, 1994. **263**(5154): 1710-1715.

260.	Saraswathi, R.Chen S.-M., *Dendrimers in electrochemical biosensors* in *Nanostructured Materials for Electrochemical Biosensors*, Y. Umasankar, S.A. Kumar, and S.-m. Chen, Editors. 2009, Nova Science Publishers: New York, USA.

261.	Arotiba, O. A., Ignaszak A., Malgas R., Al-Ahmed A., Baker P. G. L., Mapolie S.

F., and Iwuoha E. I., *An electrochemical DNA biosensor developed on novel multinuclear nickel (II) salicylaldimine metallodendrimer platform* Electrochimica Acta, 2007. **53**((4)): 1689-1696.

262.   Arotiba, O. A., Songa E. A., Baker P. G., and Iwuoha E. I., *Dendrimeric gold-poly(propylene imine) electrochemical DNA nanobiosensor.* chimica oggi • Chemistry Today •, 2009. **27**: 55-58

263.   Arotiba, O., Owino J., Songa E., Hendricks N., Waryo T., Jahed N., Baker P., and Iwuoha E., *An electrochemical DNA biosensor developed on a nanocomposite platform of gold and poly(propyleneimine) dendrimer.* Sensors, 2008. **8**(11): 6791-6809.

264.   Caminade, A.-M., Padié C., Laurent R., Maraval A., and Majoral J.-P., *Uses of Dendrimers for DNA Microarrays.* Sensors, 2006. **6**(8): 901-914.

265.   Guangjiu, L., Li X., Wan J., and Zhang S., *Dendrimers-based DNA biosensors for highly sensitive electrochemical detection of DNA hybridization using reporter probe DNA modified with Au nanoparticles.* Biosensors and Bioelectronics, 2009. **24**(11): 3281-3287.

266.   Ningning, Z., Gao H., Xu Q., Lin Y., Su L., and Mao L., *Sensitive impedimetric DNA biosensor with poly(amidoamine) dendrimer covalently attached onto carbon nanotube electronic transducers as the tether for surface confinement of probe DNA.* Biosensors and Bioelectronics, 2010. **25**(6): 1498-1503.

267.   Arotiba, O. A., Owino J. H., Baker P. G., and Iwuoha E. I., *Electrochemical impedimetry of electrodeposited poly(propylene imine) dendrimer monolayer.* Journal of Electroanalytical Chemistry, 2010. **638**(2): 287-292.

268. Hall, E. H., *On a new action of the magnet on electric currents.* American Journal of Mathematics, 1879. **2**(3): 287-292.

269. Solymar, L.Walsh D., *Lectures on the electrical properties of materials, 5th Ed., (Oxford University Press, Oxford, 1993).*

270. Griffiths, D. J., Introduction to Electrodynamics, 3rd Ed., (Addison Wesley, Upper Saddle River, NJ, 1999).

271. Pauw, L. J. v. d., *A Method of measuring the resistivity and hall coefficient on lamellae of arbitrary shape.* Philips Technical Review, 1958: 220-224.

272. Blood, P.Orton J. W., *The electrical characterization of semiconductors: majority cCarriers and electron States* (Academic Press Limited, San Diego,1992).

273. Reggiani, S., Valdinoci M., Colalongo L., Rudan M., Baccarani G., Stricker A. D., Illien F., Felber N., Fichtner W., and Zullino L., *Electron and hole mobility in silicon at large operating temperatures. I. Bulk mobility.* IEEE Transactions on Electronic Devices, 2002. **49**(3): 490-499.

274. Borthen, P.Wachutka G., *Testing semiconductor devices at extremely high operating temperatures.* Microelectronics Reliability. **48**(8-9): 1440-1443.

275. Chalker, P. R., *Wide bandgap semiconductor material for high temperature electronics.* Thin Solid Films, 1999. **343**: 616-622.

276. Cullity, B. D., *Elements of X-rRay diffraction.* 2nd ed. 1978: Reading Massachusetts:Addison-Wesley Publishing Co.

277. Albani, J. R., *Principles and application of fluorescence spectrocopy.* Wiley-

Blackwell Science, 2007.

278.   Bindell, J., *Scanning electron microscopy*, in *Encyclopedia of Materials Characterization: Surfaces, Interfaces, Thin Films*, R. BrundleC. Evans, Editors. 1992, Greenwich: Manning Publication Company.

279.   Bard , A. J., and Faulkner , L.R *Electrochemical Methods : Fundamentals and applications (2nd edition)* Newyork: John Willey & Sons, 2000.

280.   David K. Gosser, J., *Cyclic voltammetry, simulation and Analysis of Reaction Mechanisms, .* VCH publishers, 1994: 42-43.

281.   P.M, M., *Fundamentals of electroanalytical chemistry. Newyork, USA: .* John Willey & Sons., 2001: 158-159.

282.   Haines, F. W. F. a. P. J., *Environmental analytical chemistry.* blackie academic and professional, an imprint of chapman & hall, 2nd edition, 1995: 197-223.

283.   Milner, G. W. C.Slee L. J., *Analytical applications of the barker square-wave polarograph. Part III. orthophosphoric acid as a solvent and base electrolyte in direct inorganic polarographic analysis.* Analyst, 1957. **82**(972): 139-151.

284.   Williams-Dottin, A. R., *Monosubstituted Squarate Ligands and their transition metal and Lanthanide Complexes: Structural and Electrochemical Studies, PhD Thesis in Chemistry,.* University of the West Indies, St. Augustine, 2001.

285.   Kounaves, S. P., *Voltammetric Techniques: Handbook of Instrumental Techniques for Analytical Chemistry,.* 2007 **Chapter 37,**: 709-725. .

286.   Akinyenye, R. O., *Nanostructured polypyrrole impedimetric sensors for*

anthropogenic organic pollutants, PhD Thesis in Chemistry,. University of the Western Cape, South Africa., 2008.

287.   Delahay, P., *Double layer and electrode kinetics*. 1965, New York: Wiley-Interscience.

288.   D.M, *Mohilner in electroanalytical chemistry*, ed. A.J. Bard. 1966, New York: Dekker.

289.   Breyer, B.Bauer H. H., *Alternating current polarography and tensammetry, chemical analysis series, P.J. Elving and I.M. Kolthoff, Eds*. 1963, New York: Wiley-Interscience.

290.   Smith, D. E., *Electroanalytical chemistry, A.J. bard, Ed*. Vol. 1. 1966, New York: Dekker.

291.   Gileadi, E., *Electrode kinetics for chemists, engineers, and material scientists*. 1993, VCH, New York.

292.   Delahay, P., *New instrumental methods in electrochemistry*. 1954, New York: Interscience.

293.   Kang, X. M., Zhibin Zou, Xiaoyong, Cai, Peixiang Mo, Jinyuan, *A novel glucose biosensor based on immobilization of glucose oxidase in chitosan on a glassy carbon electrode modified with gold-platinum alloy nanoparticles/multiwall carbon nanotubes*. Analytical Biochemistry, 2007. **369**(1): 71-79.

294.   Fernàndez-Sańchez, C., McNeil, C.J. & Rawson, K. , *Electrochemical impedance spectroscopy studies of polymer degradation : application to biosensor development ,* . Trends in Analytical Chemistry 2005. **24 (1),** : 37-48.

295. Smith, G., Chen R., and Mapolie S., Journal of Organometallic Chemistry, 2003. **673**: 111-115.

296. Salmon, A.Jutzi P., Journal of Organometallic Chemistry, 2001. **637-639**: 595-608.

297. Turcu, R., Giurgia L. V., Ordean R., Grecu R., and Brie M., Synth.Met, 2001. **119**: 287-288.

298. Baleg, A. A. A., Jahed N. M., Arotiba O. A., Mailu S. N., Hendricks N. R., Baker P. G., and Iwuoha E. I., *Synthesis and characterization of poly(propylene imine) dendrimer - Polypyrrole conducting star copolymer.* Journal of Electroanalytical Chemistry, 2011. **652**(1-2): 18-25.

299. Depaoli, M. A.Waltaman R. J., Polym. Sci. Polym. Chem, 1985. **23**: 1687-1698.

300. Kang, H. C.Geckeler K. E., *Enhanced electrical conductivity of polypyrrole prepared by chemical oxidative polymerization: effect of the preparation technique and polymer additive* Polymer, 2000. **41**(18): 6931-6934.

301. Berg, E. M. M. D. B.-V. d.Meijer E. W., *Poly (propylene imine) dendrimers: large scale synthesis by heterogeneously catalyzed hydrogenation.* Angew Chemical International Edition English, 1993. **32**: 1308-1310.

302. yan, L., Zhang W., Guangtao, and Yong J., *Electrochemical synthesis and characterization of novel bile acid functionalized polypyrroles* Polymer, 2007. **49**(1): 225-233.

303. Cheung, K. M., Bloor D., and Stevens G. C., Polymer, 1988. **29**: 1709-1717.

304.   Gardner, J. W.Bartlett P. N., *Potential applications of electropolymerized thin organic films in nanotechnology* Nanotechnology, 1991. **2**: 19-32.

305.   Wang, D., Imae T., and Miki M., J. Colloid Interface Sci, 2007. **306**(2,15): 222-227.

306.   Chen, G., Wang Z., Xia D., Zhang L., Hui R., and Zhang J., *Whelk-like helixes of polypyrrole synthesized by electropolymerization.* Advanced Functional Materials, 2007. **17**: 1844-1848.

307.   Van-Genderen, M. H. P., M E. M., and Meijer E. W., *Poly(propylene imine) dendrimers*, in *Advances in dendritic macromolecules*, G.R. Newkome, Editor. 1999, Elsevier. p. 69.

308.   M. H. P. VAN GENDEREN, M. H. A. P. MAK, and E.W. Meijer, *Synthesis and characterization of poly (propylene imine) dendrimers*, in *Dendrimers and other dendritic polymers* J.j. FrechetD.A. Tomalia, Editors. 2001, John Wiley. p. 630-634.

309.   Ningyuan, L., Shan D., and Huaiguo X., European Polymer Journal, 2007. **43**: 2532-2539.

310.   Ouyang, J.Li Y., *Great improvement of polypyrrole films prepared electrochemically from aqueous solutions by adding nonaphenol polyethyleneoxy (10) ether* Polymer, 1997. **38**(15): 3997-3999.

311.   Bard, A. J.Faulkner L. R., in *Electrochemical Methods: Fundamentals and Applications*, 2nd, Editor. 2000, Wiley, New York.

312.   Rusling, J. F.Forster R. J., Journal of Colloid and Interface Science, 2003. **262**: 1.

313.   Arotiba, O., A, Owino J., Songa E., Hendricks N., Waryo T., Jahed N., Baker P., and Iwuoha E., Sensors 2008. **8**: 6791-6809.

314.   Orazem, M. E.Tribollet B., in *Electrochemical Impedance Spectroscopy*. 2008, John Wiley & Sons, Inc.: Hoboken, New Jersey. p. 315.

315.   Chronakis, I. S., Grapenson S., and Jakob A., *Conductive polypyrrole nanofibers via electrospinning: Electrical and morphological properties*. Polymer, 2006. **47**(5): 1597-1603.

316.   Metin, A.Toppare L., *Synthesis of star-shaped pyrrole and thiophene functionalized monomers and optoelectrochemical properties of corresponding copolymers*. Materials Chemistry and Physics, 2009. **114**: 789-794.

317.   Roovers, J.Comanita B., Advanced in polymer science, Branched Polymers I, 1999. **142**: 179-228.

318.   Hedrick, J. L., Trollsas M., Hawker C. J., Atthoff B., Claesson H., and Heise A., *Dendrimer-like star block and amphiphilic copolymers by combination of ring opening and atom transfer radical polymerization*. Macromolecules, 1998. **31**(25): 8691-8705.

319.   Roovers, J., Zhou L. L., Toporowski P. M., Vanderzwan M., Iatrou H., and Hadjichristidis N., *Regular star polymers with 64 and 128 arms. Models for polymeric micelles*. Macromolecules, 1993. **26**(16): 4324-4331.

320.   Wang, F., Rauh R. D., and Rose T. L., J. Am. Chem. Soc., 1997. **119**: 11106-11107.

321. Olowu, R. A., Ndangili P. M., Ikpo C. O., Williams A., Ngece R. F., Mailu S. N., Njomo N., Wyk V. D. V., Baker P., and Iwuoha E., *Impedimetry and microscopy of electrosynthetic poly(Propylene imine)-co-poly(3,4 ethylene dioxythiophene) dendritic star copolymer.* International Journal of Electrochemical Science, 2011. **6**: 1855-1870.

322. Smith, G., Chen R., and Mapolie S., *The synthesis and catalytic activity of a first-generation poly(propylene imine) pyridylimine palladium metallodendrimer.* Journal of Organometallic Chemistry, 2003. **673**(1-2): 111-115.

323. Salmon, A.Jutzi P., *Water soluble ferrocenyl and polyferrocenyl compounds: synthesis and electrochemistry.* Journal of Organometallic Chemistry, 2001. **637-639**: 595-608.

324. Tian, B.Zerbi G. J., *Lattice dynamics and vibrational spectra of pristine and doped polypyrrole: Effective conjugation coordinate* Journal of Chemical Physics, 1990. **92**(6): 3892.

325. Wang, D., Imae T., and Miki M., *Fluorescence emission from PAMAM and PPI dendrimers.* Journal of Colloid and Interface Science, 2007. **306**(2): 222-227.

326. Gosser, J. D. K., *Cyclic voltammetry: simulations and analysis of reaction mechanisms.* 1993: VCH Publishers Inc., New York.

327. E.Laviron, Journal of Electroanalytical Chemistry, 1979. **101**: 29.

328. Greef, R., Peat R., Peter L. M., Pletcher D., and J. Robinson E., *Nstruental methods in electrochemistry.* 1990: Elis Horwood, New York.

329. Orazem, M. E.Tribollet B., Electrochemical impedance spectroscopy, Wiley (reprint 2008) Charpter 13.

330. M.S. B.Speiser In :A.J. Bard, P. R. U., WILEY-VCH Verlag GmgH &Co. KGaA, Weinhein, (2003) chapter 2.

331. L. Niu, Q. L., F. Wei, X. Chen and H. Wang, . *Electrochemical impedance and morphological characterization of platinum-modified polyaniline film electrodes and their electrocatalytic activity for methanol oxidation.* Journal of Electroanalytical Chemistry, **544** (2003) 121-128.

332. Sarac, A. S., Ates M., and Kilic B., *Electrochemical impedance spectroscopic study of polyaniline on platinum, glassy carbon and carbon fiber microelectrodes.* International Journal of Electrochemical Science, 2008. **3**: 777-786.

333. Ates, M., *Monomer concentration effects of poly (3-methylthiopene) on electrochemical impedance spectroscopy.* International Journal of Electrochemical Science, 2009. **4**: 1004-1014.